NASA CR-66832

DEVELOPMENT OF LIGHTWEIGHT SOLAR PANELS

By J. A. Carlson

Distribution of this report is provided in the interest of information exchange. Responsibility for the contents resides in the author or organization that prepared it.

Prepared under Contract No. NAS7-428 by
ELECTRO-OPTICAL SYSTEMS
Pasadena, California

for

NATIONAL AERONAUTICS AND SPACE ADMINISTRATION

DEVELOPMENT OF LIGHTWEIGHT SOLAR PANELS

By J. A. Carlson

Electro-Optical Systems

SUMMARY

This report summarizes the results of Phase I and Phase II of Contract NAS7-428, Development of Lightweight, Rigid Solar Panels. Electro-Optical Systems began work on Phase I in January 1966 under contract to NASA Headquarters, the Office of Solar and Chemical Power Systems of the Office of Advanced Research and Technology. Phase I was concluded in January 1967. The Phase II portion of the contract, which has been monitored through Langley Research Center, was started in July 1967. The fabrication and testing of the Phase II demonstration panels was completed in March 1969.

This report covers the work on Phase I which was not reported (Ref. 1). The specific areas of Phase I which are documented in this report are related to the fabrication, assembly, and testing of the demonstration panel. CR-75370 (Ref. 1) contains the design tradeoffs, optimization studies, and array and mechanisms designs which were completed during Phase I.

The results of the Phase II effort are also presented.

CONTENTS

SUMMARY 1

INTRODUCTION 2

PHASE I SUMMARY 5

Task Description 5

Program Achievements 6

DESCRIPTION OF THE PHASE I DEMONSTRATION PANEL 6

Structure 6

Electrical 11

ELECTROFORMING OF NICKEL HOLLOWCORE SUBSTRATE 14

Electroforming Setup 14

Mandrel Fabrication 15

Electroforming 17

Etching 19

ASSEMBLY OF PHASE I DEMONSTRATION PANEL 19

Assembly of Structure 19

Electrical Assembly 23

PHASE I DEMONSTRATION PANEL VIBRATION TESTS 31

Test Setup 31

Test Procedure 34

Test Results 37

PHASE II SUMMARY 38

Task Descriptions 38

Program Achievements 39

DESIGN AND ANALYSIS 44

Design Criteria 44

Structural Design 45

Electrical Design 59

Thermal Analysis 61

Dynamic Analysis 61

ILLUSTRATIONS

1	25-sq ft Panel with Electroformed Nickel Hollowcore Substrate Supported in Aluminum Double-Box-Beam Frame	2
2	Phase II Demonstration Panels with Electroformed Aluminum Hollowcore Substrate and Beryllium Frame	4
3	Completed Nickel Hollowcore Substrate	9
4	Two-Piece Aluminum Attachment Clip	10
5	Details of Frame Assembly	12
6	Details of Frame Assembly	13
7	Electroforming Setup-- Hollowcore Structure	16
8	Demonstration Panel Assembly Flow Plan	20
9	Substrate Subassembly Riveted to Lower Beam Assembly	24
10	Vacuum Pickup Tool	25
11	Bus Bar Forming Tool	26
12	Vacuum Hold-Down Tool	27
13	Masking Tool	28
14	Completed Submodule with Adhesive Applied	29
15	Submodule Being Placed on Precleaned H-Film Surface	30
16	Demonstration Panel on Vibration Test Shake Fixture	32
17	Accelerometer Location and Attachment of Demonstration Panel to Shake Fixture	33
18	Location of Vibration Test Control Accelerometer (No. 1)	35
19	Placement of Accelerometers on Demonstration Panel Surface	36
20	Geometry of Substrate	46
21	Hollowcore Substrate Section	47
22	Cell Layout	49
23	Beryllium Beam Cross Section	52
24	Magnesium Hinge Fitting	55
25	Hinge Fitting Cover Plate	56
26	Aluminum Clip Extrusion Cross Section	57
27	Wiring Diagram	60

ILLUSTRATIONS (Contd)

61 thru 62	Electrical Performance Test Plotted Before Environmental Testing	119
63 thru 64	I-V Curves for the Standard Cell During Sunlight Tests	121

INTRODUCTION

The objective of Contract NAS7-428 was to design, fabricate and test solar panels which confirm the feasibility of erecting large area, 25 lb/kW solar arrays. During Phase I, the panel pictured in Fig. 1 was built and tested. This 25 sq-ft panel utilized an electroformed nickel "hollowcore" substrate supported in an aluminum, double-box-beam frame to achieve a weight-to-power ratio of 42 lb/kW, based on the ground rule that the power output of the 4-mil silicon cells used in the design is 10 watts per square foot. This hardware and the supporting analysis demonstrated:

1. The stiffness-to-weight advantage inherent in the curved shell concept;

2. The feasibility of fabricating large, foil gage structures using the electroforming technique;

3. The advantages of lower total weight and lower thermal resistance which are obtained with the one-piece electroformed hollowcore structure as compared to adhesive-bonded structures.

Concurrently with the Phase I effort on NAS7-428, work performed at Electro-Optical Systems under Contract NAS1-6218, had led to the development of a process for electroforming aluminum with sufficient strength to be useful as a structural material. The Phase II objective was to develop the technology necessary to successfully fabricate a solar panel using an electroformed, aluminum, hollowcore substrate and a beryllium frame. The two demonstration panels which resulted from the Phase II work are shown in Fig. 2. These panels weigh approximately 6 lb and have a calculated power output of 210W, giving a weight-to-power ratio of 28.5 lb/kW. Calculations show that, with minor design modifications and manufacturing controls, the program goal of 25 lb/kW can be achieved.

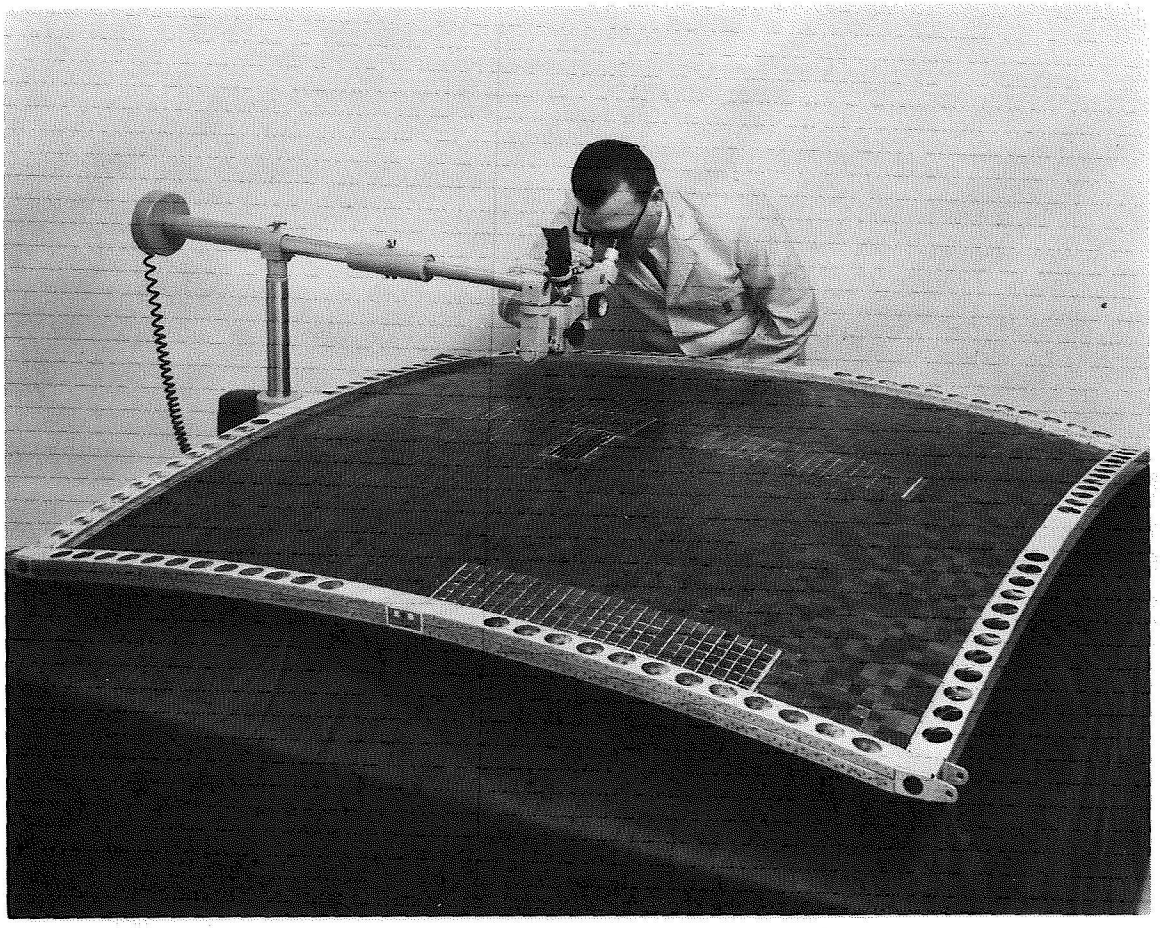

EC-16743

Figure 1. 25-sq ft Panel with Electroformed Nickel Hollowcore Substrate Supported in Aluminum Double-Box-Beam Frame

169104

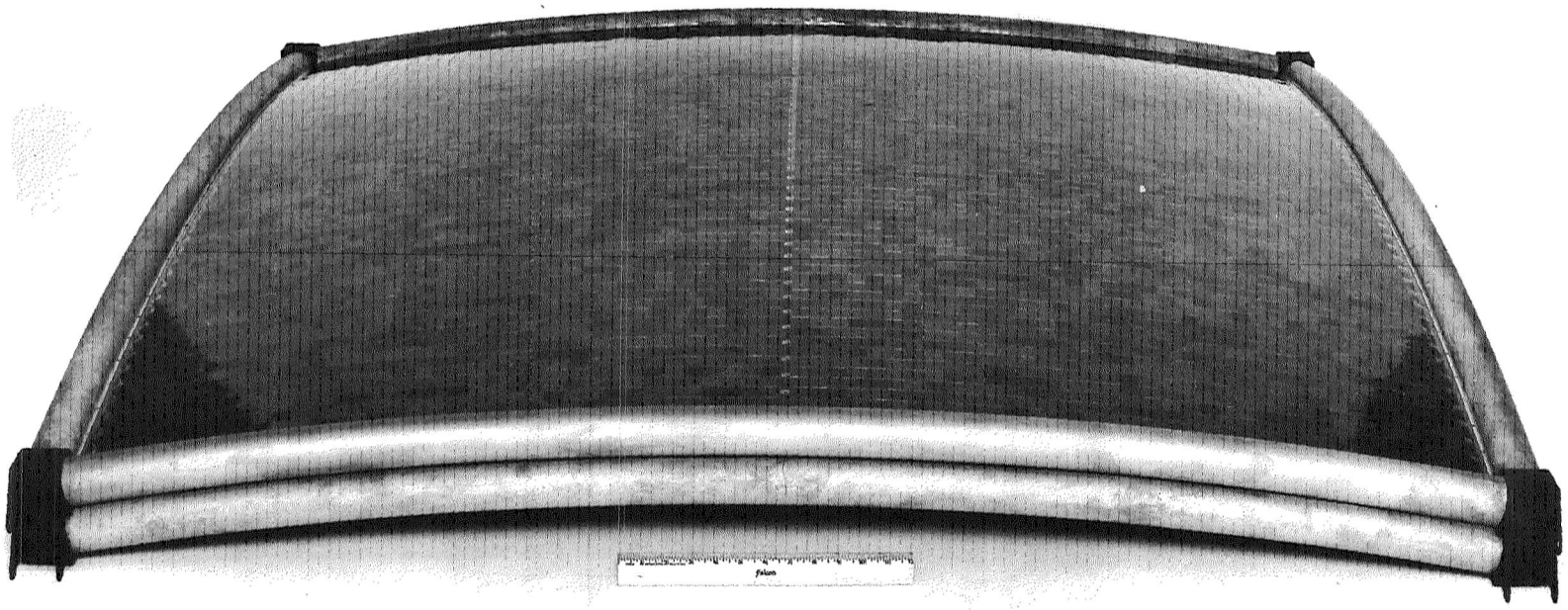

Figure 2. Phase II Demonstration Panels with Electroformed Aluminum Hollowcore Substrate and Beryllium Frame

PHASE I SUMMARY

Task Description

The Phase I development program was divided into four major tasks:

1. Task I - Perform tradeoff analyses and produce a solid, workable design for a representative photovoltaic solar cell array;

2. Task II - Fabricate a demonstration panel including assembly of structure, attachments, solar cells, and coverglass;

3. Task III - Complete testing of demonstration panel including tests of small sample panel sections and vibration test of the demonstration panel;

4. Task IV - Interpret data obtained from panel tests and recommend a program plan for Phase II.

The results of Task I and general information including mission/spacecraft assumptions, design criteria, functional specifications, and definitions of terms and nomenclature were reported in NASA CR-75370 (Ref. 1). Included in CR-75370 are designs for 5 kW and 10 kW deployable arrays which use the 25-sq-ft demonstration panel as a basic building block. A description of the Phase I demonstration panel hardware is provided in this report. A detailed report on the electroforming process used to fabricate the nickel hollowcore substrate is also presented here. The assembly procedure, which completes Task II, is also documented in this report. The results of the Phase I vibration tests, Task III, are discussed. Completion of Task IV resulted in the program plan for Phase II of NAS7-428, which is the subject of the last part of this report.

TABLE I

PHASE I DEMONSTRATION PANEL WEIGHT SUMMARY

Item	Description	Weight/unit	No. of units	Total weight in lb	Specific weight in lb/ft^2*
Structure					
Substrate	Nickel hollowcore - 1.00-in. holes 3 mil skin	0.116 lb/ft^2	23.4 ft^2	2.714	0.10267
Frame and hinge fittings	Aluminum box beams - 10 mil nominal	1.916 lb	1	1.916	0.07248
Attachment clips	Aluminum sheet - 10 mil	0.015 lb/ft	19.22 ft	0.288	0.01089
Dielectric film	Kapton H-film - 2 mil	0.0144 lb/ft^2	23.4 ft^2	0.340	0.01286
Adhesives:					
H-film to substrate	Narmco 7344/7119 2-part epoxy	0.13 lb/ft^2	4.12 ft^2	0.537	0.02031
clip to hollowcore	Narmco 7344/7119 2-part epoxy	0.08 lb/ft^2	0.8 ft^2	0.064	0.00242
frame assembly	Narmco 7344/7119 2-part epoxy	0.06 lb/ft^2	1.2	0.072	0.00272
Rivets	MS-20604-AD3K1; 0109 dia	0.00019	1.20	0.0228	0.00086
			Structure Subtotals	5.954	0.22521
Electrical					
Solar cells	4-mil silicon; 2 cm x 2 cm	0.1199 grams	150	0.0396	0.00150
	8-mil silicon; 2 cm x 2 cm	0.1813 grams	150	0.0600	0.00227
	15-mil dendritic; 1 cm x 15 cm	1.900 grams	6	0.0251	0.00095
Filters	3-mil microsheet; 2 cm x 2 cm	0.0704 grams	300	0.0466	0.00176
Interconnections	1-mil molybdenum; silver plated	0.303 grams	60	0.0401	0.00152
Weight simulation	7-mil aluminum platelets; 2 cm x 2 cm	0.19686 grams	4380	1.9010	0.07191
Adhesives:					
filters to cells	RTV-602	0.021 $\frac{grams}{cell}$	300	0.0139	0.00052
cells and platelets to H-film	RTV-602	0.007 lb/ft^2	23.4 ft^2	0.1640	0.00620
			Electrical Subtotals	2.2903	0.08663
			Total	8.2443	0.31184

Assuming 10 W/ft^2 of active, projected cell area, power = 195.2W

Specific power = 23.2 W/lb

Weight-to-power ratio = 42.2

A_{total} = 62.6 in. x 60.7 in. = 26.43 ft^2

*Based on total planform area of panel

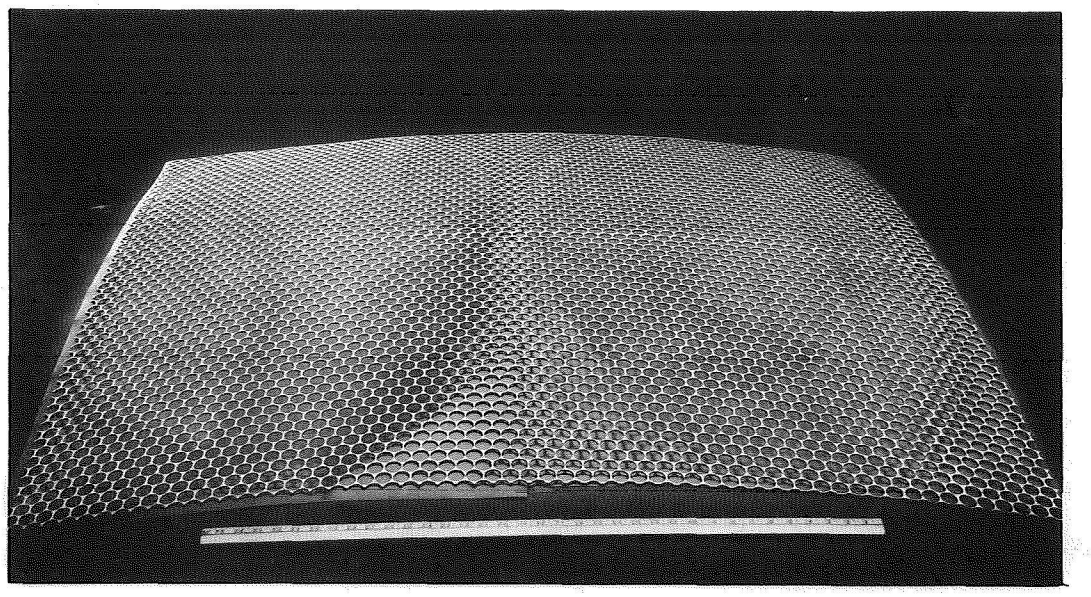

86671

Figure 3. Completed Nickel Hollowcore Substrate

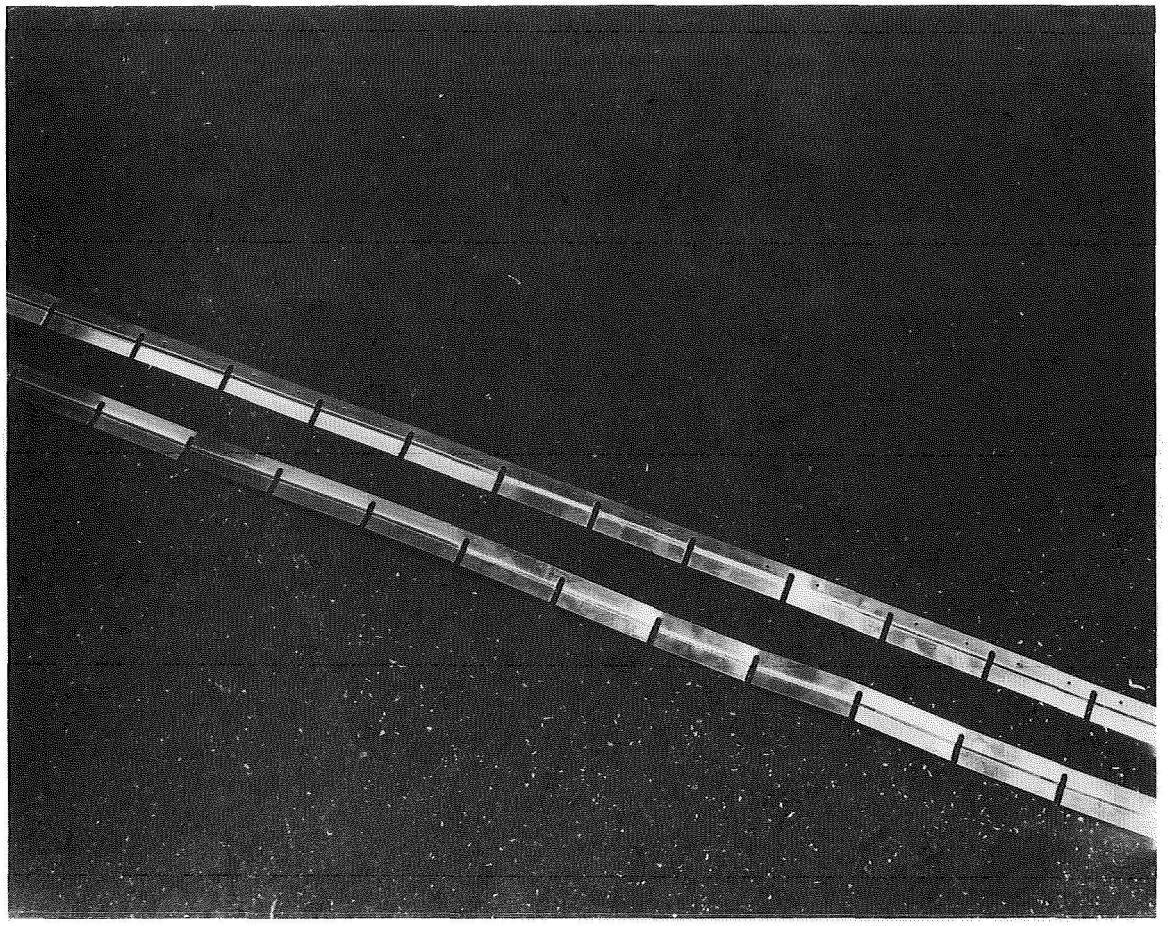

966116

Figure 4. Two-Piece Aluminum Attachment Clip

hinge brackets are inserted into the corner bracket at each corner. These were used to simulate the hinges between subpanels and were used for mounting the demonstration panel to various test fixtures.

The details of the frame assembly are shown in Figs. 5 and 6.

Electrical

Solar cells. - The Phase I demonstration panel was three types of solar cells bonded in place to confirm the feasibility of using the hollowcore structure as a solar panel substrate. The following cells are installed:

1. 150, 4-mil, 2 cm x 2 cm N/P silicon with conventional silver/titanium contacts (solderless)

2. 150, 8-mil, 2 cm x 2 cm N/P silicon with conventional silver/titanium contacts (solderless)

3. 6, 15-mil, 1 cm x 15 cm N/P dendritic with plated contacts

Filters. - The 300 silicon cells were filtered using OCLI type B-SCC-410-MS-C solar cell cover slips. These filters are 2 cm x 2 cm x 0.003 inch microsheet.

Interconnections. - The interconnections used on the demonstration panel are 1-mil molybdenum.

Weight simulation. - The area of the panel not covered by live cells is covered with 2-mil aluminum platelets, 2 cm x 2 cm, which simulate the weight of the cells, filters, and interconnections.

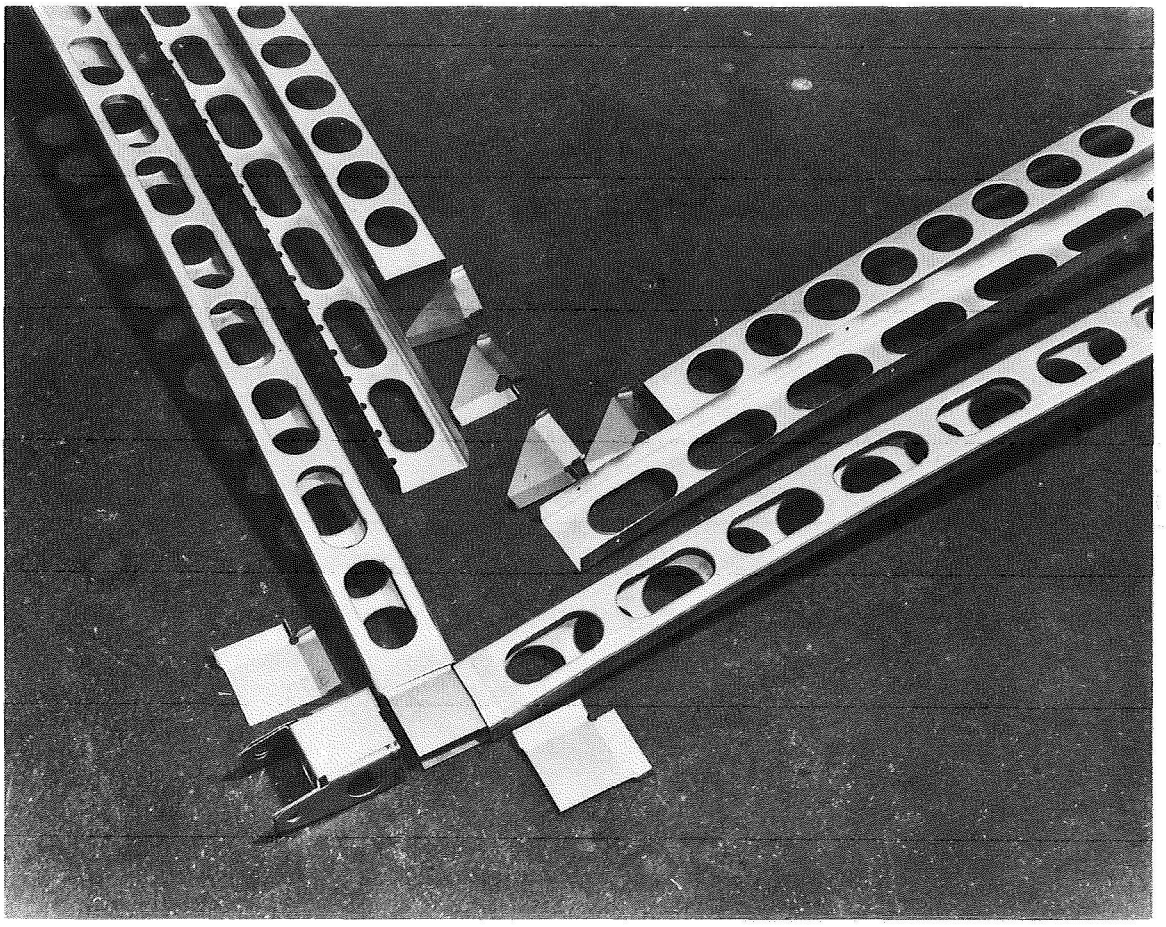

966117

Figure 5. Details of Frame Assembly

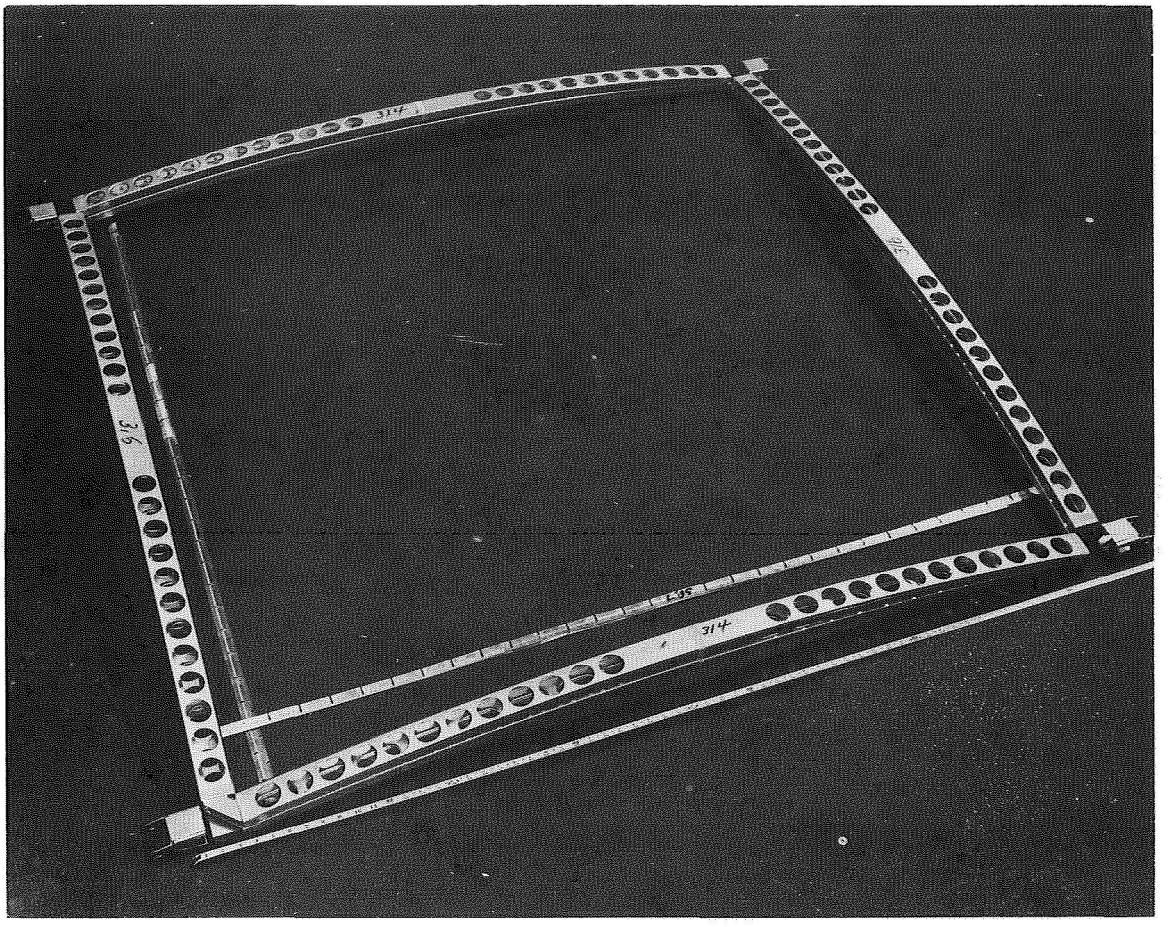

966115

Figure 6. Details of Frame Assembly

A cross-sectional view of the plating setup is shown in Fig. 7. The aluminum plating mandrel was mounted on the reciprocator as shown in the figure. After mounting, the reciprocator was placed in the plating bath between the contour masks which separated the aluminum mandrel and the anode baskets. The anode baskets were filled with sulfur depolarized nickel anode chips. The anode baskets were fabricated from titanium wire mesh to minimize possibilities of bath contamination. The anode baskets were covered with Dacron cloth to prevent the anode sludge from dispersing in the plating solution and causing a rough nickel deposit. Air agitation was supplied through a pipe placed in the bottom of the plating tank along the lower edge of the reciprocator. Air agitation was used to help remove gas bubbles that form on the surface of the mandrel during plating and thereby reduce pitting of the nickel. The part was reciprocated back and forth during the plating process to minimise the effect of variations in current density which would have resulted in thick and thin places in the final electroformed structures.

Continuous filtration of the electroforming solution was maintained throughout the plating process by the use of 50-disk Alsop Filter Assemblies supplied by Vanton pumps. Power for the electroforming process was supplied by a 1000A direct-current power supply.

Mandrel Fabrication

The electroforming mandrel for the demonstration panel was fabricated from 6061-T6 aluminum sheets 0.090 inch thick.

Material was procured from Diamond Metal Sales, Los Angeles, as prepunched flat aluminum sheets 60 inches x 144 inches. The sheets were punched with 3/4-inch-diameter holes on staggered 1-inch centers. After receiving-inspection, the prepunched sheets were cut to a blank size of 60 x 65 inches. The holes in the blanks were then drilled and

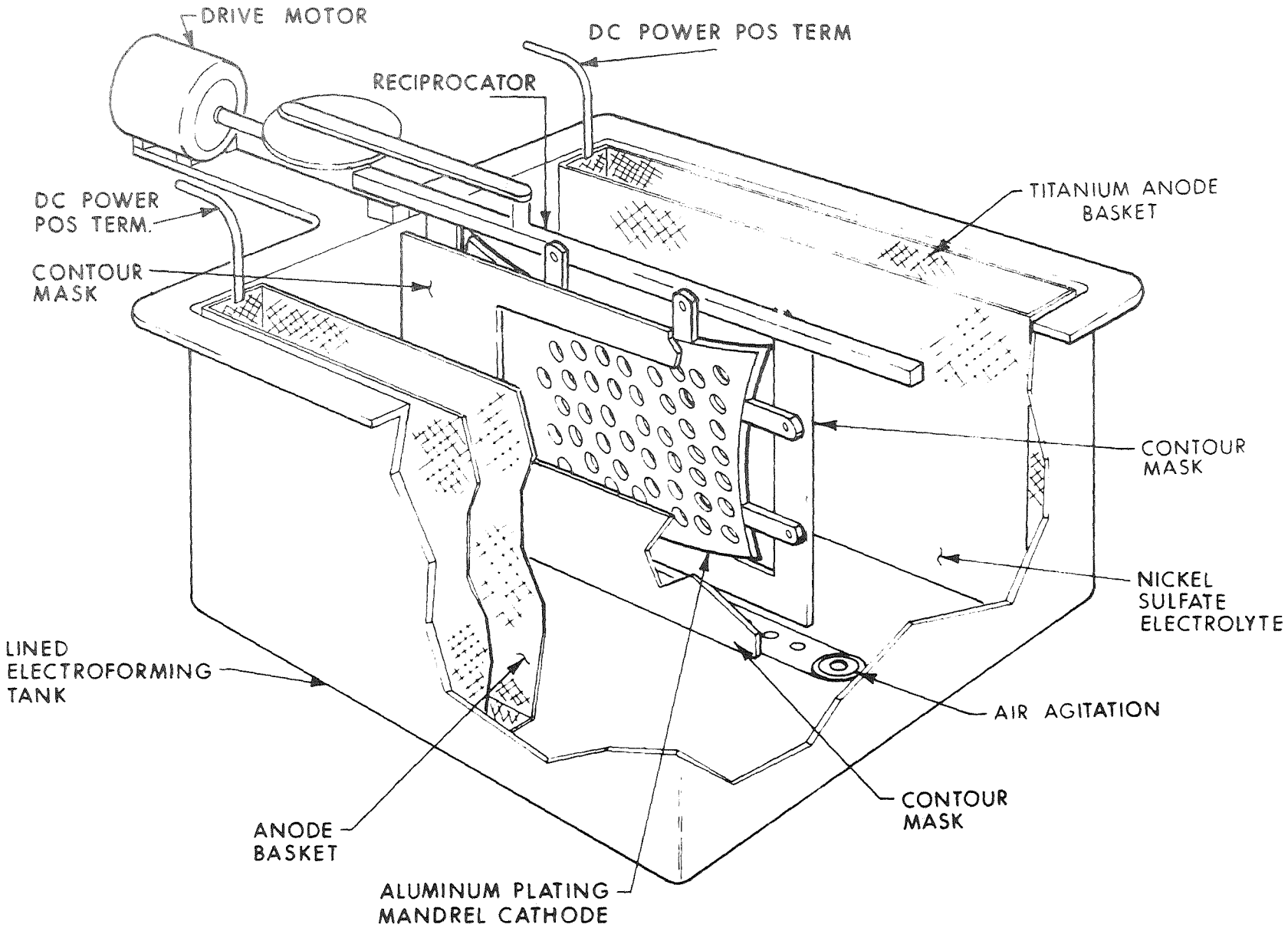

Figure 7. Electroforming Setup - Hollowcore Structure

reamed to a 15/16-inch division. This gave a final area of approximately 16 percent. The edges of each hole were radiused to minimize discontinuity stresses. It was found during the fabrication of buckling specimens that samples without this radius tended to crack in this area.

The mandrels were polished by sanding before forming to remove all scratches and dents.

A drop hammer forming process was used to obtain the biconvex shape of the panel. After forming, the contour of the panel was inspected using a master check template with the panel remaining in the die for support. At this time it was noted that some of the holes near the edges of the mandrel had deformed during the forming process. In addition, holes which had less than the 0.050-inch web between them also deformed. It is believed that these problems could be corrected on other units by increasing the blank and die size over the final required, and drilling and reaming the holes with an accurate drill jig. The prepunched sheets had somewhat greater hole location variations than should be allowed for production parts for this use.

The mandrels were completed by trimming to size and welding on six slotted tabs which were used for attaching the mandrel to the reciprocator.

Electroforming

Electroforming of the hollowcore nickel substrate consisted of two basic steps: (1) preparation and (2) electroforming.

The mandrels were prepared for electroforming by sanding to remove all scratches and burrs.

Actual electroforming of the demonstration panel was accomplished using an average current density of 20A per square foot. Electroforming was accomplished in approximately 2.5 hours.

Etching

Following electroforming the completed structure was given a visual examination for pits, cracks, or tears.

The mounting tabs were trimmed off and the nonconductive tape was removed, exposing the etching holes. Etching the aluminum mandrel out of the electroformed nickel was accomplished by immersing the panel vertically in 30 percent solution of muriatic acid. The etching process required approximately 7 days because of the limited surface area available for the HCL to attack.

After the etching process was completed, the lightweight structure was rinsed several times with deionized water.

The fabrication of the nickel biconvex substrate was completed by placing it on the forming die and checking the contour with the master check template. The completed nickel substrate is shown in Fig. 3.

ASSEMBLY OF PHASE I DEMONSTRATION PANEL

Assembly of Structure

Assembly flow plan. - The flow plan for the assembly of the structure is shown in Fig. 8. The drawing numbers in the figure refer to drawings included in NASA CR75370 (Ref. 1).

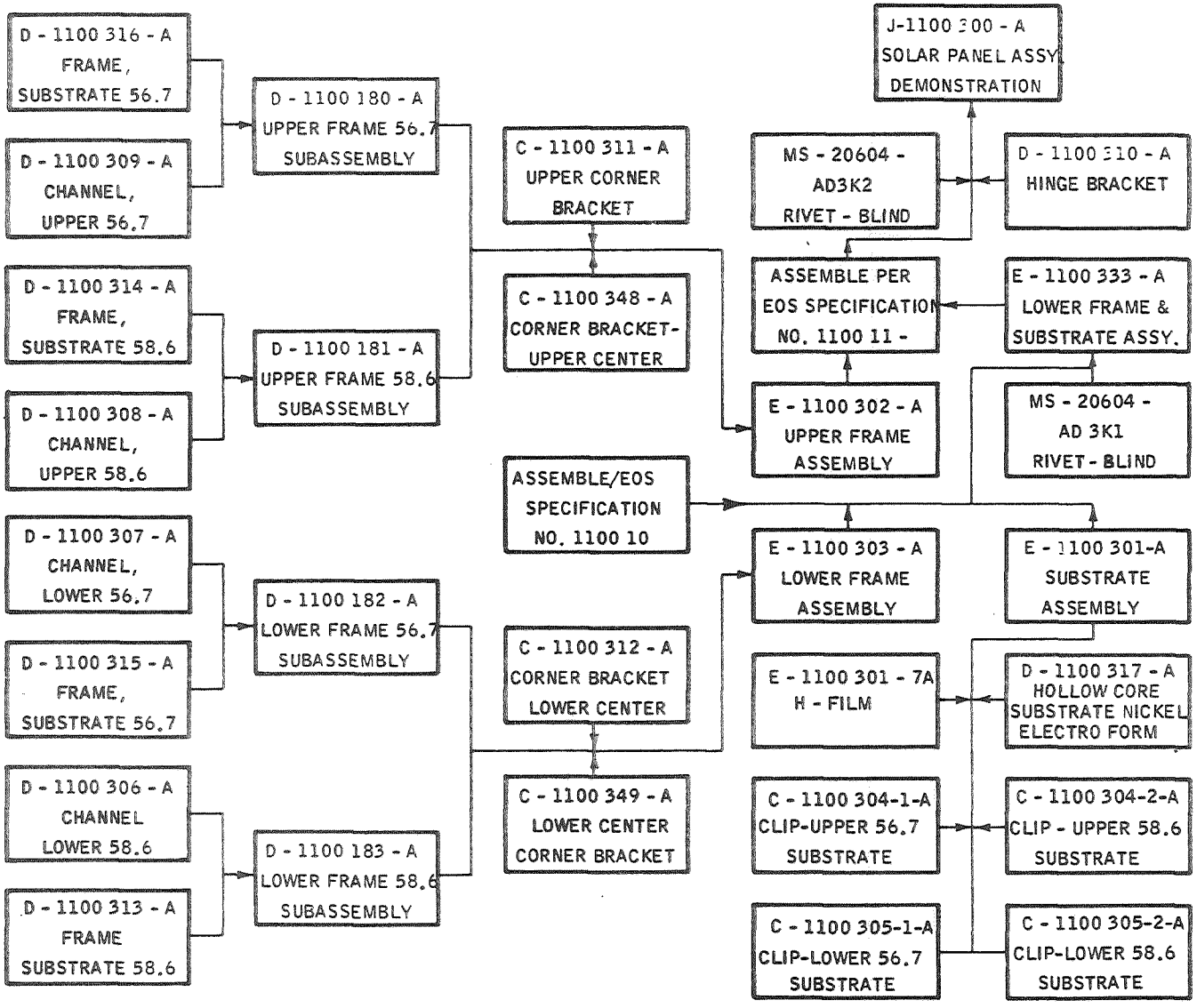

73628187

Figure 8. Demonstration Panel Assembly Flow Plan

Bonding of the dielectric film to the nickel hollowcore substrate. - Following is a discussion of the bonding of the dielectric film to the nickel hollowcore substrate.

Evaluation of adhesives. - A series of pull tests was conducted on nickel-H film lap shear samples to evaluate the following types of adhesives; Du Pont Silicon, General Electric SR-585, Dow Corning DC-280, Bloomingdale Rubber Company BR-1000 and FM-47, Shell Chemicals 422, and Narmco 7344 with Narmco Catalyst 7119. Most of these adhesives developed maximum bond strength in high pressure, elevated temperature, cure cycles. The room temperature, low pressure cure cycle required to bond the H-film to the fragile nickel hollowcore substrate would develop bond strengths of less than 200 psi for all of these adhesives except Narmco 7344. Narmco 7344 with Narmco Catalyst 7119 developed bond strengths between 1000 psi and 1200 psi using a room temperature cure and 2 psi bonding pressure. Based on the results of these tests, Narmco 7344 was chosen as the adhesive to be used to bond the H-film to the nickel hollowcore.

Preparation of surfaces. - The H-film was precut in 16 x 56.7 in. sections and mechanically etched, using No. 400 grit abrasive paper. The sections were suspended during the etching process to prevent imperfections in the surface beneath the H-film from wearing through. The H-film was first etched along the long side of the section and then rotated 90° and etched across the short length to produce a uniform matt surface. The film was then washed with warm tap water and a detergent soap, and rinsed in tap water with a final rinsing in distilled water. It was dried in a 150°F oven for 45 minutes. Just prior to bonding, the H-film was wiped with a clean cloth saturated in methyl ethyl ketone.

combination. The corner pieces and hinge brackets were riveted to the beam assemblies using MS-20648D3K2 blind rivets to complete the assembly.

The substrate subassembly riveted to the lower beam assembly is shown in Fig. 9.

Electrical Assembly

Submodule fabrication. - The 4- and 8-mil cells which were used to fabricate the submodules were tested and electrically grouped into ±1 mA lot at 0.45V.

All handling of the cells was done using the vacuum pickup tool shown in Fig. 10.

The bus bar forming tool is shown in Fig. 11. This tool is a dual purpose device and was also used to jig the bus bars and cells for soldering. Figure 12 shows the bending tool replaced with a vacuum hold-down tool upon which the cells were placed and indexed under the preformed bus bar for the soldering operation. The large vacuum pickup tool which is shown in this figure was used to handle the completed submodules.

Laydown of submodules. - The masking tool used to apply the RTV 602 to the submodules is shown in Fig. 13. A completed submodule with the adhesive applied is shown in Fig. 14. Figure 15 shows a submodule about to be placed on the precleaned H-film surface. This figure also shows the geometric layout and straight edge arrangement used to position the submodules on the substrate.

The aluminum platelets which were used to simulate the solar cells for the demonstration panel were mounted to the substrate using the

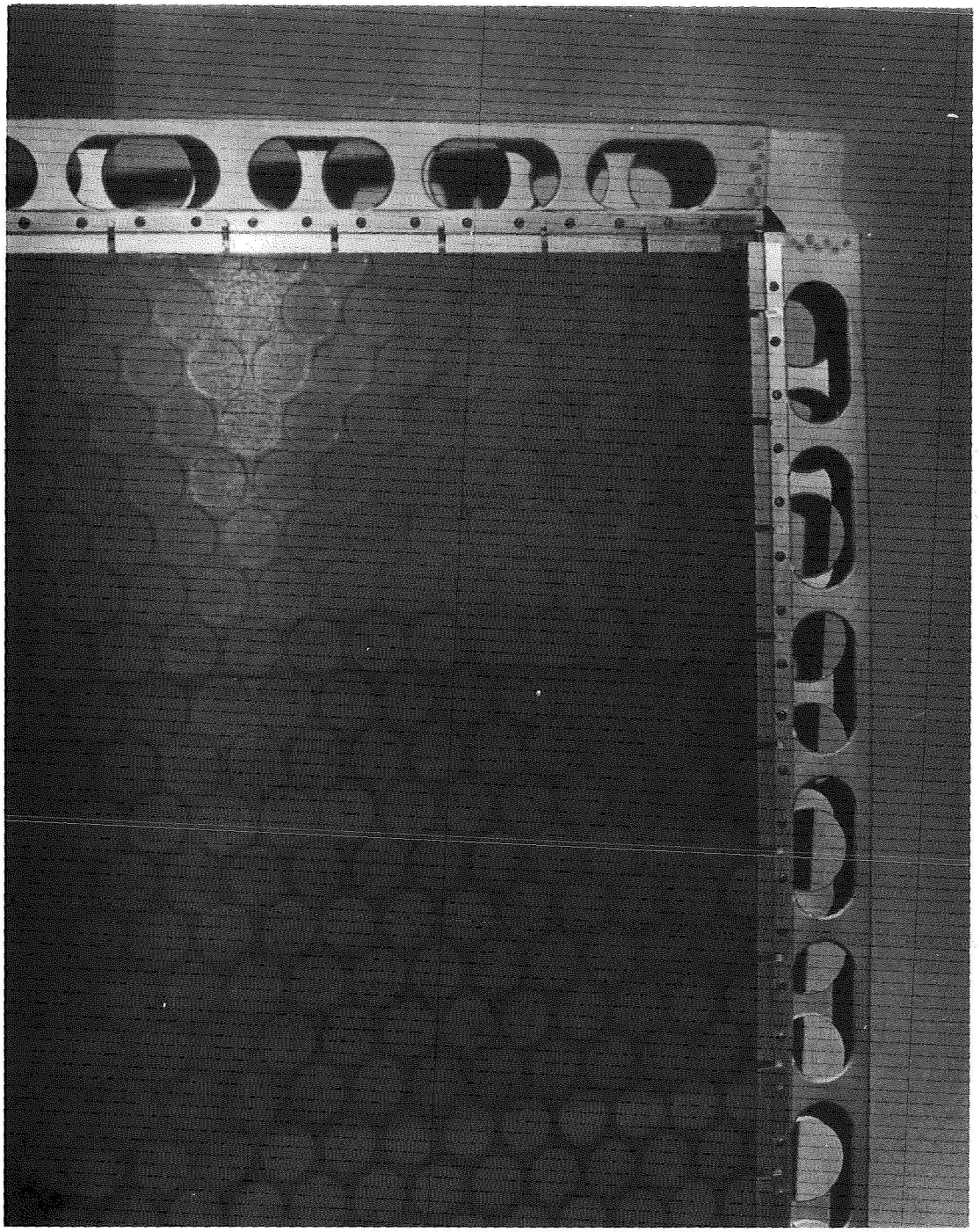

374

Figure 9. Substrate Subassembly Riveted to Lower Seam Assembly

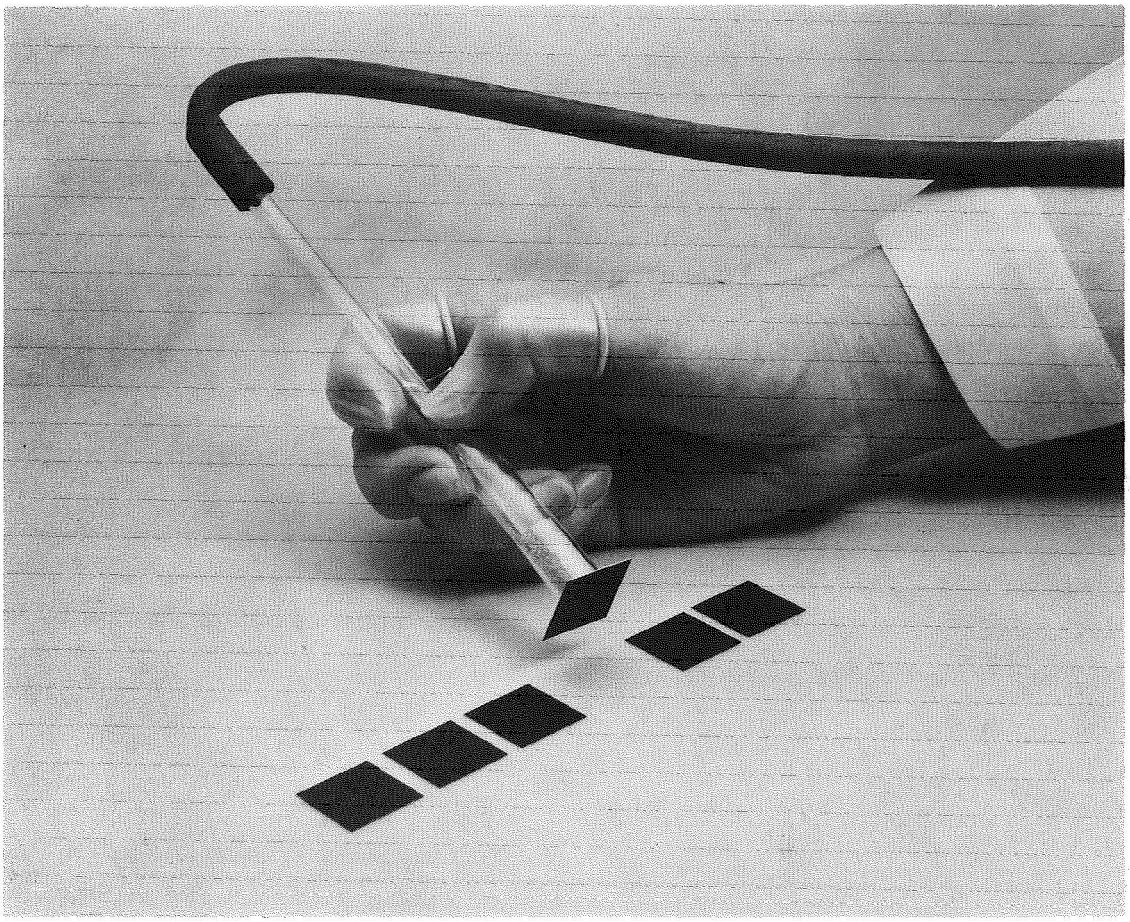

EC-126638

Figure 10. Vacuum Pickup Tool

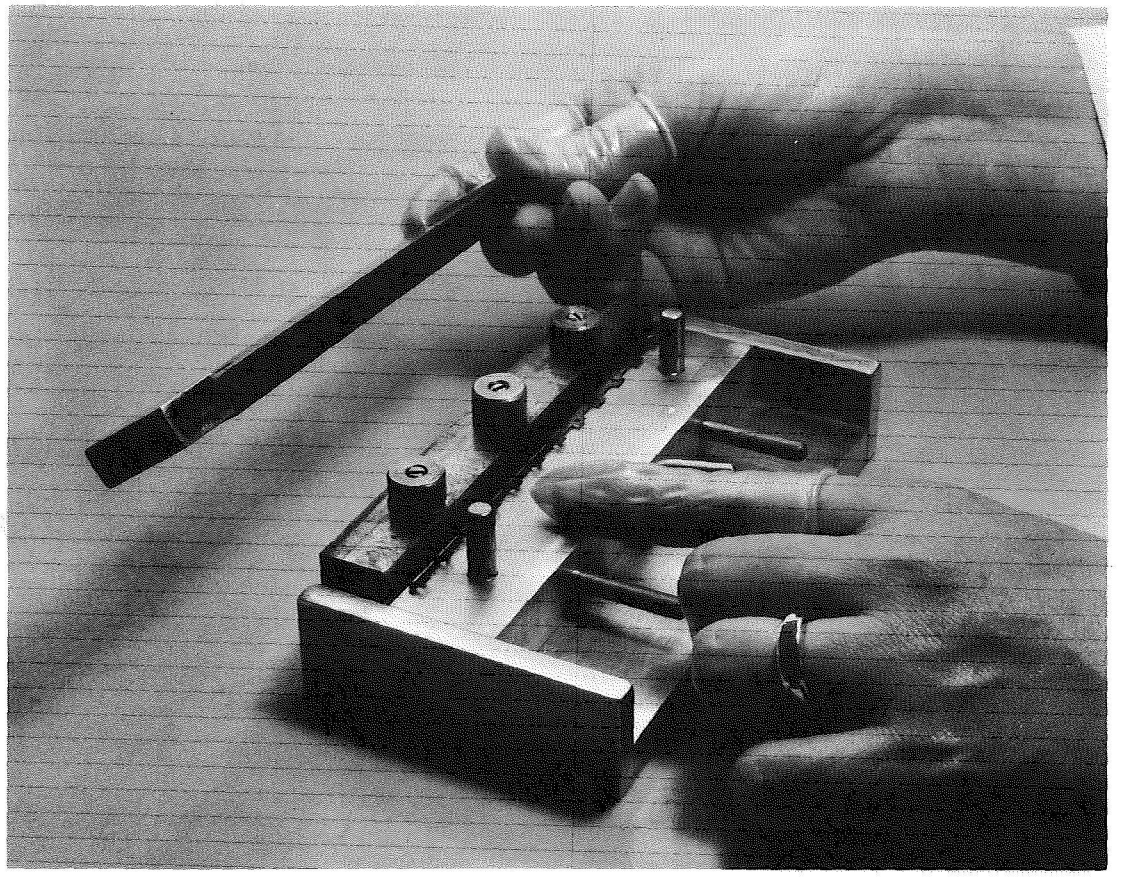

EC 126633

Figure 11. Bus Bar Forming Tool

EC 126637

Figure 12. Vacuum Hold-Down Tool

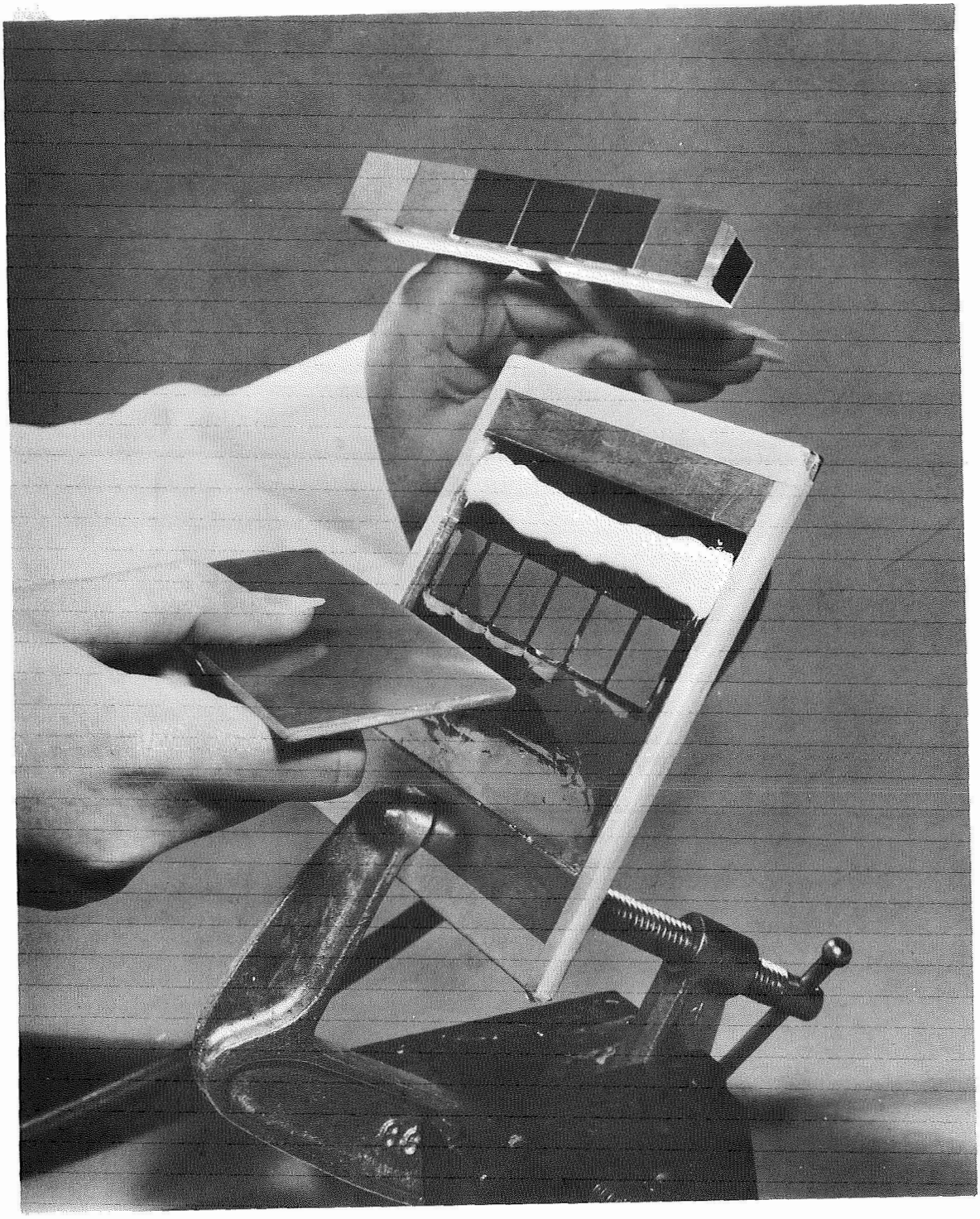

C-367140

Figure 13. Masking Tool

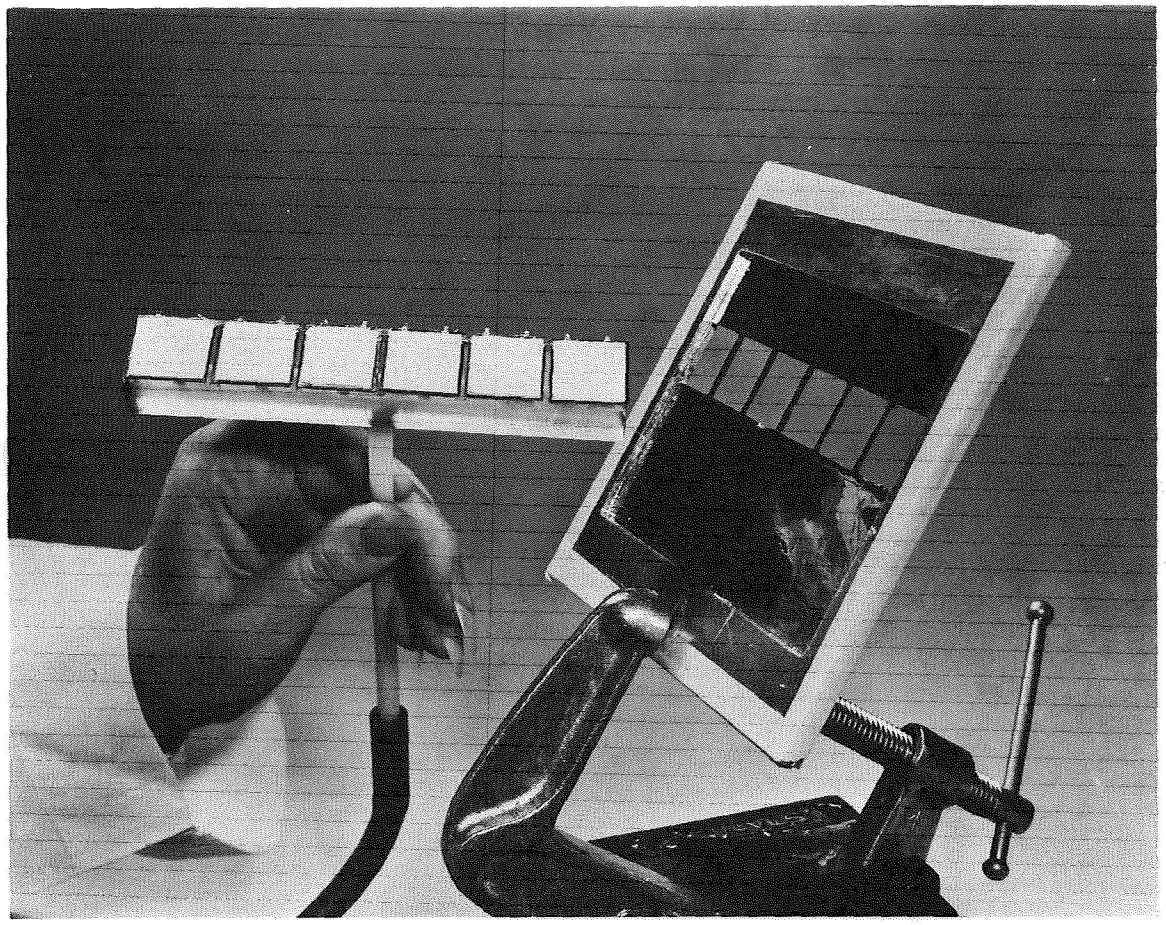

C-367141

Figure 14. Completed Submodule with Adhesive Applied

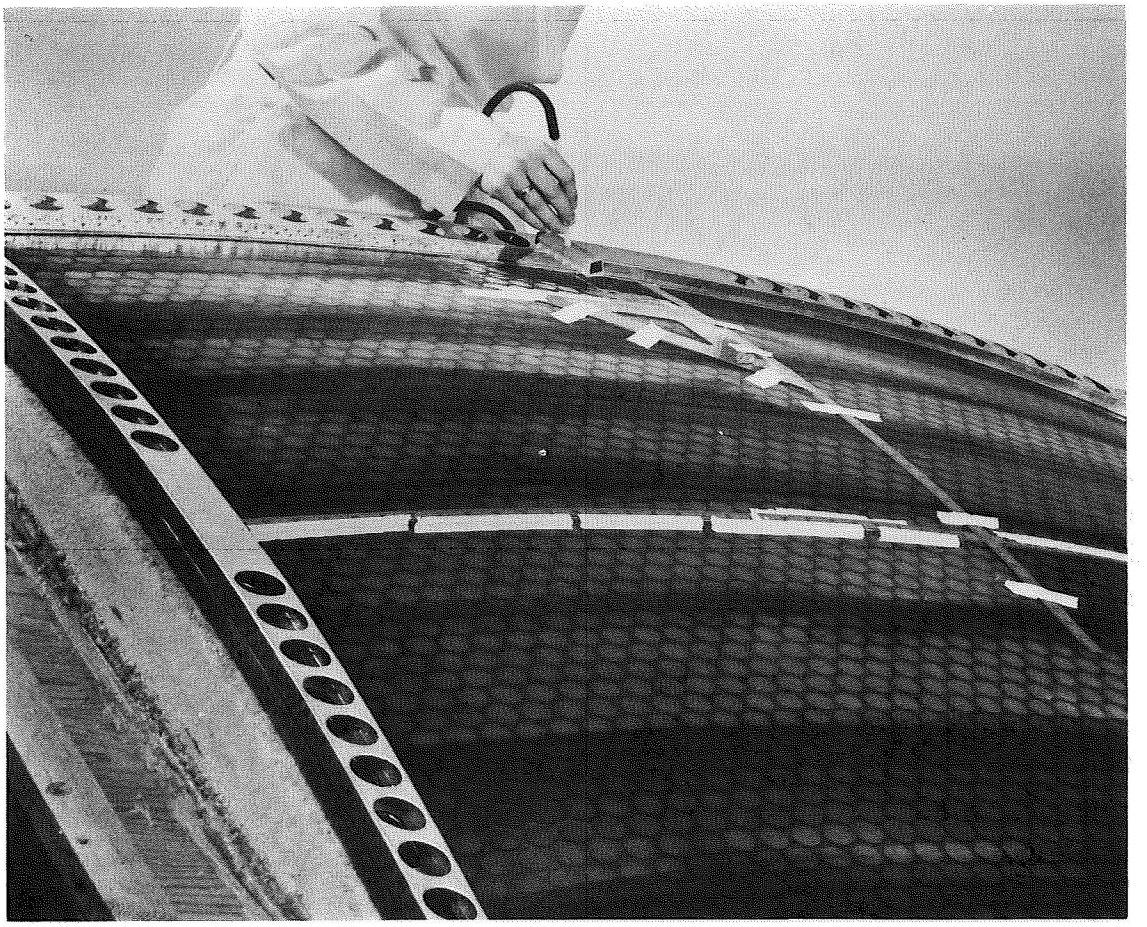

EC-1266128

Figure 15. Submodule Being Placed on Precleaned H-Film Surface

same technique as that used for the actual submodules. The cover slides were bonded to the solar cells after all submodules and solar cell simulators had been mounted to the substrate. The terminal standoffs were then bonded to the H-film and the final wiring of the demonstration panel was completed.

PHASE I DEMONSTRATION PANEL VIBRATION TESTS

A series of low-input-level vibration tests was performed to determine the resonant frequencies and gains at resonance of the biconvex demonstration panel. The results of the tests verified the assumptions and analyses used in the design of the structure.

Since these tests were not intended to be design qualification tests the input levels were maintained below the design limit loads. The excitation for all tests in this series was normal to the plane tangent to the biconvex panel at its center. All excitation was sinusoidal.

The test specimen was the biconvex solar panel, EOS Part No. J1100300. The area which was not celled was covered with aluminum platelets which simulate the weight of the solar cells.

Test Setup

The test setup at Wyle Laboratories (El Segundo, California) is shown in Fig. 16. Two Ling 249 electrodynamic shakers were used to drive the fixture to which the panel was mounted. The attachment of the panel to the fixture is shown in Fig. 17. The armatures of the shakers were series connected to insure proper phasing.

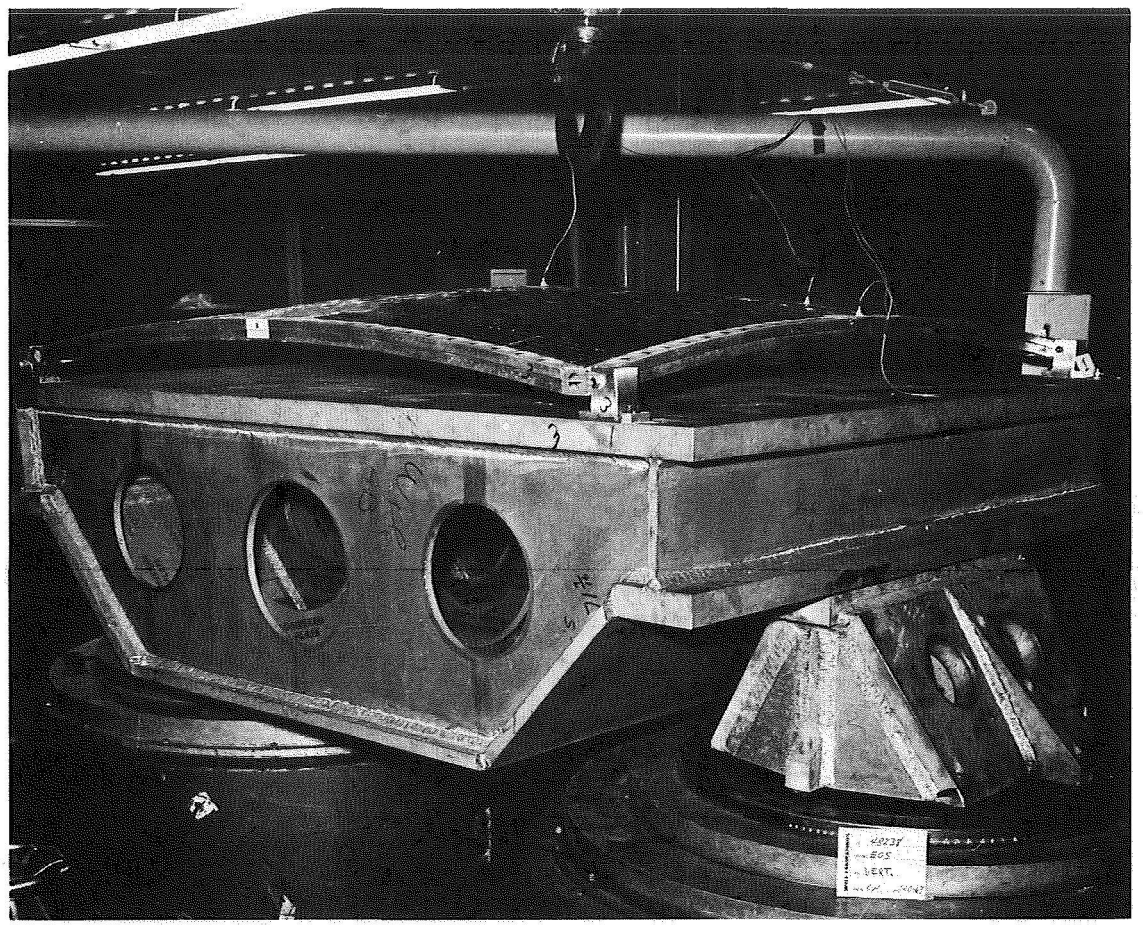

EC-16732

Figure 16. Demonstration Panel on Vibration Test Shake Fixture

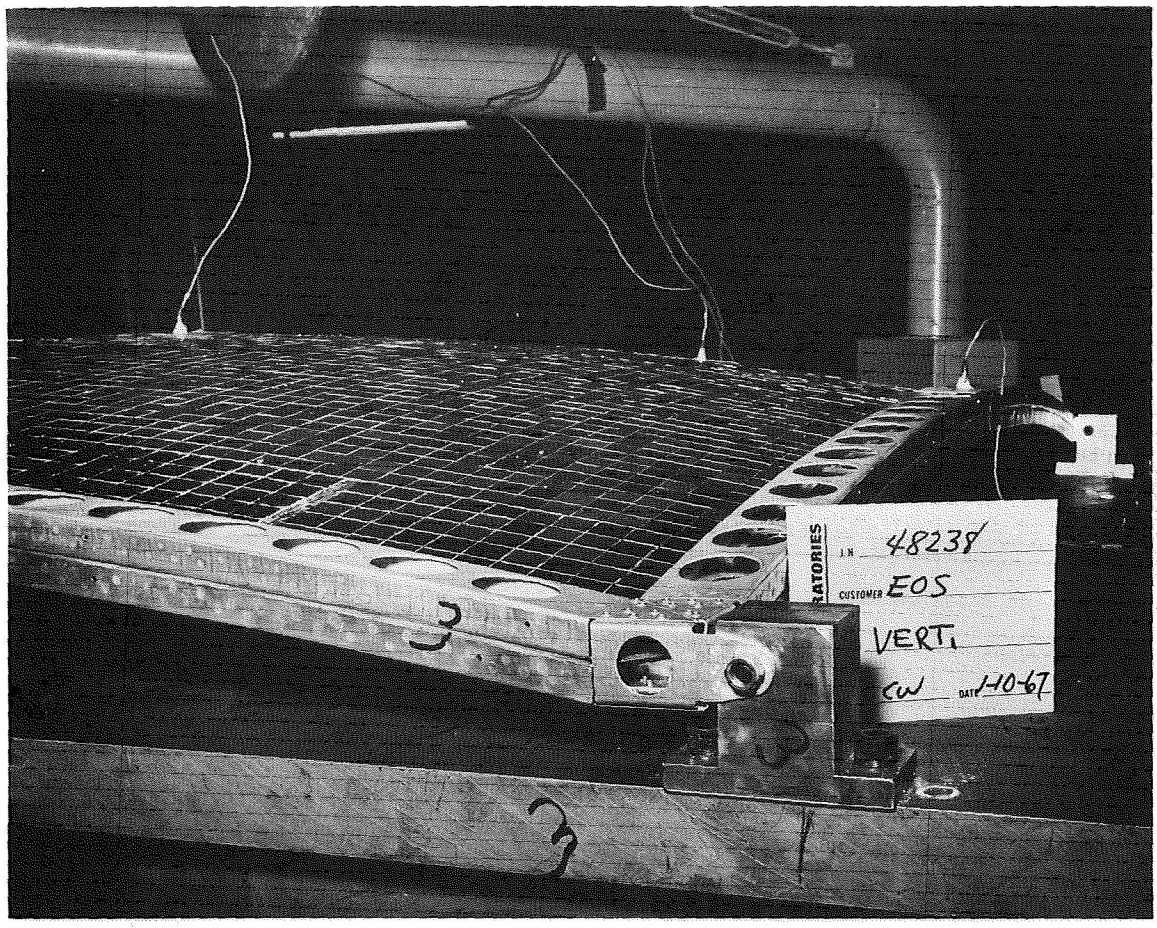

EC 16735

Figure 17. Accelerometer Location and Attachment of Demonstration Panel to Shake Fixture

EC-16733

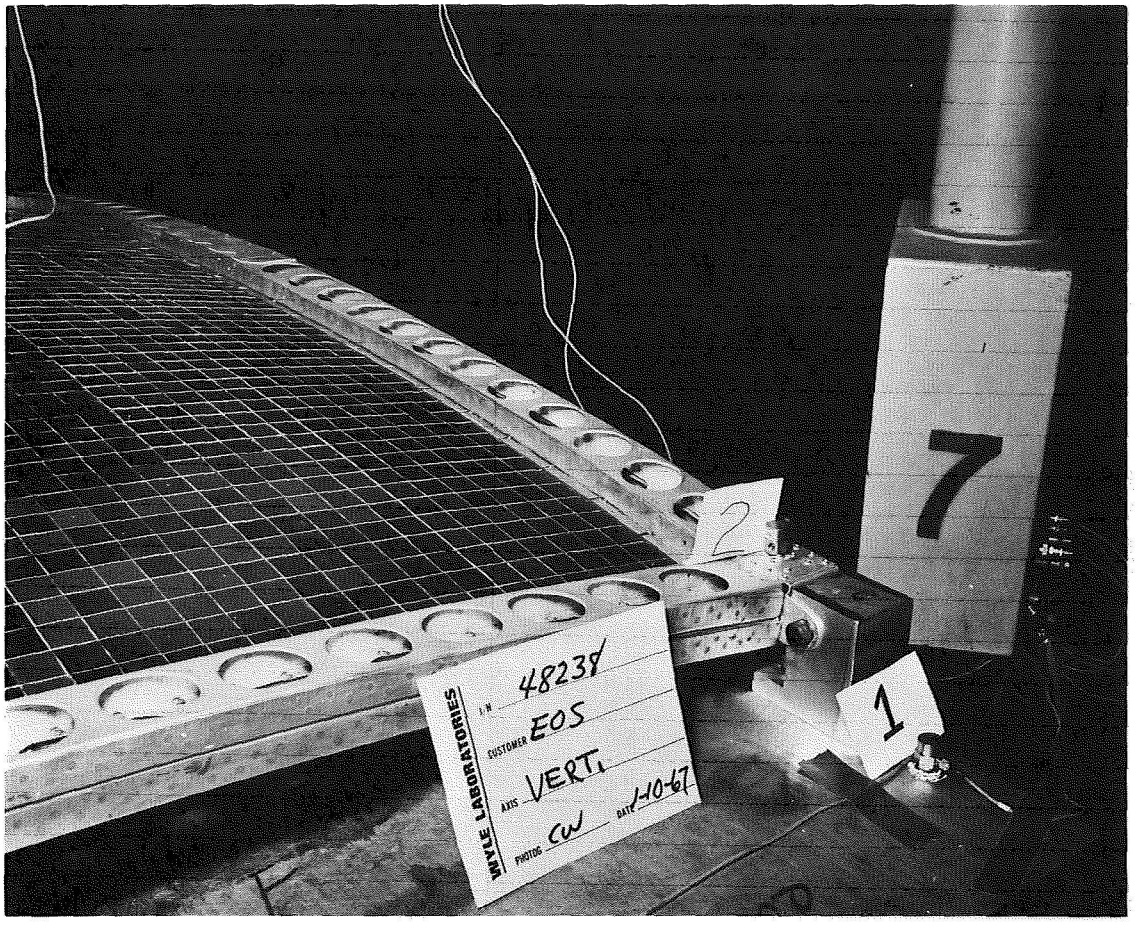

Figure 18. Location of Vibration Test Control Accelerometer (No. 1)

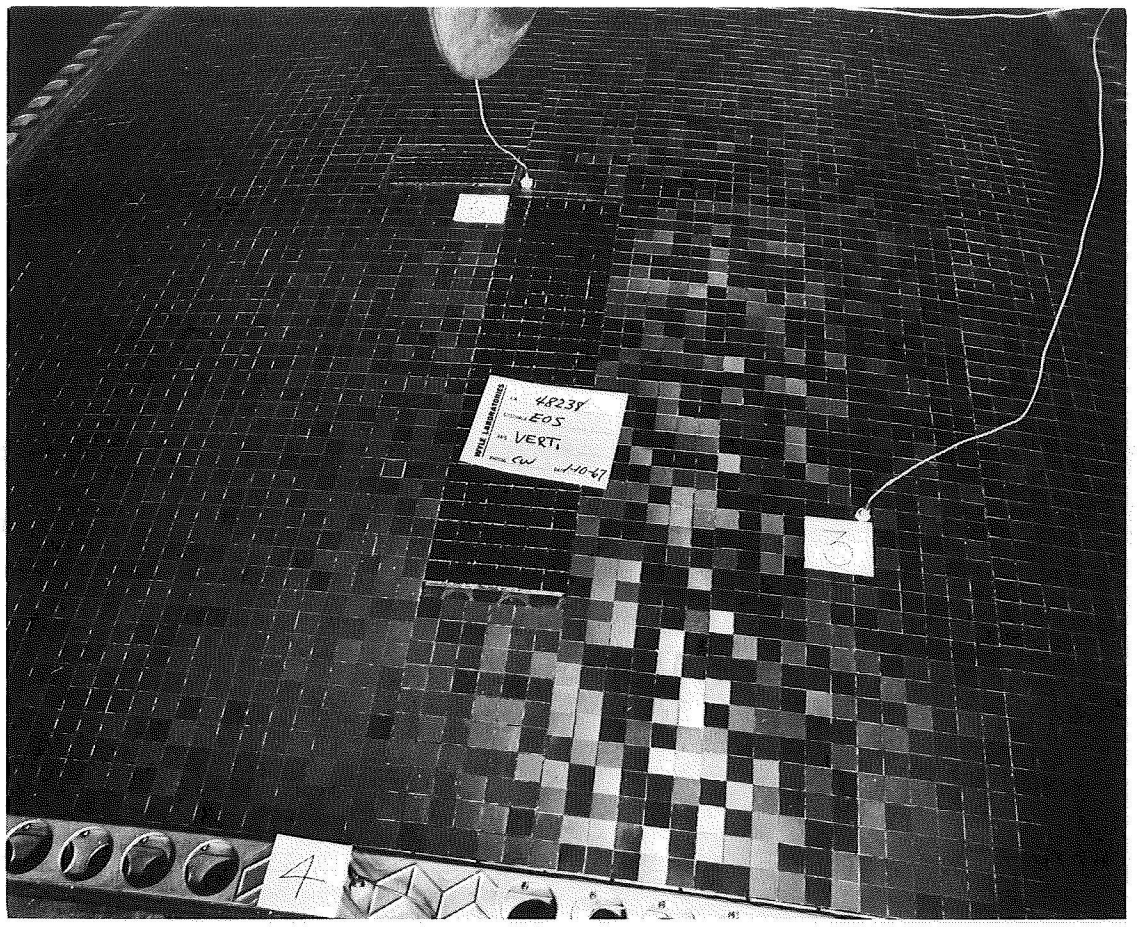

EC-16734

Figure 19. Placement of Accelerometers on Demonstration Panel Surface

Test Results

During the fixture evaluation tests it was discovered that the No. 1 Ling 249 shaker was resonating at 16 Hz with a gain of approximately 3. By controlling the servo system with a control accelerometer on the end of the fixture driven by the No. 1 shaker, the resonance could be controlled out. The effect of controlling this resonance was a lowered input at 16 Hz (by a factor of 3) from the No. 2 shaker. This resonance in the shaker did not affect the test results since the panel was responding as a rigid body at 16 Hz.

The only other significant resonance in the shaker-fixture system was at 105 Hz and had a gain of approximately 1.5.

The panel resonant frequencies and the gains at resonance are tabulated in Table II.

TABLE II

BICONVEX PANEL RESONANT FREQUENCIES AND GAINS

Frequency Hz	Gain g's/g	Remarks
26	38.5	The motion at this frequency was a combination frame and panel resonance.
46	38.6	Panel resonance. Frame rigid
56	48.5	Panel resonance
75	50.0	Panel resonance
100	67.0	Combination frame and panel resonance. This gain was adjusted to account for the fixture resonance at this frequency.
120	67.0	Combination frame and panel resonance
160	70.0	Panel resonance

DEVELOPMENT OF LIGHTWEIGHT SOLAR PANELS

By J. A. Carlson

Electro-Optical Systems

SUMMARY

This report summarizes the results of Phase I and Phase II of Contract NAS7-428, Development of Lightweight, Rigid Solar Panels. Electro-Optical Systems began work on Phase I in January 1966 under contract to NASA Headquarters, the Office of Solar and Chemical Power Systems of the Office of Advanced Research and Technology. Phase I was concluded in January 1967. The Phase II portion of the contract, which has been monitored through Langley Research Center, was started in July 1967. The fabrication and testing of the Phase II demonstration panels was completed in March 1969.

This report covers the work on Phase I which was not reported (Ref. 1). The specific areas of Phase I which are documented in this report are related to the fabrication, assembly, and testing of the demonstration panel. CR-75370 (Ref. 1) contains the design tradeoffs, optimization studies, and array and mechanisms designs which were completed during Phase I.

The results of the Phase II effort are also presented.

PHASE II SUMMARY

Task Descriptions

The Phase II development program was divided into four major tasks:

1. Task I - Design and analysis of a solar cell panel utilizing an aluminum hollowcore biconvex substrate and beryllium frame

2. Task II - Scaling up of aluminum electroforming process development reported in NASA CR-66427 (Ref. 2), and fabrication of aluminum hollowcore biconvex substrates

3. Task III - Fabrication of beryllium frame

4. Task IV - Assembly and test of Phase II demonstration panels.

The results of Task I, including descriptions of the resulting designs for the hardware to be fabricated and discussions of the criteria and methods used to define the configuration are presented in this part of the report. This section also contains a description of the electrical layout for the demonstration panel and thermal and dynamic analyses of the system.

The Task II subtasks including process parameter studies, design and construction of the large electroforming cell, and the electroforming of the substrates for the demonstration panels are described in this part of the report.

The Task III discussion covers the fabrication of the beryllium beams, magnesium hinge fittings, and aluminum attachment clips which constitute the frame hardware.

The assembly of the two Phase II demonstration panels is described, and the vibration, acoustic, thermal, and electrical tests, which are required to complete Task IV, are also reported.

Program Achievements

The weight breakdown for the two panels fabricated during Phase II is given in Tables III and IV. The projected weight of a fully celled panel using the technology developed during Phase II is given in Table V. The total weights are 6.054 pounds for S/N 1, 5.974 pounds for the partially celled panel S/N 2, and 5.137 pounds (projected) for a fully celled panel. The projected weight for the fully celled panel can be obtained by imposing controls in two areas of fabrication.

1. The specified wall thickness for the beryllium tube frame members was 0.010 ±0.002 inch. The manufacturer of the tube held the high side of the tolerance, giving a nominal wall thickness of 0.012 inch. The total weight of the beams can be reduced from 1.40 pound as used in the demonstration panels to 1.17 pound by specifing a tolerance of $0.010 \begin{smallmatrix} +0.000 \\ -0.004 \end{smallmatrix}$ inch on wall thickness. The design contains sufficient margin of safety to allow this change with no sacrifice in performance. The shift in the tolerance band will not cause difficulty in the fabrication process.

2. The skin thickness of the electroforming holowcore substrate specified for the demonstration panel is 0.004 inch. The substrate for S/N 1 was plated to this thickness but required repair of thin spots and holes which developed during mandrel removal in the nontemperature-control acid bath. The etching of S/N 1 took place at a time when the ambient temperature, and therefore the bath temperature, was extremely high causing accelerated attack on the aluminum. The repair of the substrate using aluminum-filled epoxy raised the weight to 1.84 pound. The substrate for S/N 2 was plated to the nominal thickness of 0.008

TABLE III

PHASE II DEMONSTRATION PANEL (S/N 1) - WEIGHT SUMMARY

Item	Description	Weight/unit	No. of units	Total weight in lb	Specific weight in lb/ft^2*
Structure					
Substrate	Aluminum hollowcore - 1.25 in. holes; 4 mil skin, Ecco bond repair	0.0775 lb/ft^2	23.72 ft^2	1.840	0.06734
Beams	Beryllium tube - 2.0 in. diameter 0.012 in. wall	0.3520	4	1.408	0.05153
Hinge fittings	Machined magnesium; 0.060 wall	0.1030	4	0.412	0.01508
Attachment clip	Aluminum extrusion	0.018 lb/ft	18.42 ft	0.328	0.01200
Dielectric film	Kapton H-film - 1 mil	0.0072 lb/ft^2	23.72 ft^2	0.171	0.00626
Adhesives:					
H-film to substrate	2 mil Narmco 3135-7111 (18% area)	0.0133 lb/ft^2	4.27 ft^2	0.057	0.00209
Substrate to clip	10 mil FM-123 OST	0.060 lb/ft^2	0.3 ft^2	0.018	0.00066
Clip to beam	10 mil Narmco 3135/7111	0.060 lb/ft^2	0.58 ft^2	0.035	0.00128
Beam to fitting	10 mil Narmco 3135/7111	0.060 lb/ft^2	0.087 ft^2	0.006	0.00022
Coverplate to fitting	10 mil Narmco 3135/7111	0.060 lb/ft^2	0.028 ft^2	0.002	0.00007
			Structure Subtotals	4.277	0.15613
Electrical					
Mass simulation of 4 mil cell, 1 mil integral coverglass, and 1 mil interconnection	5 mil, 2 cm x 2 cm aluminum platelet, 1145-H-19	0.138 grams	5040	1.533	0.05610
Adhesive:					
Cell mounting	2 mil RTV 511	0.0103 lb/ft^2	23.72 ft^2	0.244	0.00893
			Electrical Subtotals	1.777	0.06503
			Totals	6.054	0.22116

Assuming 10 W/ft^2 of active, projected cell area; power = 209.2W

Specific power = 34.56 W/lb

Weight-to-power ratio = 28.96 lb/kW

*Based on total planform area of panel - $A_{total} = 62.72 \times 62.72 = 27.32\ ft^2$

TABLE IV

PHASE II DEMONSTRATION PANEL (S/N 2) - WEIGHT SUMMARY

Item	Description	Weight/unit	No. of units	Total weight in lb	Specific weight in lb/ft^2*
Structure					
Substrate	Aluminum hollowcore - 1.25 in. holes; 8 mil skin	0.070 lb/ft^2	23.72 ft^2	1.672	0.06119
Beams	Beryllium tube - 2.0 in. diameter 0.012 in. wall	0.358	4	1.432	0.05241
Hinge fittings	Machined magnesium; 0.060 in./wall	0.103	4	0.412	0.01507
Attachment clip	Aluminum extrusion	0.015 lb/ft	18.42 ft	0.328	0.01200
Dielectric film	Kapton H-film - 1 mil	0.0072 lb/ft^2	23.72 ft^2	0.171	0.00625
Adhesives:					
H-film to substrate	2 mil Narmco 3135/7111 (18% area)	0.0118 lb/ft^2	4.27 ft^2	0.051	0.00186
Substrate to clip	10 mil FM-123 OST	0.060 lb/ft^2	0.23 ft^2	0.014	0.00051
Clip to beam	10 mil Narmco 3135/7111	0.060	0.3 ft^2	0.035	0.00128
Beam to fitting	10 mil Narmco 3135/7111	0.060	0.087 ft^2	0.006	0.00021
Cover plate to fitting	10 mil Narmco 3135/7111	0.060	0.028 ft^2	0.002	0.00007
			Structure Subtotals	4.123	0.15085
Electrical					
Solar cells	4 mil, 2 cm x 2 cm, n-p silicon	0.119 grams	210	0.055	0.00201
Interconnections	2 mil moly	0.168 grams	37	0.014	0.00051
Mass simulation	5 mil, 2 cm x 2 cm aluminum platelets	0.138 grams	4830	1.469	0.05376
Cabling	No. 22 AWG wire (spot bonded)	0.005 lb/ft	14	0.065	0.00237
Terminals	Copper on epoxy-glass board	0.003 lbs	1	0.003	0.00011
Adhesive:					
Cells mounting	2 mil TRV 511	0.0103 lb/ft^2	23.72	0.245	0.00896
			Electrical Subtotals	1.851	0.06772
			Totals	5.974	0.21857

Assuming 10 W/ft^2 of active, projected cell area, power = 209.2

Specific power = 35.02 W/lb

Weight-to-power ratio = 28.56 lb/kW

*Based on total planform area of panel - A_{total} = 62.72 x 62.72
= 27.32 ft^2

TABLE V

PROJECTED WEIGHT SUMMARY FOR FULLY CELLED PANEL USING PHASE II TECHNOLOGY

Item	Description	Weight/unit	No. of units	Total weight in lb	Specific weight in lb/ft^2
Structure					
Substrate	Aluminum hollowcore; 1.25 in. diameter holes, 4-mil skin	0.035 lb/ft^2	23.72 ft^2	0.830	0.03038
Beams	Beryllium tube; 2.0 in. diameter, 0.10 in. wall	0.293 lb	4	1.172	0.04289
Hinge fittings	Machined magnesium; 0.060 in. wall	0.103 lb	4	0.412	0.01508
Attachment clips	Aluminum extrusion	0.018 lb/ft	18.42 ft	0.328	0.01200
Dielectric film	Kapton-H-film; 1-mil	0.0072 lb/ft^2	23.72 ft^2	0.171	0.00626
Adhesives:					
H-Film to substrate	2 mil Narmco 3135/7111 (18% of area)	0.0133 lb/ft^2	4.27 ft^2	0.057	0.00209
Substrate to clip	10 mil FM-123 OST	0.060 lb/ft^2	0.30 ft^2	0.018	0.00066
Clip to beam	10 mil Narmco 3135/7111	0.060 lb/ft^2	0.58 ft^2	0.035	0.00128
Beam to fitting	10 mil Narmco 3135/7111	0.060 lb/ft^2	0.09 ft^2	0.006	0.00022
Coverplate to fitting	10 mil Narmco 3135/7111	0.060 lb/ft^2	0.03 ft^2	0.002	0.00007
			Structure Subtotals	3.031	0.11093
Electrical					
Solar cells	4 mil, 2 cm x 2 cm, n-p silicon	0.120 grams	5040	1.333	0.04879
Coverglass	1 mil, integral (spray-on)	0.022 grams	5040	0.243	0.00890
Interconnections	1 mil moly foil	0.084 grams	864	0.160	0.00585
Terminals	Copper on epoxy glass board	0.003 lb	2	0.006	0.00021
Diodes	Unitrode UR-220	0.215 grams	8	0.004	0.00014
Cabling	No. 22 AWG wire (spot bonded)	0.005 lb/ft	20 ft	0.100	0.00366
Adhesives:					
Cell mounting	2 mil, RTV 511	0.011 lb/ft^2	23.72 ft^2	0.260	0.00951
Coverglass mounting	None				
			Electrical Subtotals	2.106	0.07706
			Totals	5.137 lb	0.18800 lb/ft^2

Assuming 10 W/ft^2 of active, projected cell area; Power = 209.2W

Specific power = 40.7 W/lb

Weight-to-power ratio = 24.6 lb/kW

*Based on total planform area of panel - $A_{total} = 62.72 \times 62.72 = 27.32\ ft^2$

DESIGN AND ANALYSIS

Design Criteria

The Phase II demonstration panels were designed to withstand the following environments:

1. Vibration environment
   a. Three sweeps of sinusoidal vibration from 2 to 200 Hz at 1.0 octave/min with levels of 1.5 g-rms (2.12 g-0-peak) from 2 to 50 Hz and 2.0 g-rms (2.83 g-0-peak) from 50 to 200 Hz.
   b. Three minutes of gaussian vibration at 0.2 g^2/Hz, band limited between 200 Hz and 2000 Hz.

2. Thermal environment

   Exposure in an oven at 90°C until the panel temperature stabilizes.

3. Acoustic environment

   Atlas/Centaur acoustic spectrum; overall sound pressure level of 146 dB.

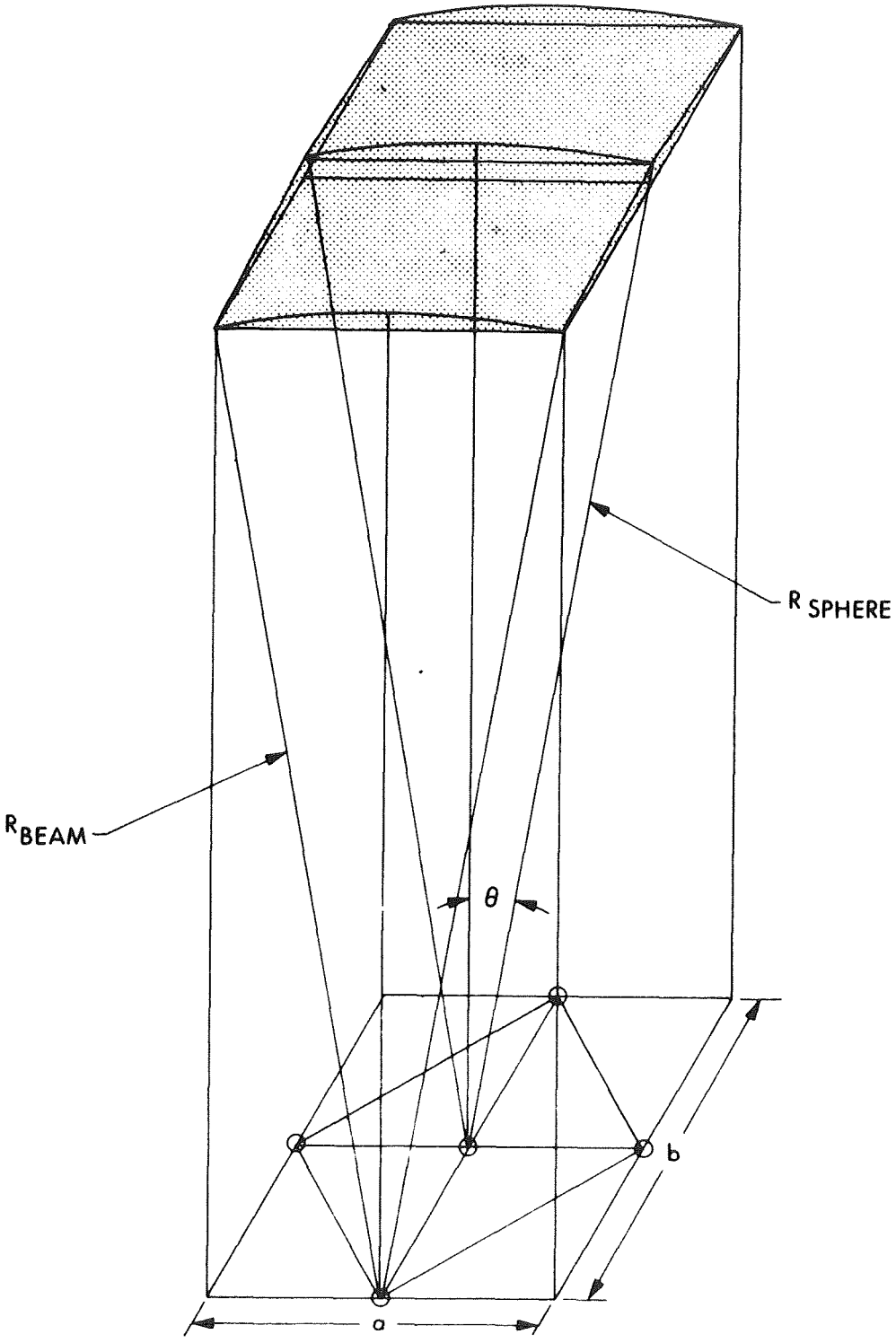

Figure 20. Geometry of Substrate

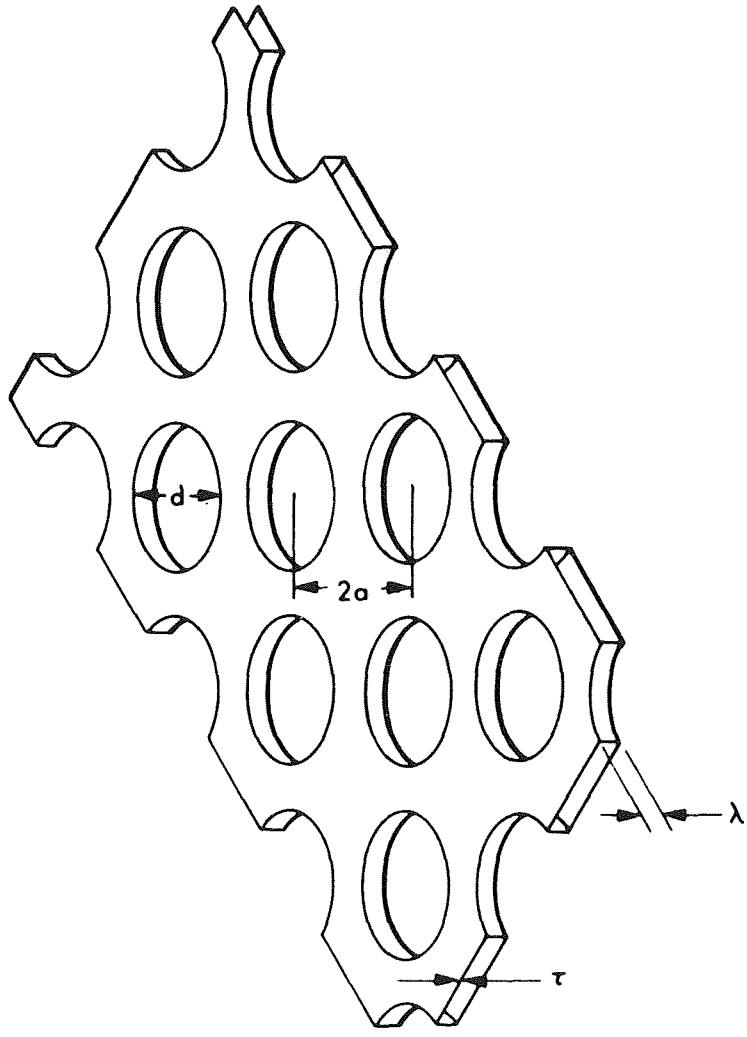

Figure 21. Hollowcore Substrate Section

(Fig. 1) to an arbitrarily chosen value of 10 degrees. The same radius was used in Phase II to allow use of Phase I tooling for the forming of the mandrel.

The planform dimensions specified were a = b = 58.13 inches. This area was chosen to accommodate the cell layout shown in Fig. 22. The square planform is used for the following reasons:

1. the area/perimeter is maximum
2. the four beams which support the substrate can be identical, which minimizes the tooling requirements for the beryllium forming operations.

The planform dimensions and spherical radius specified produce a substrate which has a projected area which is 98.9 percent of the surface area. The edges of the substrate are segments of small circles with a radius of 100.64 inches.

The material properties for the electroformed aluminum which were used in the design were:

yield strength	-	20,500 psi
ultimate strength	-	24,600 psi
modulus of elasticity	-	7.8×10^6 psi
elongation in 1 inch	-	10%
poisson's ratio	-	0.33

The steps of the procedure, which was used to establish the values of the remaining parameters (d, h, 2a, and t) which produce the optimum hollowcore configuration, are listed below. This procedure is based on the results of testing conducted in Phase I, which established that the allowable stress for the hollowcore design is determined by the crippling strength of the skin under compression loading.

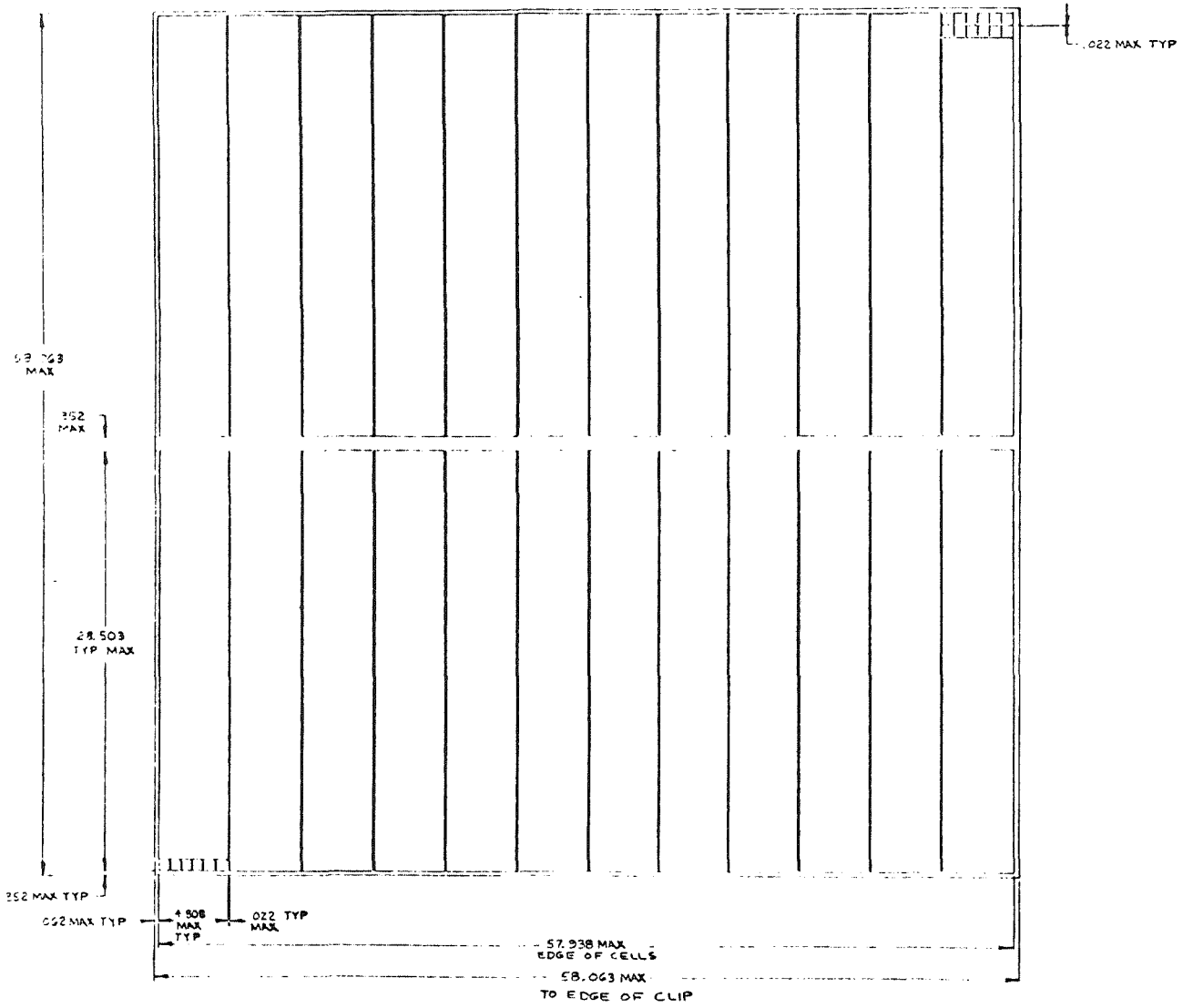

Figure 22. Cell Layout

1. Establish the limits on parameters which are dictated by fabrication considerations.

2. Determine the stiffness requirement for the substrate; i.e., determine the desired frequency range for the first resonance of the substrate.

3. Establish the critical external loading condition and applicable dynamic magnification factors.

4. Determine the dead load (solar cell stack) to be carried by the substrate.

5. Calculate the membrane forces for the critical external loading condition with dead load and structure weight applied.

6. Calculate the design limit stress produced by the membrane forces as a function of hollowcore geometry.

7. Apply a safety factor of 1.25 to the design limit stress to determine the ultimate stress.

8. Calculate allowable stress in the hollowcore skin as a function of geometry using theoretical buckling coefficients.

9. Superimpose the results from steps 6 and 8 to determine the hollowcore geometries for which the ultimate stress equals the allowable crippling stress.

10. Calculate the weight of each of the configurations which satisfy the conditions of step 9 to find the optimum configuration.

11. Check the resonant frequency of the substrate against the criteria established in step 2. Check the amplitude of input vibration at the panel of resonance to see that it agrees with the value used in step 5.

12. Check the overall buckling condition for the panel.

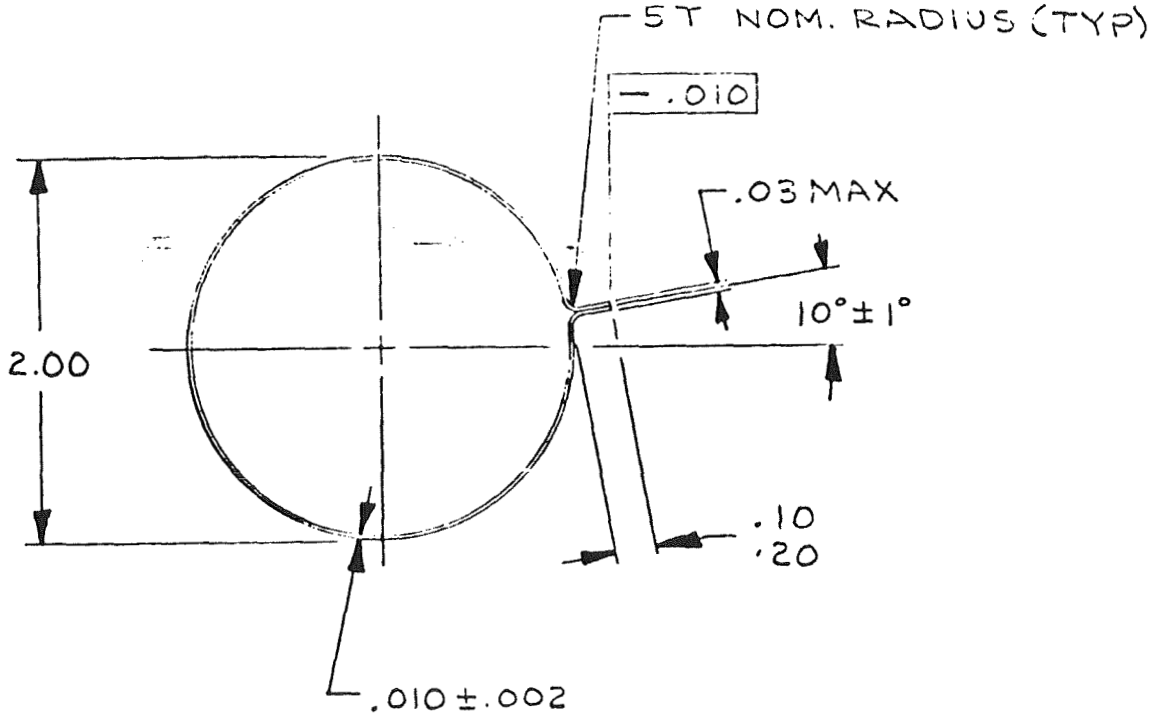

Figure 23. Beryllium Beam Cross Section

Hinge fitting design. - The design which was chosen for the fitting which is bonded to the beryllium beams in each corner is shown in Fig. 24. This fitting is essentially a hollow block with a hinge clevis on one side and two collet-like sleeves on an adjacent side to provide the bonding surfaces for the beams. The last operation in the frame assembly procedure is the bonding of the machined cover plate (Fig. 25) to close the open side of the box.

The one-piece machined fitting design was selected for this application to minimize the number of bonding operations or mechanical fasteners required to assemble the frame. This approach simplifies the assembly procedure and increases the structural reliability of the frame.

The wall thickness of the fitting has been made as thin as the machine operation will allow without the use of elaborate tooling. This restriction results in a part which is overdesigned for the loading conditions. In summary, the fitting is designed by fabrication, assembly, and functional requirements rather than stiffness or strength criteria.

The hinge fitting was machined from magnesium tooling plate, AZ31B, since this material is of low density and is easily machined. Dow 19 surface treatment was specified to provide corrosion protection.

Attachment clip design. - The attachment clip which is bonded to the edge of the hollowcore and to the flange of the beryllium beams is an aluminum extrusion. The cross section of the extrusion is shown in Fig. 26. The clip runs the full length of the edge of the hollowcore. The part of the clip which attaches to the beam is mill cut at 2-inch intervals to allow for the differential thermal expansion between beryllium and aluminum.

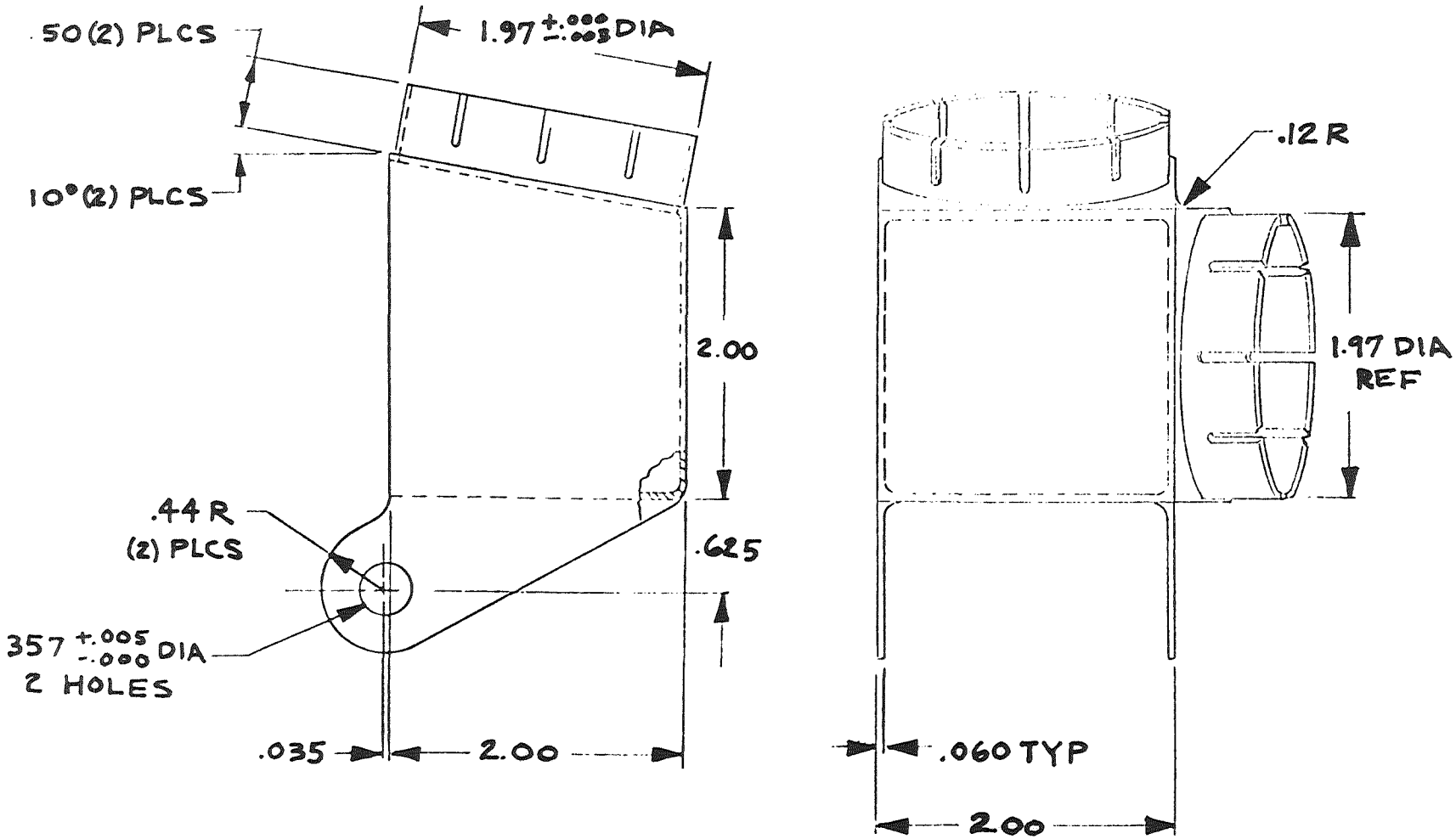

Figure 24. Magnesium Hinge Fitting

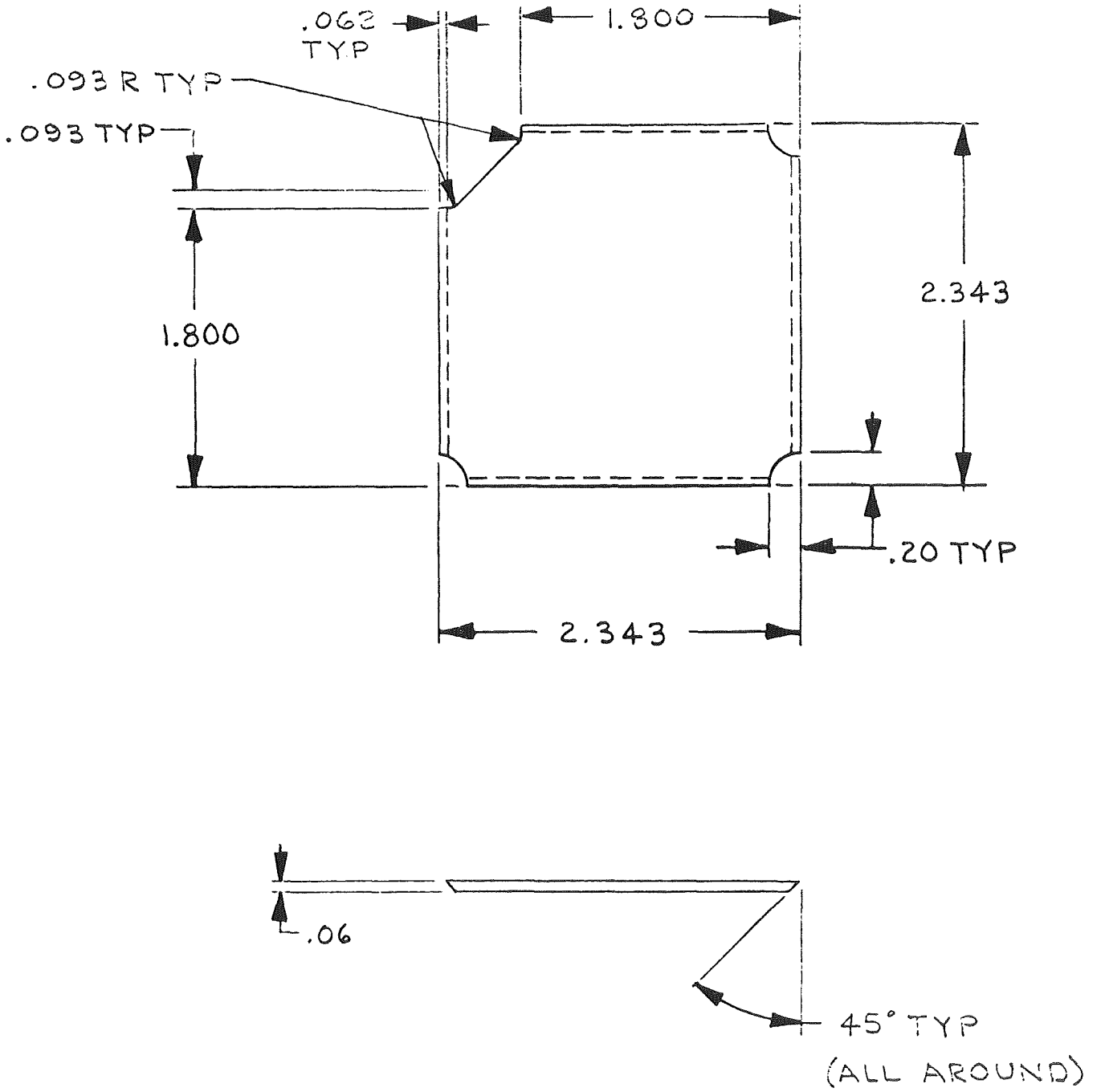

Figure 25. Hinge Fitting Cover Plate

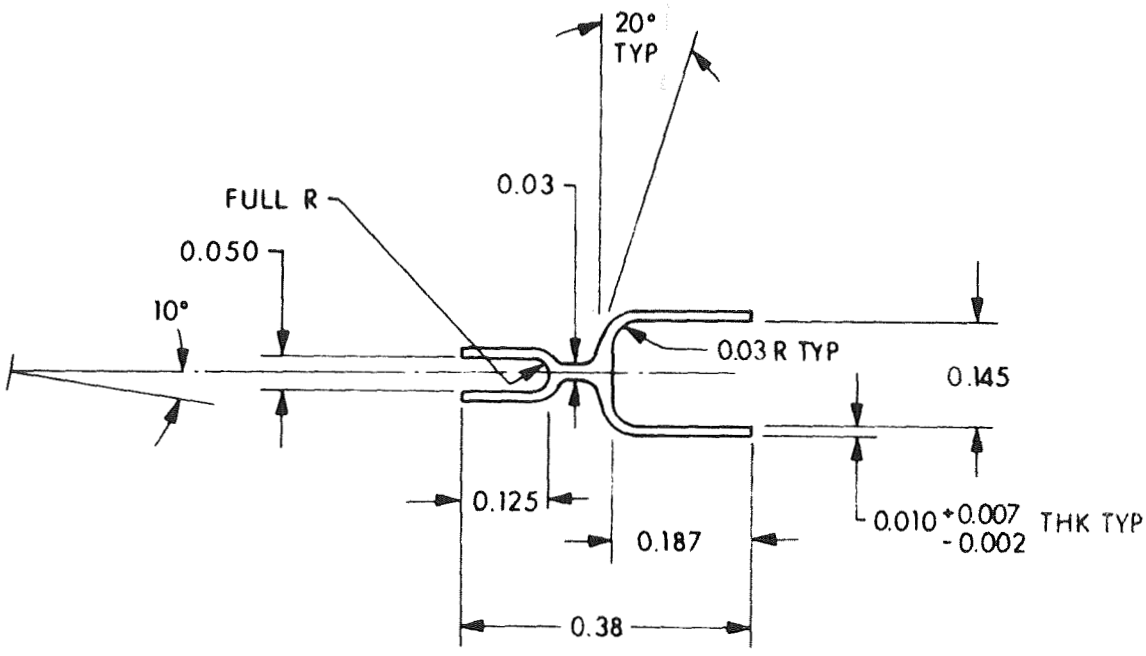

Figure 26. Aluminum Clip Extrusion Cross Section

The cross section of the extrusion is designed to provide sufficient bond area to ensure a positive attachment to the hollowcore and beam flange, and to provide a hinge joint between these attachments. The hinge joint eliminates bending moments and out-of-plane forces at the boundary which is necessary to justify the assumption of a membrane state of stress used in the analysis of the substrate.

Dielectric. - The dielectric material specified for use on the demonstration panels is 1 MIL Kapton H-film. This material was selected for its mechanical strength and stability and for its high dielectric strength.

Adhesives. - The solar panel structure has been designed to use structural adhesives for all fastening requirements. This approach was taken for the following reasons:

1. To achieve a uniform distribution of load into the hollowcore skin

2. To avoid the use of mechanical fasteners where joints are being made to the beryllium beams

3. To minimize weight.

The 0.004-inch skin on the hollowcore precludes the use of mechanical fasteners which produce high local stresses. The continuous adhesive joint along the edge of the substrate distributes the load from the hollowcore skin into the attachment clip by using a large surface area and minimizing the local stress.

Riveted and bolted joints can be made in beryllium structures if proper precautions are taken, but a more reliable design can be obtained by avoiding the potential problems of local cracking and spalling in the areas where fasteners bear on the brittle beryllium.

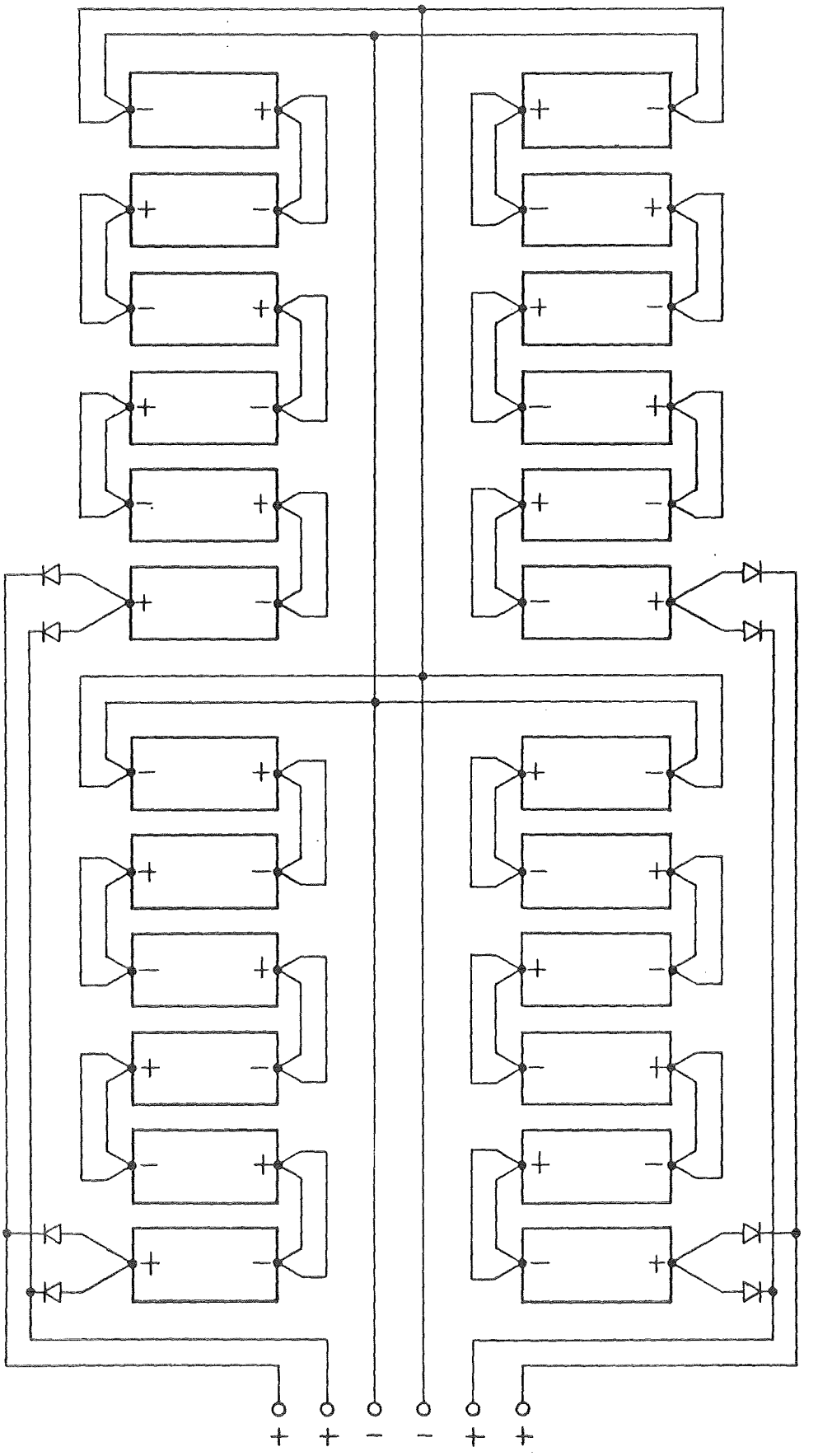

Figure 27. Wiring Diagram

ELECTROFORMING OF ALUMINUM HOLLOWCORE BICONVEX SUBSTRATE

Background of Electrodeposition of Aluminum

The first criterion in the electrodeposition of any metal from an electrolyte is that the metal deposition potential is lower than the decomposition potential of the electrolyte. If this is not the case, the solution will decompose prior to the deposition of the desired metal. To illustrate this, Table VI shows the half cell potential of various metals in acid solution. By convention, the deposition or evolution of hydrogen is taken at a zero reference point; therefore, in an aqueous electrolyte which has a free hydrogen ion, it is theoretically impossible to deposit any metal which requires a voltage greater than the hydrogen, as zinc or nickel, should not deposit from aqueous baths.

However, hydrogen deposition generally does not occur at its theoretical potential, and a hydrogen overvoltage exists which allows the deposit of metals up to approximately 0.8V above the hydrogen potential. In the deposition of such metals, the parallel processes of hydrogen evolution and metal deposition usually occur. Since the light metals (aluminum, magnesium, beryllium, and lithium) have potentials which are well above the hydrogen voltage, it is clearly impossible to deposit them from an aqueous solvent electrolyte. To solve this problem, two classes of electrolyte solvents (molten salt and organic solvents) which have decomposition potentials above the light metal potentials have been used. Molten salt electrolytes require high operating temperatures, and considerable difficulty can be expected in making any relatively large part. Therefore, the efforts at EOS have revolved around the use of organic solvents. In addition to the requirement that the solvent has a high decomposition potential, the electrolyte must contain dissolved salts of the metal to be deposited, must be reasonably conductive, and must enable deposition of an adherent, cohesive deposit.

Work conducted previously by Brenner and Conner at the National Bureau of Standards has demonstrated the ability to electrodeposit aluminum from a diethyl ether solvent, aluminum chloride salt, lithium aluminum hydride salt bath. Since then, several laboratories have duplicated and or have improved upon the NBS process.

The earlier attempts to electroform aluminum all resulted in a metal too soft to be useful. Under contract NAS-16218, EOS has successfully improved the aluminum plating bath to provide electrodeposited aluminum with physical characteristics 2-1/2 times harder than those from the NBS bath. Table VII gives the comparative physical properties of the two baths.

TABLE VII

PHYSICAL PROPERTIES OF ALUMINUM ELECTRODEPOSITS

	Standard ether bath	Mixed ether bath
Yield strength (psi)	8,200	21,400
Yield ultimate (psi)	10,400	25,700
Modulus of elasticity (psi x 10^6)	8	10
Hardness, knoop No.	32	71

Electroform Process

Aluminum electroforming may be described as "the production or reproduction of aluminum articles by electrodeposition upon a mandrel or mold that is subsequently separated from the deposit."

Electroforming is accomplished by placing the mandrel of the article to be formed in an electrolyte solution. Aluminum anodes are placed in the electrolyte in an arrangement that will produce the desired metal distribution over the mandrel. A direct current is passed

Laboratory study of process parameters. - The materials used in the aluminum plating solution must be originally anhydrous and, subsequently, be stored and be handled in a dry atmosphere that is free of oxygen and carbon dioxide.

Two laboratory units of aluminum electroforming assembly were set up to ascertain the process parameters. These units were to have the same essential features as the final 500-gal assembly, except that they were designed to prepare small hollowcore samples of 6 x 7 inches. Pictures showing the setup and the inside of the plating tank are given in Figs 28, 29, and 30.

The 8 x 9 x 11 inch-plate tank was constructed of 304 stainless steel. Both the tank and the removable top were coated with Kisite 100. This coating protected the tank from corrosion, which in turn reduced the level of contamination of the solution, and acted as an electrical insulator for better current distirubtion. The top had fittings for nitrogen gas and vacuum lines, and a vacuum pressure gage.

The plating tank had a sight glass to determine the level of solution. In each tank were two 3/8-inch-diameter tubes to fill and empty it and for circulation. The anodes and workpiece connections were transmitted through three spark plug-type, insulated feedthroughs.

The combination storage tanks and heat exchanger measured 9 inches in diameter by 16 inches high, and were constructed of 304 stainless steel. The storage tank had fittings for nitrogen gas and vacuum and a vacuum-pressure gage. There was approximately 20 feet of 3/8-inch-diameter stainless steel tubing coiled in the bottom 6 inches of the tank. This tubing performed as the heat exchanger. The tank had two 3/8-inch-diameter tube openings, one near the top and one at the bottom, for filling and circulation of solution.

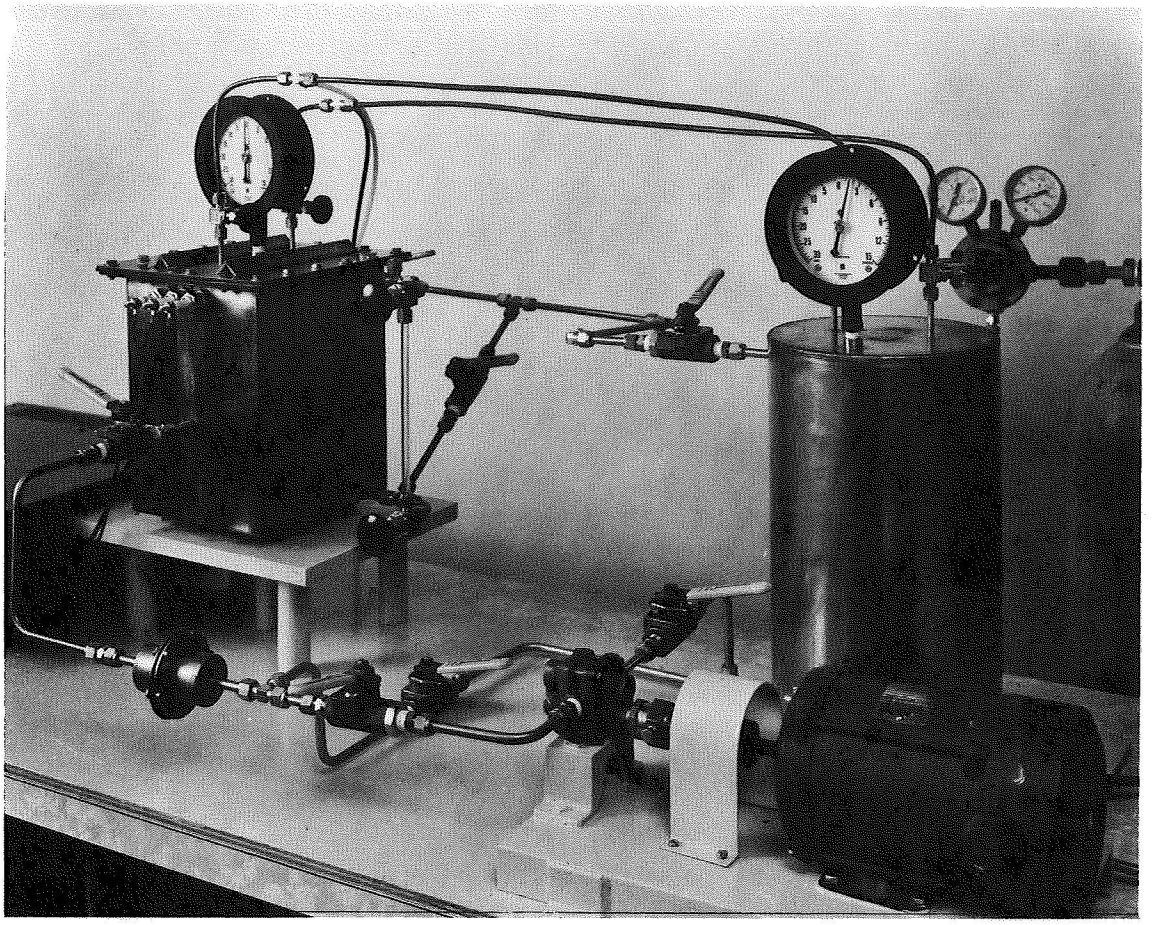

ES-96715

Figure 28. Closeup of Laboratory Electroforming Assembly

ES-96714

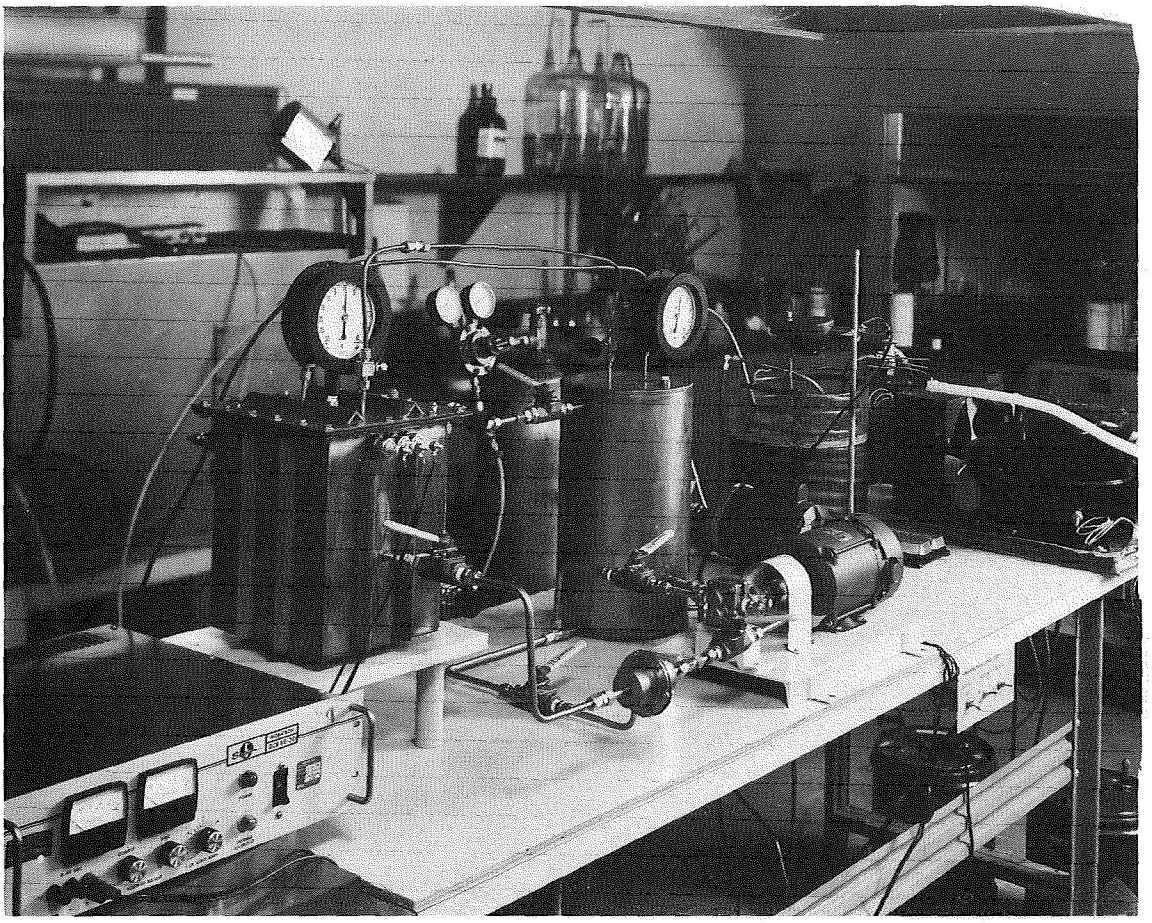

Figure 29. Complete View of Laboratory Electroforming Assembly

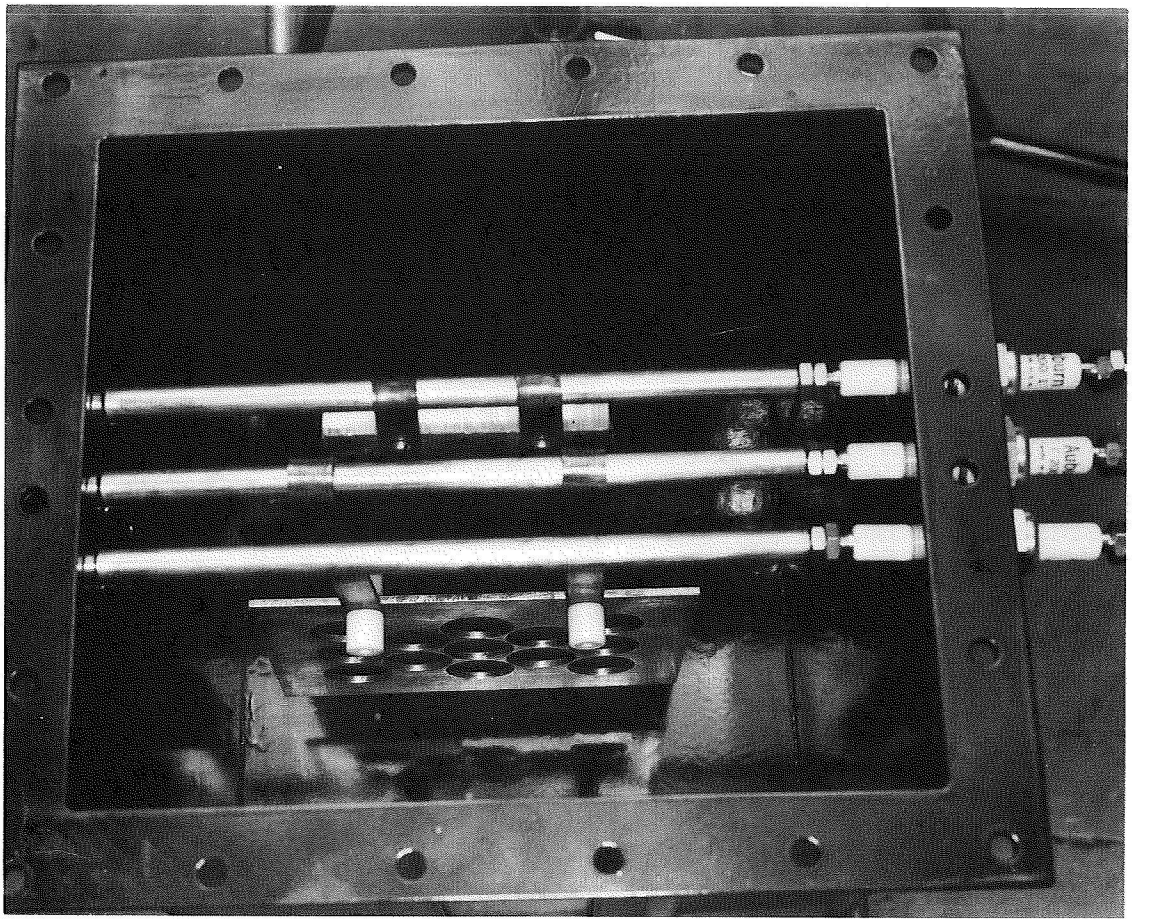

ES-96716

Figure 30. Inside of Plating Tank of Laboratory Electroforming Assembly

For a plating study operation, the solution was pumped from the bottom of the storage tank through the filter. The filter consists of a stainless steel housing with tetrafluoro ethylene gaskets containing the selected filter element. The electrodeposition process was started by applying power through the feed-throughs in the tanks. The organic plating solutions had comparatively high resistivities compared to aqueous plating baths, and substantial voltage drops were encountered in the plating because of this internal resistance. These IR losses result in considerable heat generation during the plating; it was therefore necessary to cool the electrolyte. This was accomplished by circulating the electrolyte through a cooling coil. It was found that due to the high I^2R heat generation, extremely high-rate plating was not practical beyond the operating currents of 10 to 30 A/sq ft. The corresponding voltage was 5 to 15V.

The results of the process parameter studies are described below.

Current distribution: Uniform thickness was the desirable feature in the hollowcore. A uniform current distribution over the surface must be attained to achieve uniform thickness. The geometry of the position of the anode and mandrel must be such that the distance between the two is constant. The uniform spacing was accomplished by placing one-inch tetrafluoroethyl spacers all along the four edges of the two electrodes. The one-inch spacing was chosen based on the tradeoff between the minimum IR drop distance and the minimum allowable distance. This avoids electrical shorting across the electrodes because of the possible formation of long fine trees growing from the mandrel. The edges of the mandrel are normally the high-current-density areas. Treeing, which is more profuse under high current density, increases the probability of electrical shorting. The method used very successfully in preventing this edge shorting was to entirely shield off the edge areas of the mandrel with TFE sheets.

temperature and current density. The bath temperature must be kept below the point where surface boiling occurs at the mandrel surface. The lower limit of the temperature is governed by unreasonable lowering of the conductivity and the crystallizing out of the aluminum chloride from its ethereal solution. When the bath temperature is maintained in the 15°C to 27°C range it is well within the upper and lower limits; at the same time, it causes no appreciable change in the electrodeposit. The lower limit of current density is governed by the occurrance of voids, and the upper limit is governed by the advancing of dendrite formation (trees) and voltage. When electrodeposition takes place at current densities of 10 to 25 amperes per square foot, voids are negligible, dendrite formation is limited to a tolerable level, and operating voltages are in a practical range.

Laboratory electroforming cell. - Laboratory scale electroforming cells were constructed and operated for two purposes. The first purpose was that these cells were to have the essential features of the 500-gal cell so that operation data could be gathered to determine the scale-up factors in finalizing the optimum design of the large cell. The second purpose of these cells was to electroform flat samples (6 to 7 inches) to verify the values for modulus of elasticity, yield strength and ultimate strength which were used in the design and analysis of the hollowcore substrate. These cells were also used to electroform small hollowcore samples which were used to determine the buckling and crippling characteristics of hollowcore panels. Figures 28 and 29 show the laboratory cell assembly and Fig. 30 shows the inside of the plating tank.

Description of the laboratory plating cell. - The 8 x 9 x 11-inch plating tank was constructed of 304 stainless steel. Both the tank and the removable top were coated with baked phenolic coating. This coating protected the tank from corrosion, which in turn reduced the contamination

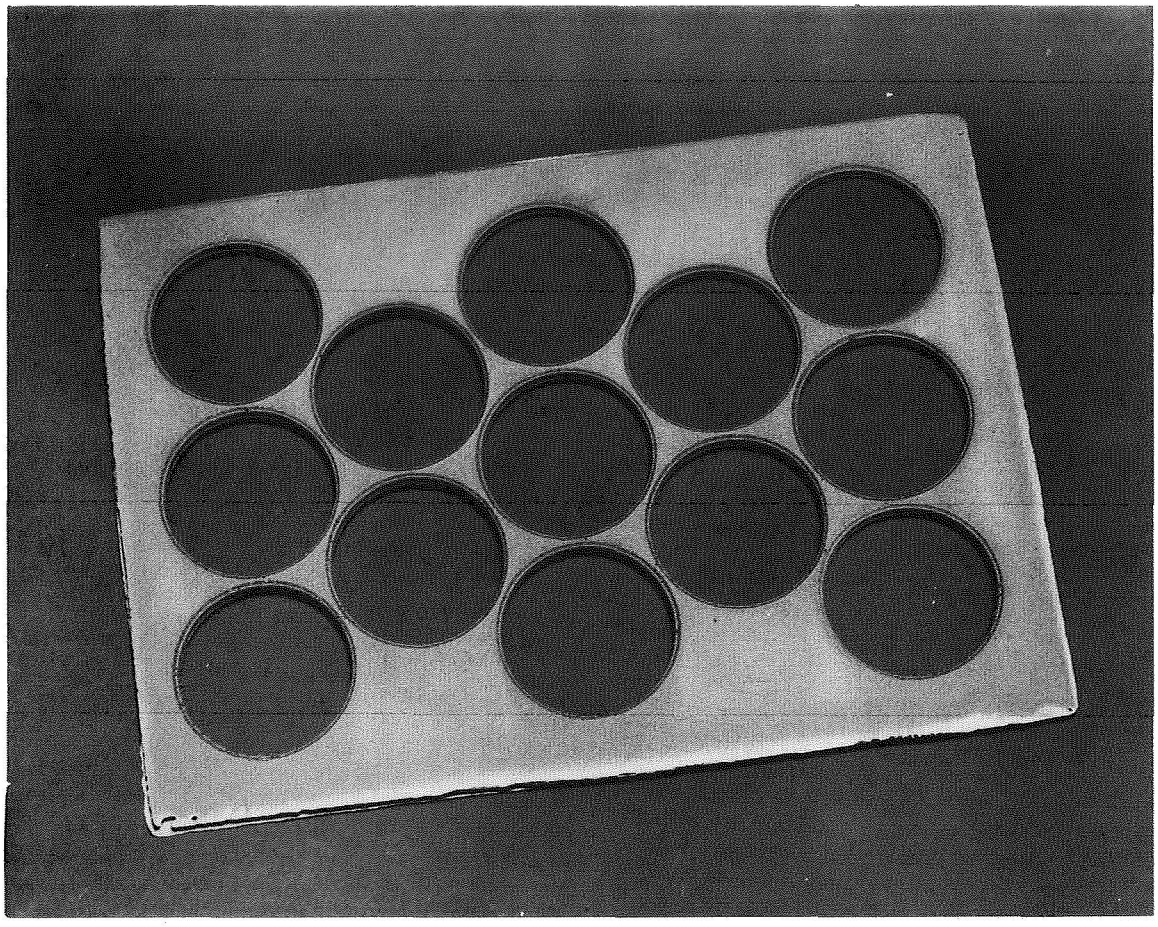

ES-116718

Figure 31. Aluminum Electroformed Hollowcore Sample

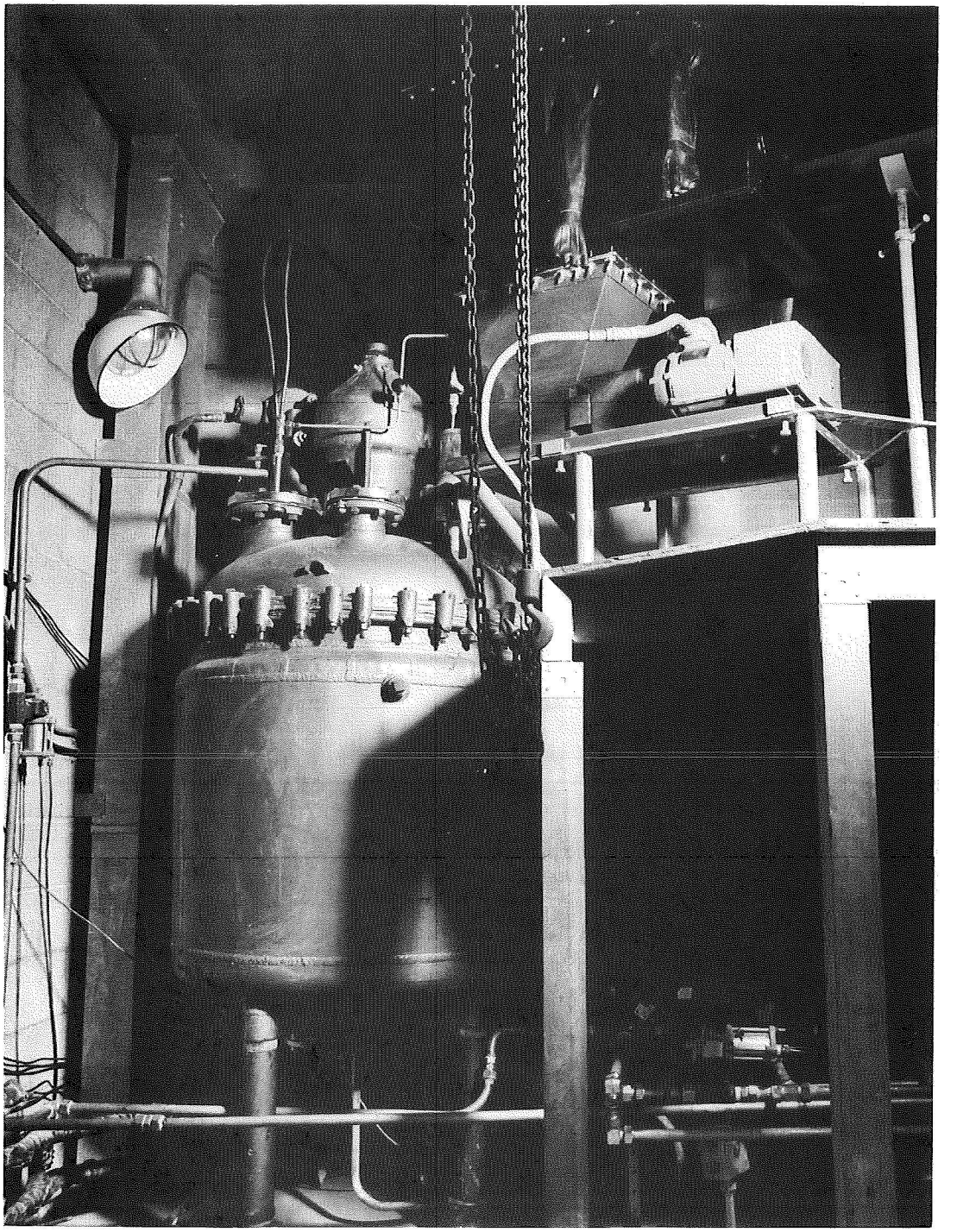

ES-468183

Figure 32. Inside View of Blockhouse Showing Electrolyte Mixing Tank

auger capable of delivering controlled amounts of aluminum chloride, 0.5 ft^3 per hour, into a mixing tank. The mixing tank was a glass-lined steel-jacketed tank with a maximum capacity of 200 gal. Mixing was promoted through an agitator rotating at a speed between 60 and 180 rpm. Heat generated from the solution was removed by the circulation of coolant through the cooling jacket. A five-ton refrigeration unit was used to meet the cooling requirement. After preparation, the electrolyte was stored in an underground tank with a 600-gal capacity.

The electroforming was performed in a plating tank which had an inside dimension of 6 x 1.5 x 6 ft high. Direct current was furnished by a power supply capable of delivering 300A at 30V. Cooling was effected by the continuous circulation of electrolyte through a tubular heat exchanger.

Transportation and circulation of electrolyte among various equipment was effected through the use of sealless pumps to avoid leakage and possible contamination. Micro-porous candle-type polypropylene filters were employed to remove particles suspended in electrolyte. A variable area flow meter was installed in-line for monitoring electrolyte flow rate. All valves in the electrolyte pipe line were pneumatically operated. Temperatures of the electrolyte at the inside of the mixing tank (at the inlets and outlets of the heat exchanger) and the plating tank were monitored by means of remotely read thermometers. Pressures in the mixing tank, plating tank, and storage tank were detected through pressure gages. A dry air pump with a capacity of 15 cfm at 5 in. Hg was provided for all evacuation operations. Dry nitrogen was fed to the system by nitrogen storage tanks. All operations were controlled at a remotely installed panel with the following features (see Fig. 33):

ES-468184

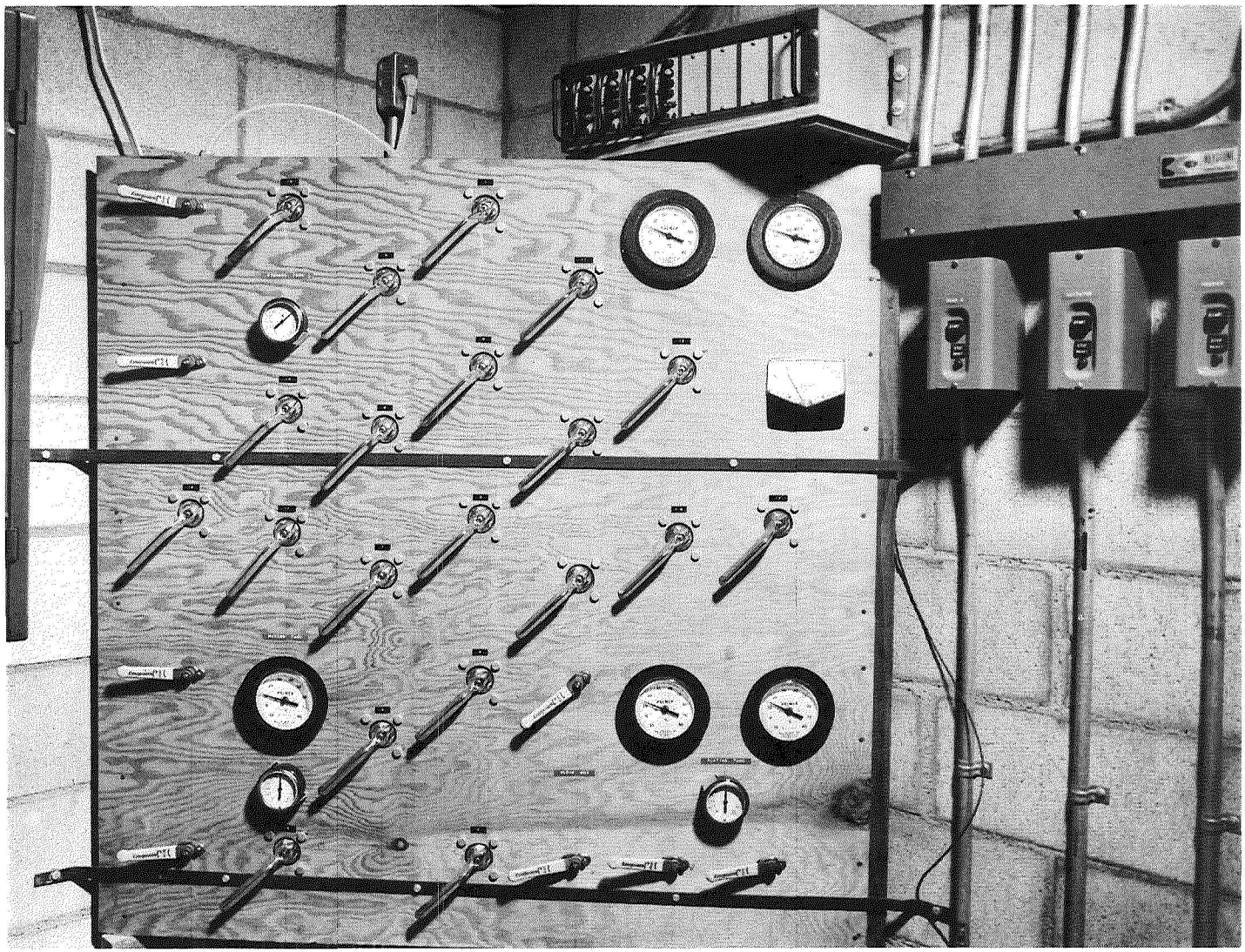

Figure 33. Electroforming Cell Remote Control Panel

Electrolyte flow diagrams

Controls for all pneumatically operated valves

Controls for vacuum valves

Controls for nitrogen valves

Switches for dry air pump, compressor, and circulation pumps

Flow rate indicator

Pressure gages

Temperature gages

A description of major equipment is given in Table VIII. The entire aluminum hollowcore facility is shown in Fig. 34.

Preparation of the aluminum plating solution. - For design, the heat of solution of aluminum chloride in water (580 cal/gram) was used as an approximation for the heat of solution of aluminum chloride in ether. However, the actual heat of solution was somewhat smaller allows mixing of the aluminum chloride at three times the designed cooling capacity. After the aluminum chloride was added to the ether, an ethereal solution of $LiAlH_4$ was added to it. The initial adding of lithium aluminum hydride was done very slowly to avoid voluminous gassing. The evolved gas was evacuated to prevent a pressure buildup in the mixing tank. The heat of solution of lithium aluminum hydride, when added into the aluminum chloride-ether solution, was fairly low and no cooling was required. The lithium aluminum hydride addition formed some precipitate. The precipitate, when suppressed in the solution, was separated out by circulation through the filter. The preparation of 500 gal of aluminum plating solution, which included the addition of aluminum chloride and lithium aluminum hydride, required 7 working days.

Mandrel and anode cleaning and assembly. - The copper mandrel must be thoroughly cleaned, otherwise, premature peeling and/or blistering of the aluminum deposit could result. The copper mandrel was wiped

ES-468182

Figure 34. View of Blockhouse Facility

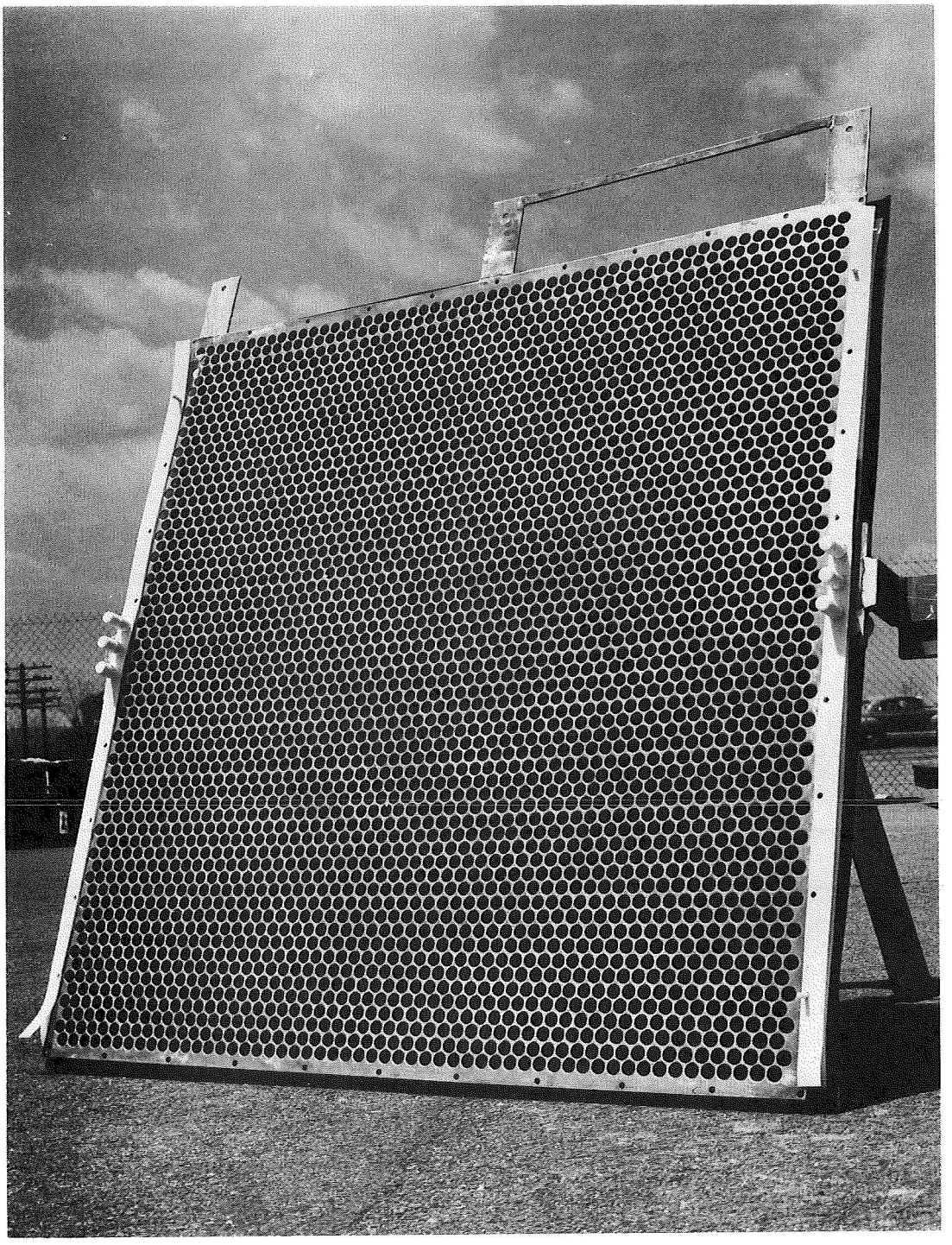

ES-468185

Figure 35. Anodes-Mandrel Package for Trial Flat Plate With Front Anode Removed

TABLE IX - Concluded

SUMMARY OF 5 FT X 5 FT ALUMINUM ELECTROFORMING RUNS

Plating No.	Type of mandrel	Plating conditions			Results and remarks	Etching conditions and remarks
		Current density A/ft^2	Bath temp. ^oC	Circula. rate/gpm		
5	Machined curved copper mandrel.	12	20	6	(a) Good Al deposit. (b) Condition (b) above was not completely corrected. Holders were coated with Kesite.	(a) Portion of hollowcore etched out in conc. HNO_3 (appr. 65%) at ambient temp. (b) Etching time, 14 days. (c) Edges and area covered by flakes of Al were attached by HNO_3 and appear as holes.
6	Machined curved copper mandrel	14	20	6	(a) Good Al deposit. (b) $LiAlH_4$ added to increase its conc. by 0.10M before electroforming.	(a) Portion of hollowcore etched out in conc. HNO_3 (appr. 65%) at ambient temp. (b) 0.050 holes were provided in every junction to facilitate acid in reaching the copper mandrel. (c) Etching time, 14 days. (d) Edges were slightly attacked by HNO_3 and appear as holes.

005020

Figure 36. Glassrock Radius Die (Being Fabricated in Model Shop)

005075

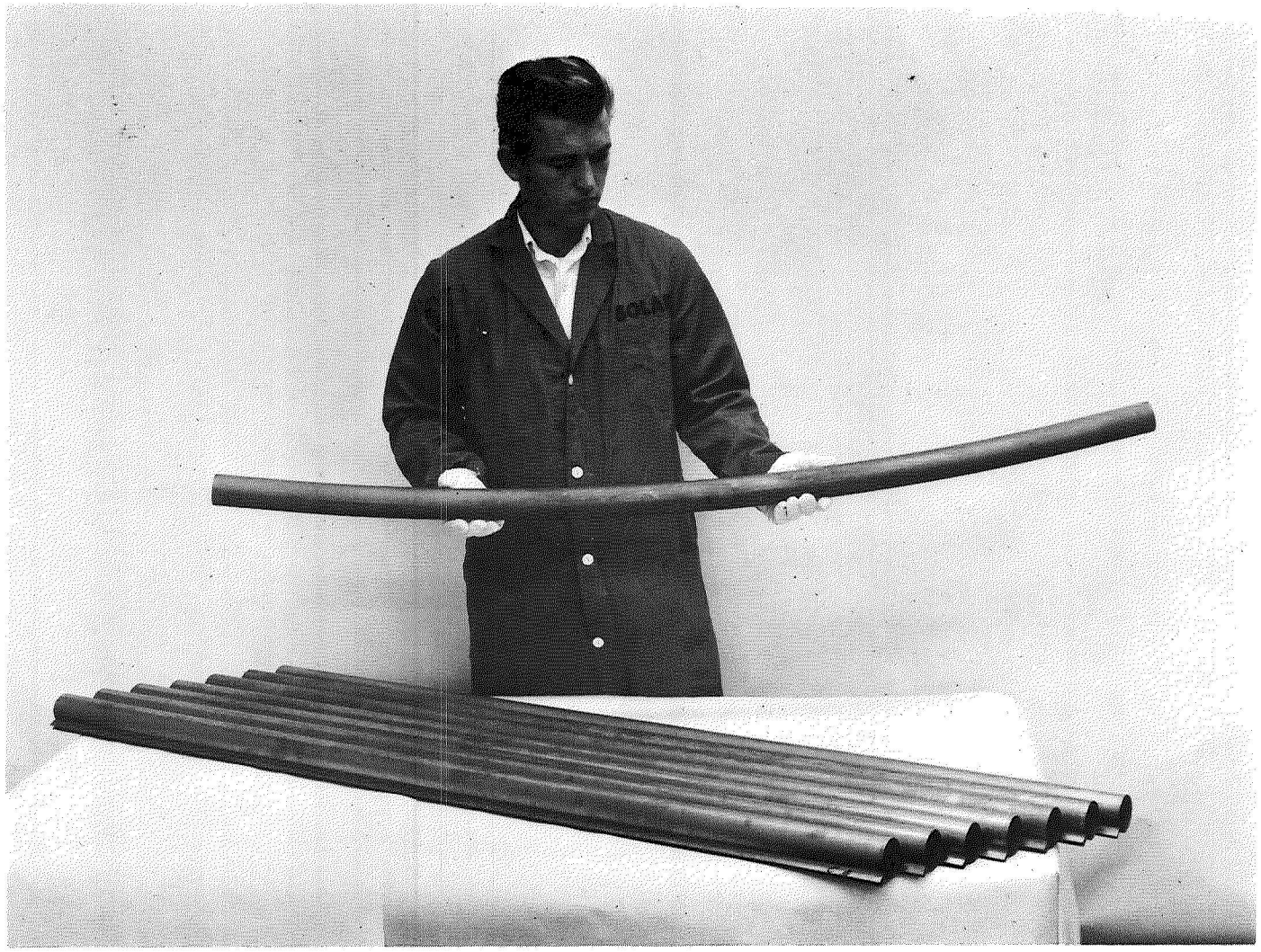

Figure 37. As-Formed Be Tubes

ENGINEERING REPORT

NO. S/N 1

SUBJECT: E.O.S. CRS Be TUBE 2" OD x 60" x .010" WALL

DATE 2/15/68

PAGE 1 OF 1 PAGES

BY: SHEARER / KAMPER

JOB NO. S.O. 6-2923-0

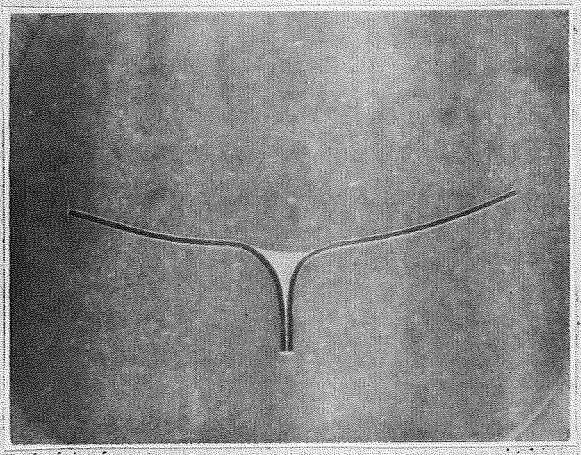

FLANGE SEAM JOINT - 3X

MATERIALS:

FILLER: AWS BAlSi-4

Be: CRS (SR-200 / PR-20)

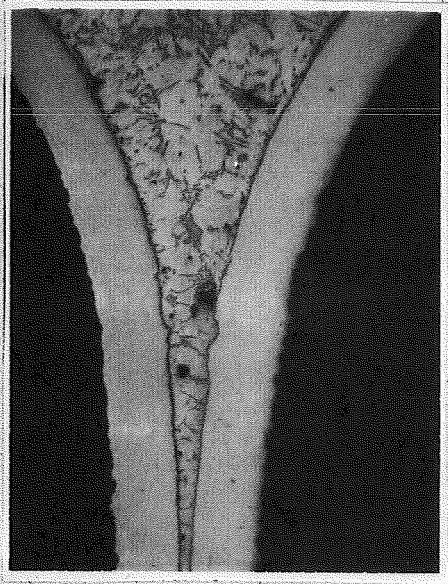

FLANGE SEAM JOINT - 30X

INTERFACE 175X

005076

Figure 38. Photomicrographs of Brazed Joint

005068

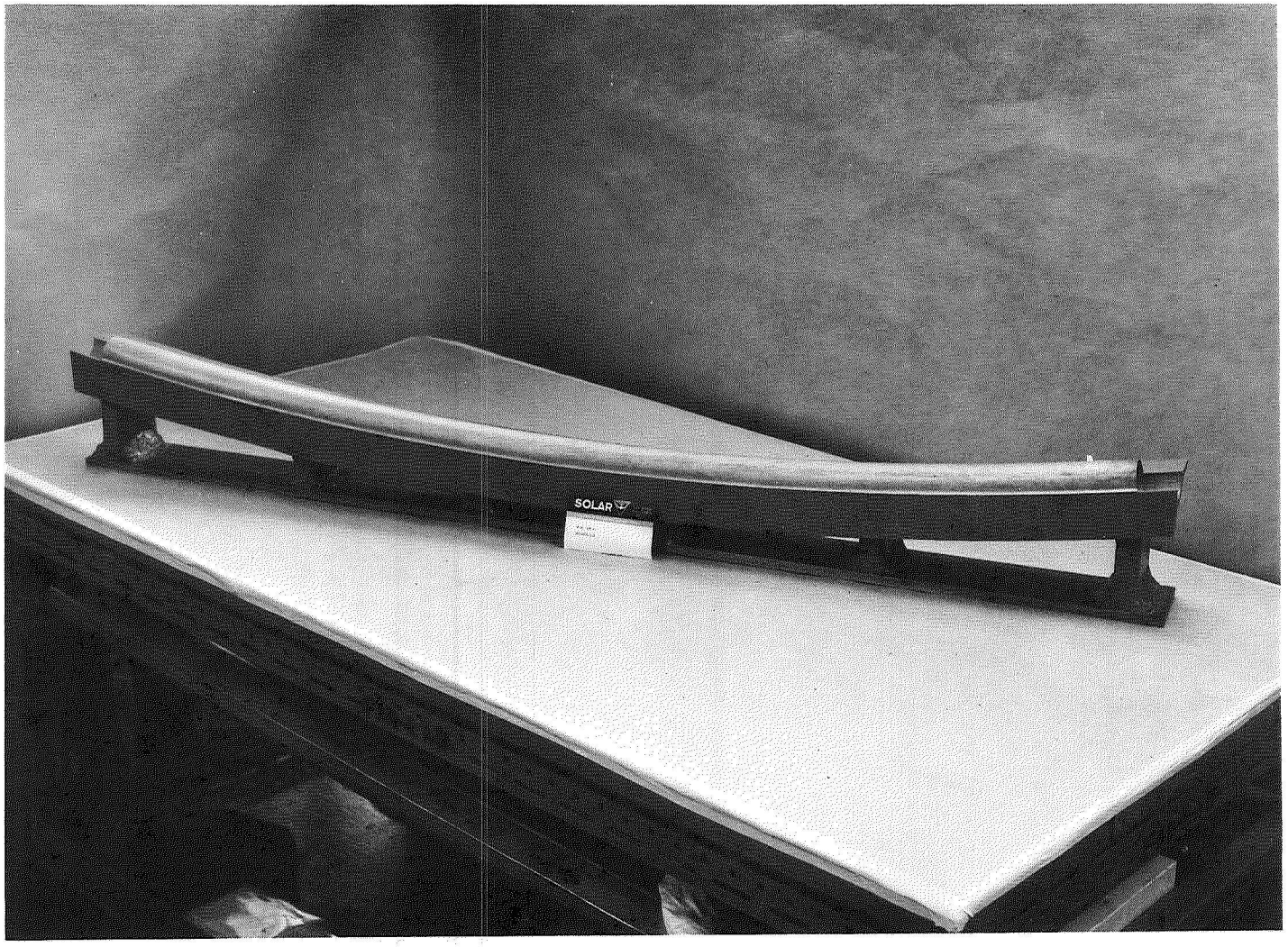

Figure 39. Completed Be Tube on Inspection Fixture

005077

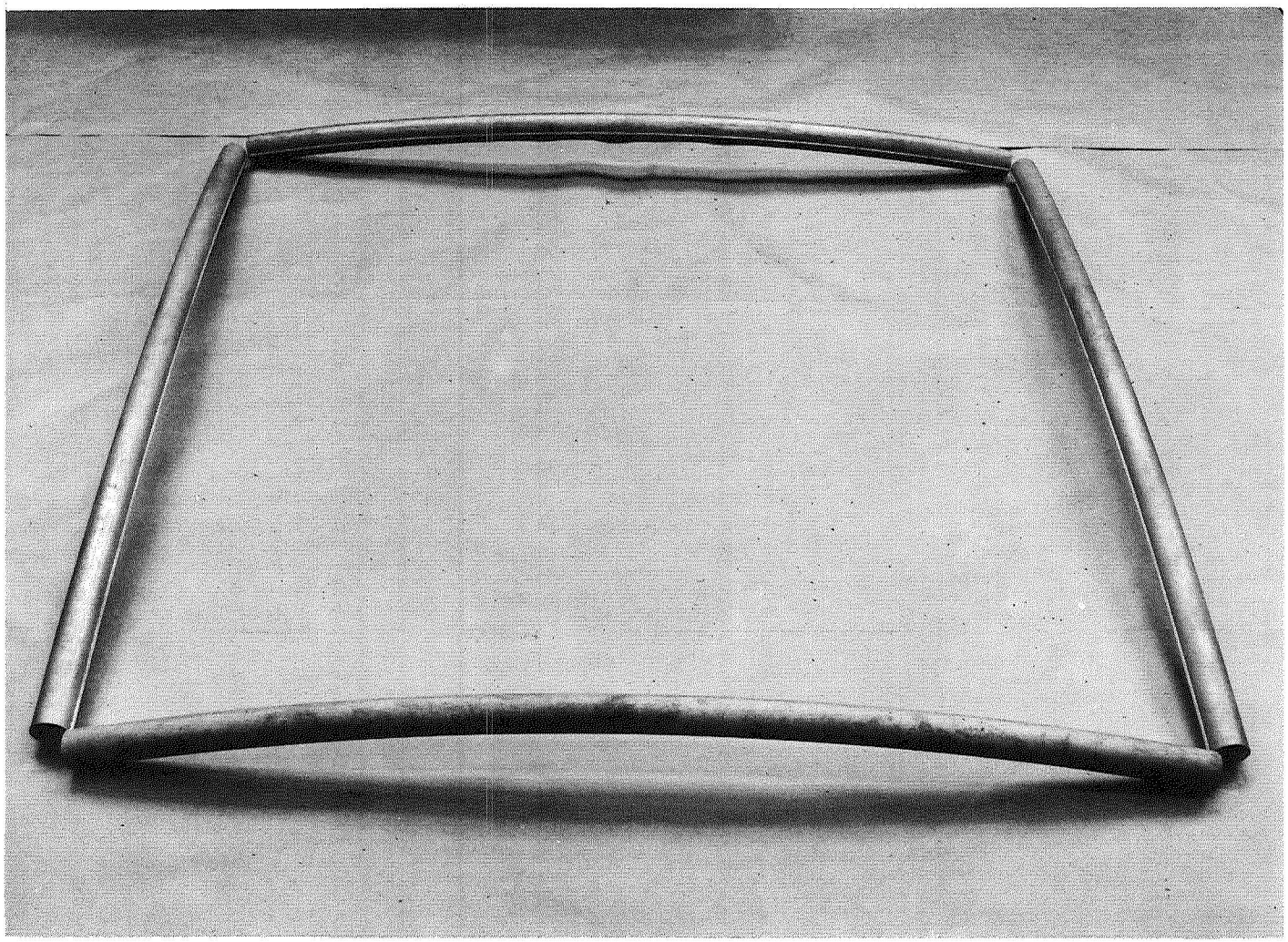

Figure 40. Completed Ship-Set of Four Be Tubes

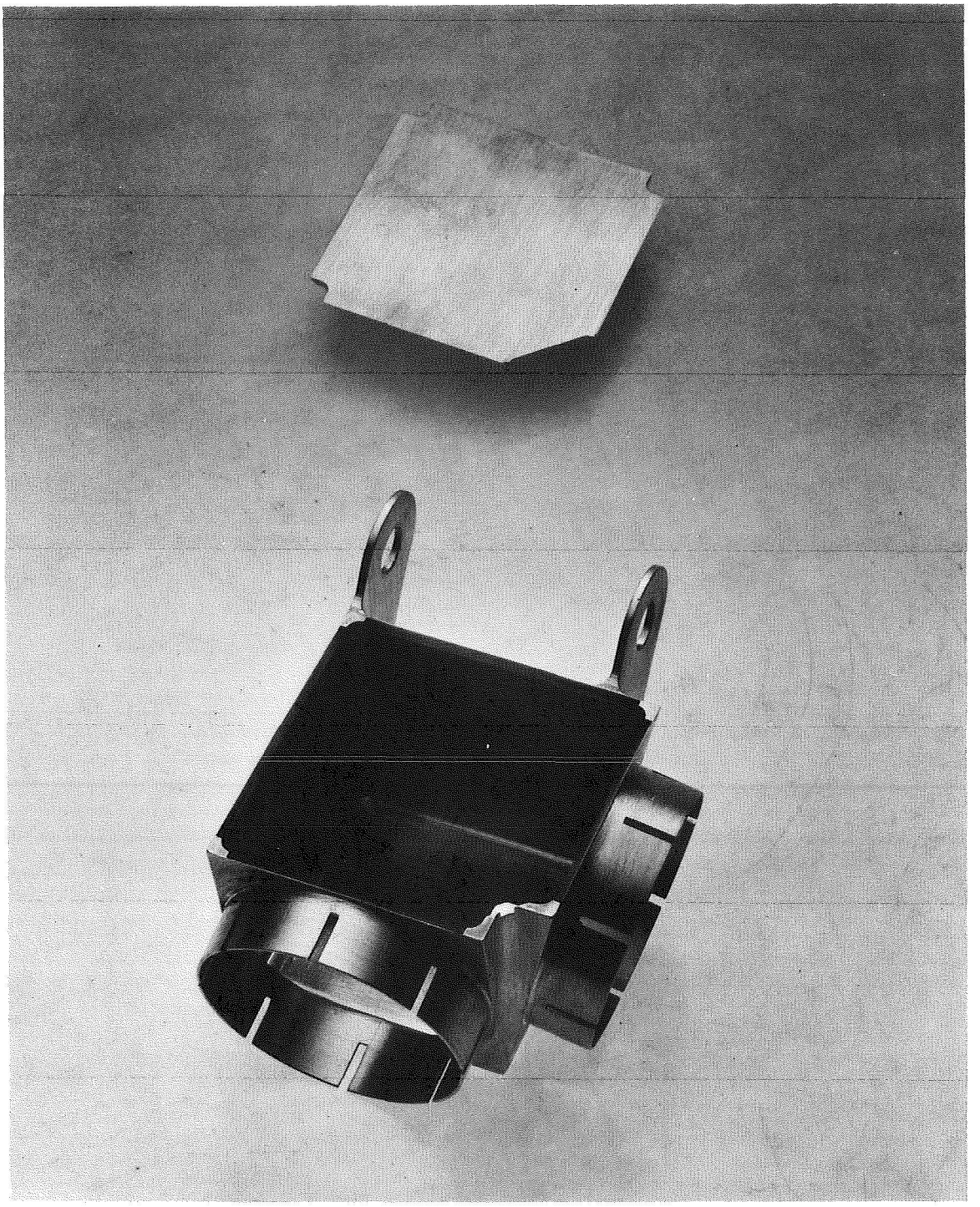

SP16876

Figure 41. Machined Magnesium Hinge Fitting

Assembly procedure. - Following are the steps in the assembly of the solar panel structure:

Step 1 - Trim the substrate to size. Place the hollowcore substrate on the concave mold, weight in position with shot bags, and grind to the exact planform dimensions using a high-speed sanding wheel with the mold edge providing the template.

Step 2 - Install the attachment clips. Clean the edges of the hollowcore with MEK, tack and trim EM-123 OST film adhesive to cover the faying surfaces. Force the clips in position along the edges and place on the convex mold, locating the clips in the grooves. Clamp the clips to the mold and cure at 250°F for one hour.

Step 3 - Apply the H-film dielectric. Clean the hollowcore convex side with MEK, mix Narmco 3135/7111 and thin with toulene. Roll adhesive on the surface with a rubber ink brayer and cut 6-inch-wide strips of H-film. Apply adhesive to the half-inch-wide overlap strip, stretch the H-film gores over the surface and hold tension. Cure at room temperature for 24 hours and then trim off excess H-film.

Step 4 - Install the frame. Inject thinned Narmco 3135/7111 in the grooves on the attachment clips using syringe. Locate and weight the substrate in place on the concave mold. Position the two beams on opposite sides of the substrate, working the flange of the beam into the groove of the clip, extruding out adhesive. Hold the beams in place with the support brackets. Apply adhesive to the collett sleeves of the hinge fittings, and insert in the ends of the two remaining beams forming dumbell-like subassemblies. Install the subassemblies by working the sleeves into the beams previously located, and the flange into the groove of the clip simultaneously. Clamp the beams in place, apply the adhesive to the hinge fitting cover plate faying surfaces,

TESTING OF THE PHASE II DEMONSTRATION PANELS

The two Phase II demonstration panels, S/N 1 and S/N 2, were subjected to tests to verify the ability of the solar panel structure to withstand the vibration, acoustic and thermal environments specified in the design criteria portion of this report. Electrical performance tests in sunlight were conducted on the partially celled panel, S/N 2, before and after the environmental testing. No electrical or structural degradation was produced by the environments. The testing procedures and results are detailed below. The environmental tests were performed in the following sequence: (1) thermal, (2) acoustics, (3) vibration. This sequence was dictated by scheduling and equipment availability at Ogden Technology Laboratories, Inc.

Thermal Tests

The demonstration panels were installed in the temperature chamber as shown in Fig. 42. The volume of the chamber was such that the installation of the panels did not interfere with the generation or maintenance of the test environment. The heat source was located where the radiant heat would not fall directly on the specimen. Four thermocouples were installed on each panel. A thermocouple was placed on each major structural component on each panel. The thermocouple locations and the temperature data taken during the heat-up period, and a 1-hour soak at a nominal chamber temperature of 90°C are given in Fig. 43.

Acoustic Tests

A plywood dummy specimen, the approximate size of the demonstration panel, was suspended by means of soft suspension cord in a reverberation-type chamber. The chamber was formed and proportioned so as to produce a diffused sound field with nearly uniform energy density throughout the enclosure. The Atlas-Centaur spectrum (internal-forward) was set

005808

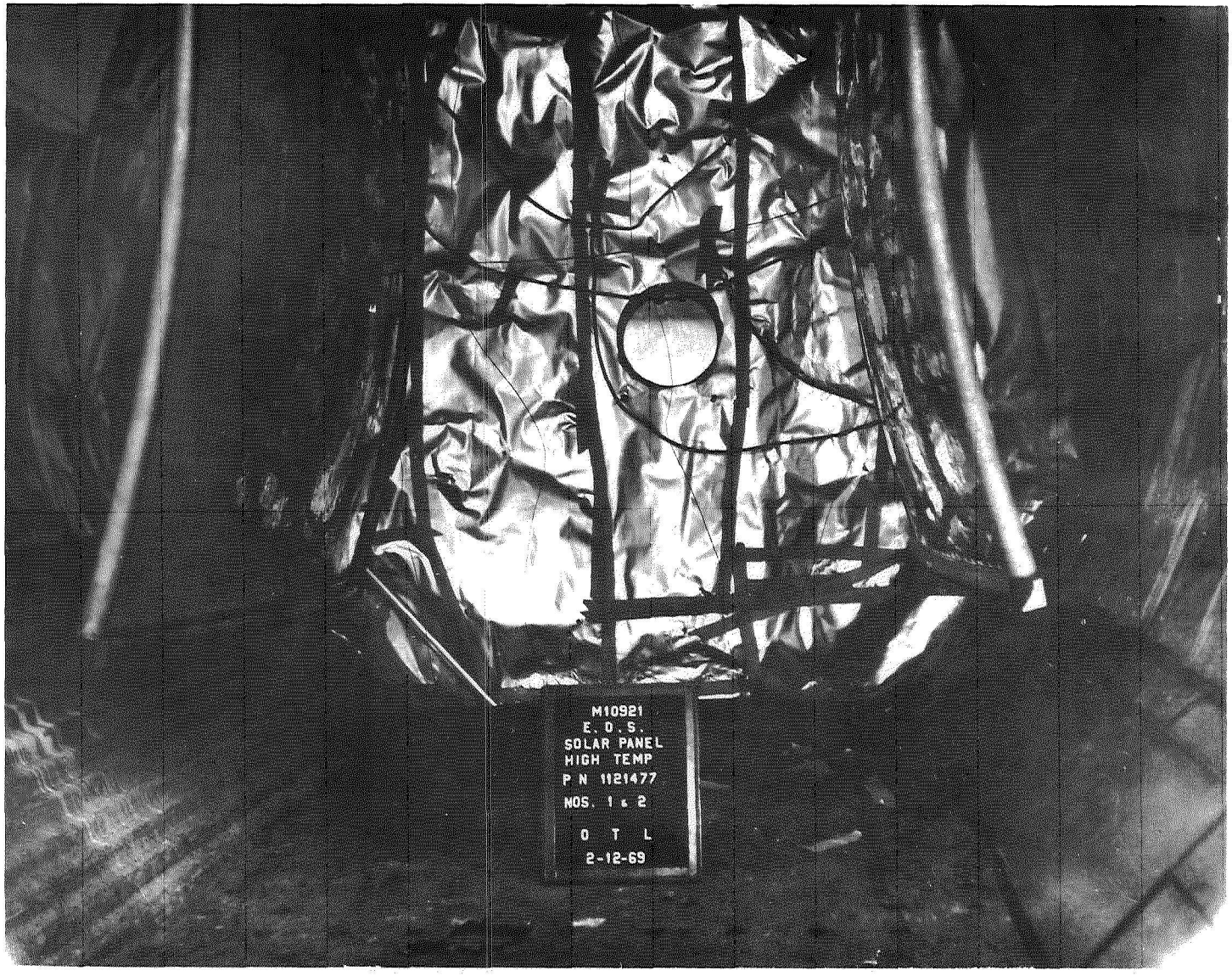

Figure 42. Demonstration Panels Installed in Temperature Chamber

Date Started: 2-12-69		TEST DATA	Performed By: Mangino
Date Completed: 2-12-69		Specimen Description: Solar Panel	OTL Q.A. H. [illegible]
Temp.: 20° C	Humidity: 57%	Test: High Temp Soak	Cust. Insp. [illegible]
J/N M-10921		Customer: E.O.S.	Gov't. Insp. N/A

Temperature in °C P/N 1121477 S/N 1 & 2

Time	#1 Magnesium Fitting	#2 Beryllium Beam	#3 Aluminum Clip	#4 Hollow Core (Corner)	#5 Hollow Core (Center)	#6 Aluminum Clip	#7 Beryllium Beam	#8 Mag Fitting	#9 Chamber Ambient
Start 1000	30	33.5	24	37	33	34.5	38.5	39	49.5
1015	50	53	53.5	56.5	53.5	50	55	57	67
1030	64	65	65	64.5	62	59.5	62.5	63	65
1040	67	69	69	70	68	64.5	69	72	80
1050	74	75	75	76	73.5	69.5	74	76	80
1100	78	79.5	80	81	78.5	76	80.5	82.5	90.5
1107	83.5	83	83.5	82.5	80	79	82.5	85	91
	85	84.5	85	84	81	80	83.5	86	91
1120	90	89.5	89.5	87	84.5	83	85.5	86.5	81.5
1130	89.75	90.5	90.5	89.5	87	84.5	87	87.75	87.5
(*) 1140	Begin		1 Hour Soak			Per Customer instructions			
1140	90	90.5	91	91	88	86	88.25	89	88
1147	91	92	92	92	89	87	90	90.5	89
1155	91	92	92.5	92.5	90	87.5	90.75	91	91
1202	89.5	90.75	91.25	92	90	88	91	92	94.75
1210	90	89.25	89.5	87.75	87	87	88.25	90	93.25
1217	91.5	90	90.75	88	87.75	87.5	87.75	88.5	90.75
1224	92	92.5	92.5	90.75	89	88.5	89.5	89.25	87.5
1233	90.5	92.25	92.5	93.5	91	88	91.25	91.75	92
1243	88	87.75	87.5	86.5	86	86.5	87.5	89	91
	Finish		1 Hour Soak						

Examination after test showed no damage or deformation.

note: thermocouples 1, 2, 3 & 4 were located on S/N [illegible] thermocouples 5, 6, 7 & 8 were located on S/N 001

Figure 43.

Date Started: 2-14-69	TEST DATA	Performed By: [illegible]
Date Completed: 2-14-69	Specimen Description: BICONVEX SOLAR PANEL STRUCTURE, ALUMINUM HONEYCOMB	OTL Q.A.
Temp.: 23°C / Humidity: N/A	Test: ACOUSTIC NOISE	Cust. Insp.
	Customer: ELECTRO OPTICAL SYSTEMS, INC.	Gov't. Insp.

FREQUENCY (OCTAVE BANDS) (CPS)	OCTAVE BAND SOUND PRES. LEVELS (DB)	OVERALL SOUND PRES. LEVEL (DB)	DURATION OF EXPOSURE (MINUTE)	TEST ITEM S/N	COMMENTS
20-75	123-126	144/	—	(DUMMY)	SIMULATED TEST ITEM
75-150	126-129	/145			SUSPENDED IN ACOUSTICS TEST
150-300	136-138				CHAMBER (TEST ITEM MTG.
300-600	140-141				MEANS <25 CPS RESONANCE).
600-1200	140-142				ADJUSTED ACOUSTIC NOISE
1200-2400	136-137				SPECTRUM PER APPLICABLE
2400-4800	131-132				SPEC. AND VERBAL INSTRUCTIONS
4800-10,000	126-127				FROM E.O.S. REP.
20-75	123-126	144/	2.0	#1	TEST ITEM S/N #1 SUBJECTED
75-150	126-129	/145			TO 2.0 MINUTE NOISE EXPOSURE.
150-300	136-138				OVERALL LEVEL 144/145 DB.
300-600	140-141				
600-1200	140-142				
1200-2400	136-137				
2400-4800	131-132				
4800-10,000	126-127				
20-75		132/	2.0	#2	TEST ITEM S/N #2 SUBJECTED
75-150		/133			TO 2.0 MINUTE NOISE EXPOSURE.
150-300					HOWEVER, OVERALL TEST LEVEL
300-600					REDUCED TO 132/133 DB,
600-1200					PER VERBAL INSTRUCTIONS OF
1200-2400					E.O.S. REP.
2400-4800					
4800-10,000					

Figure 44.

005806

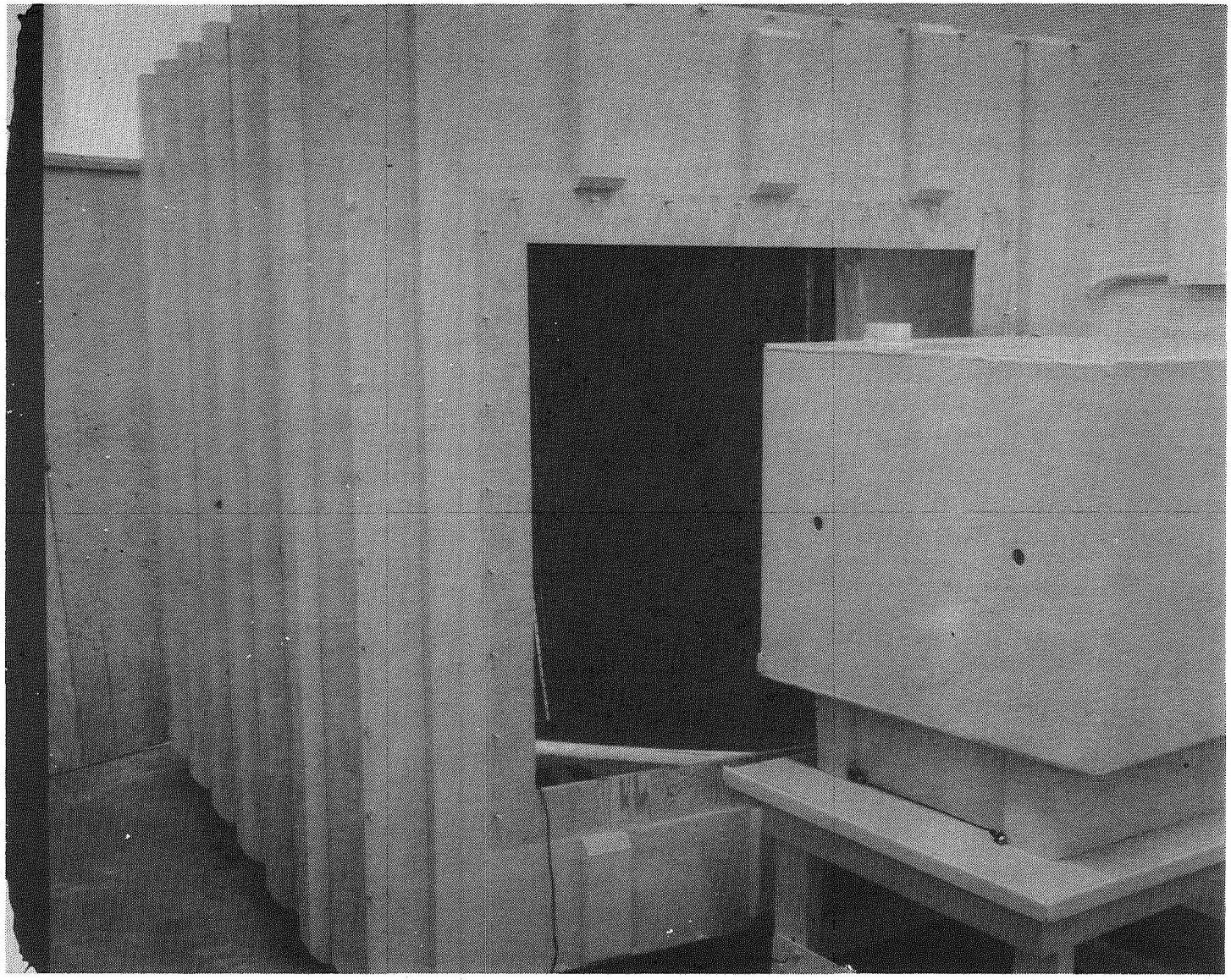

Figure 45. Demonstration Panel Suspended in Reverberation Chamber

005805

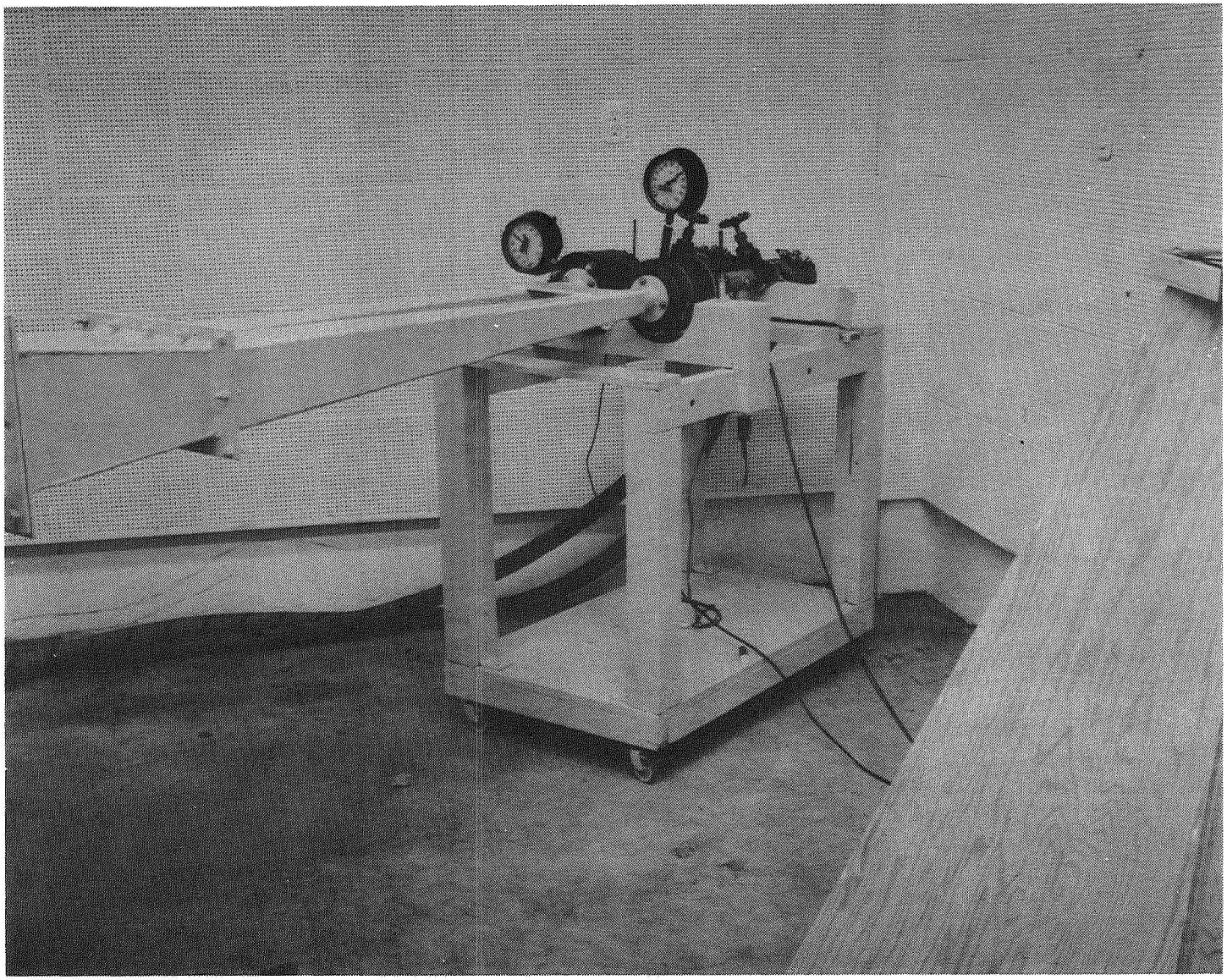

Figure 46. Air Modulation System

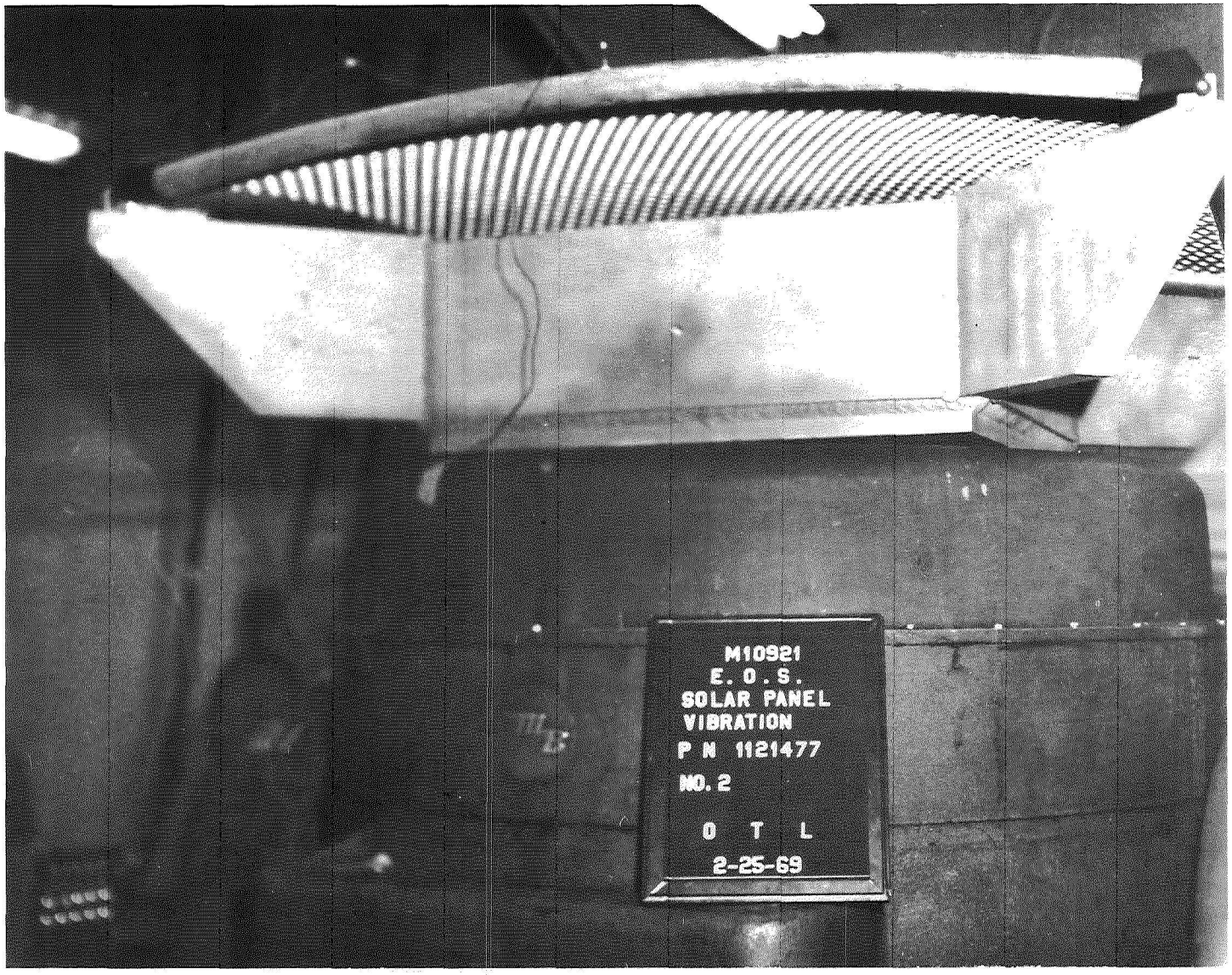

Figure 47. Fixture for Vibration Testing of Demonstration Panels

005807

Figure 48. Demonstration Panel Installed on Fixture

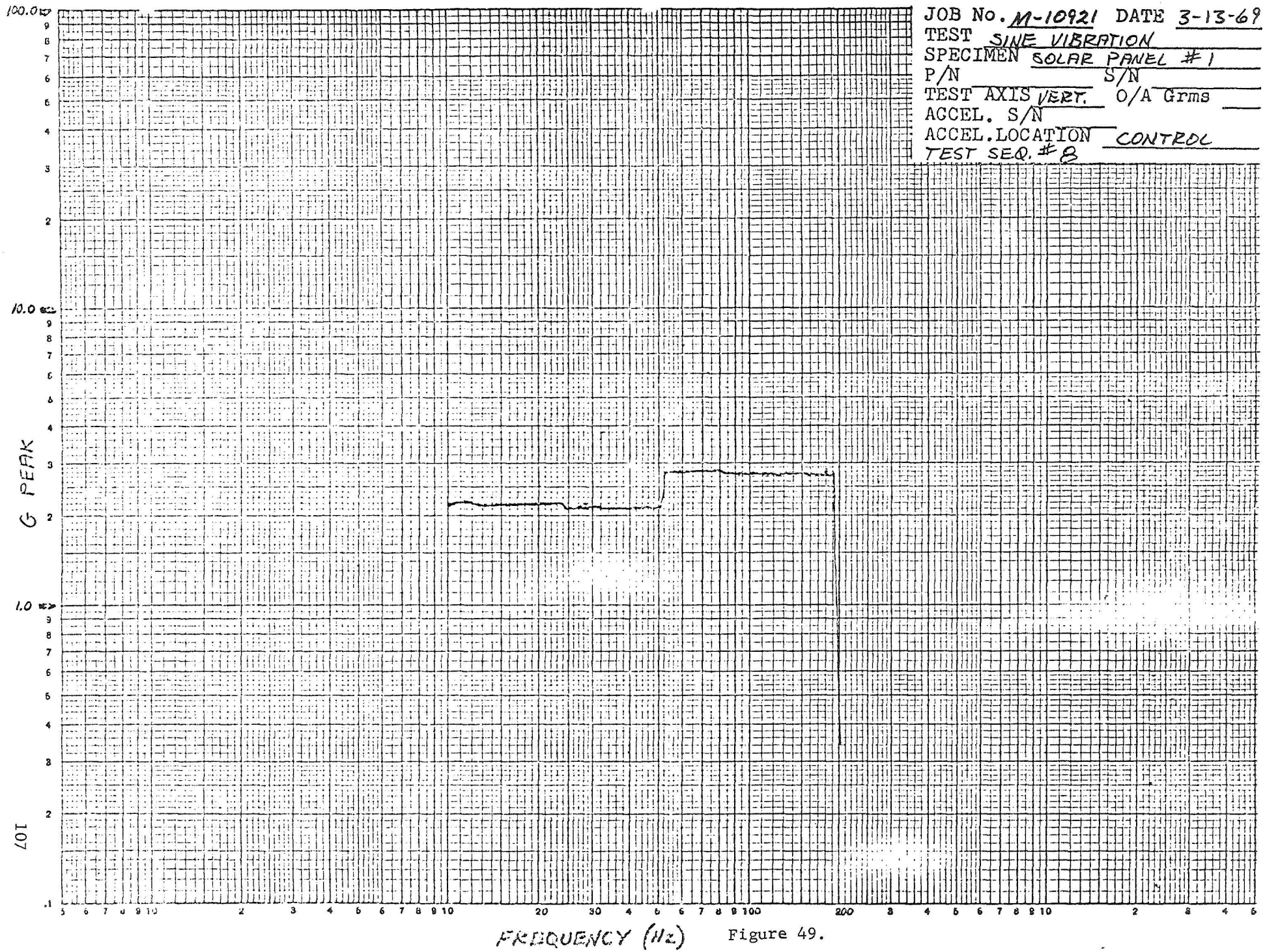
JOB No. M-10921 DATE 3-13-69
TEST SINE VIBRATION
SPECIMEN SOLAR PANEL #1
P/N S/N
TEST AXIS VERT. O/A Grms
ACCEL. S/N
ACCEL. LOCATION CONTROL
TEST SEQ. #8
G PEAK
100.0
10.0
1.0
.1
FREQUENCY (Hz)

Figure 49.

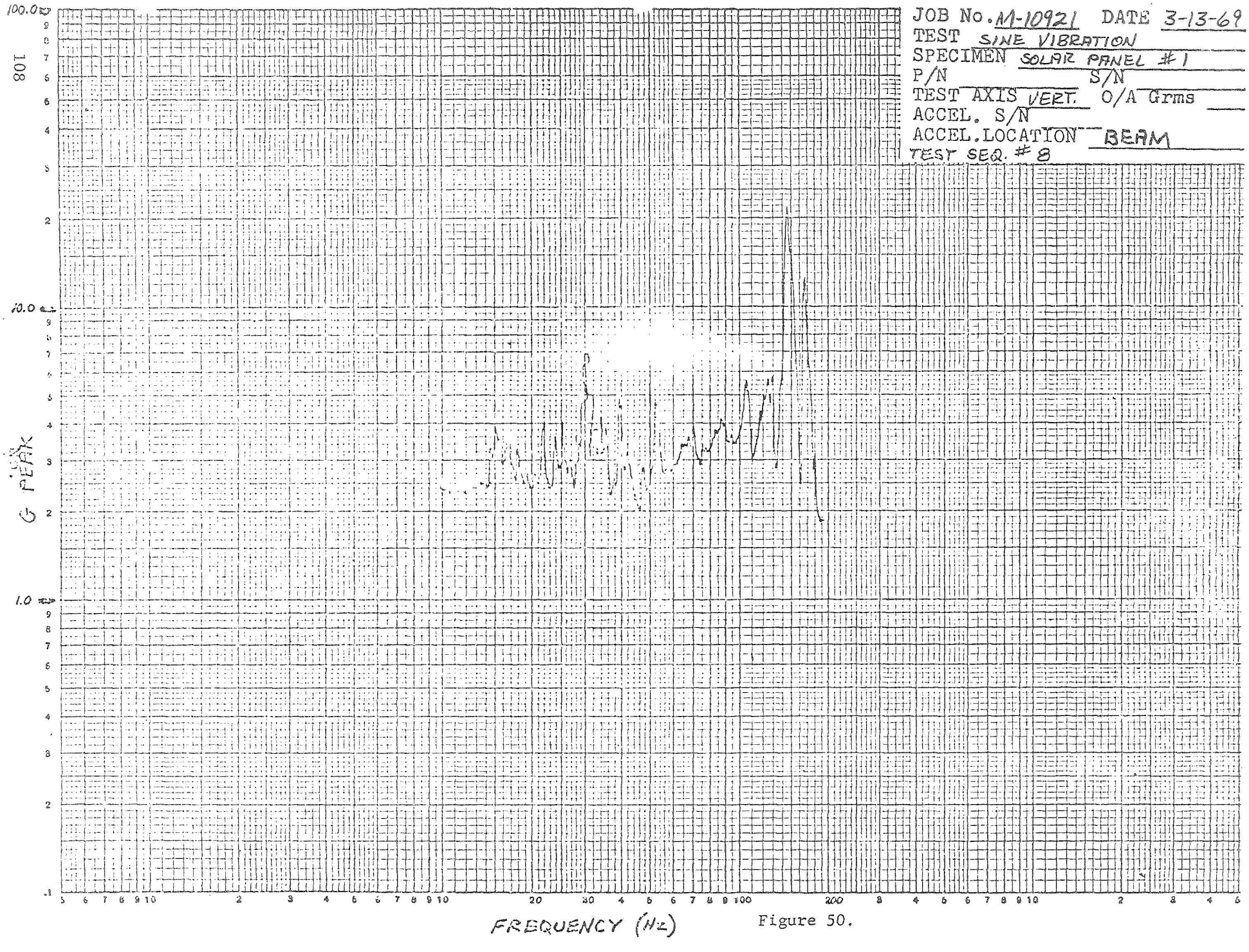
JOB No. M-10921 DATE 3-13-69
TEST SINE VIBRATION
SPECIMEN SOLAR PANEL #1
P/N S/N
TEST AXIS VERT. O/A Grms
ACCEL. S/N
ACCEL. LOCATION BEAM
TEST SEQ. #8
100.0
10.0
1.0
.1
G PEAK
FREQUENCY (HZ)

Figure 50.

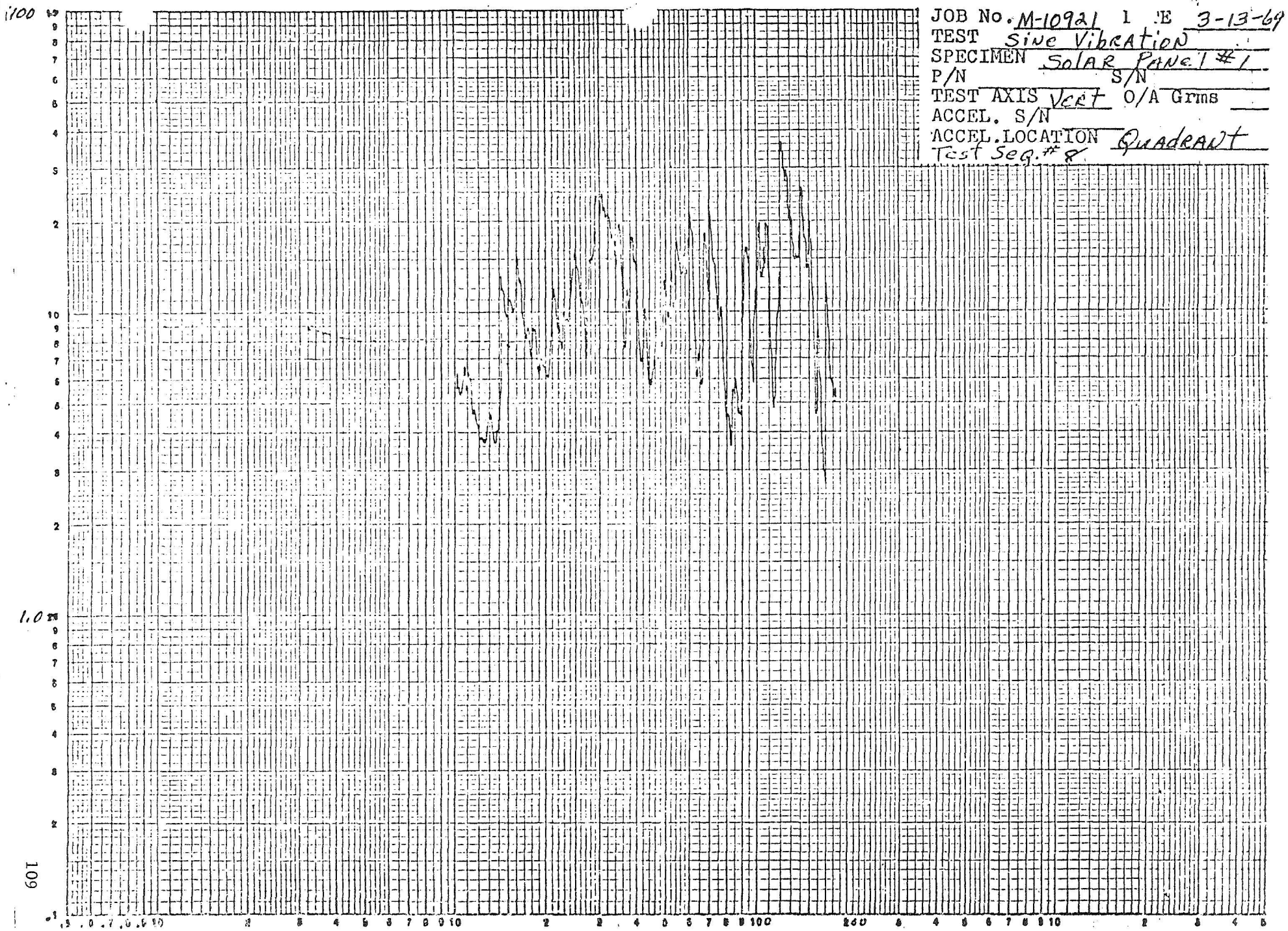
JOB No. M-10921 DATE 3-13-69
TEST Sine Vibration
SPECIMEN Solar Panel #1
P/N S/N
TEST AXIS Vert O/A Grms
ACCEL. S/N
ACCEL. LOCATION Quadrant
Test Seq. #8
100
1.0
Frequency (Hz)

Figure 51.

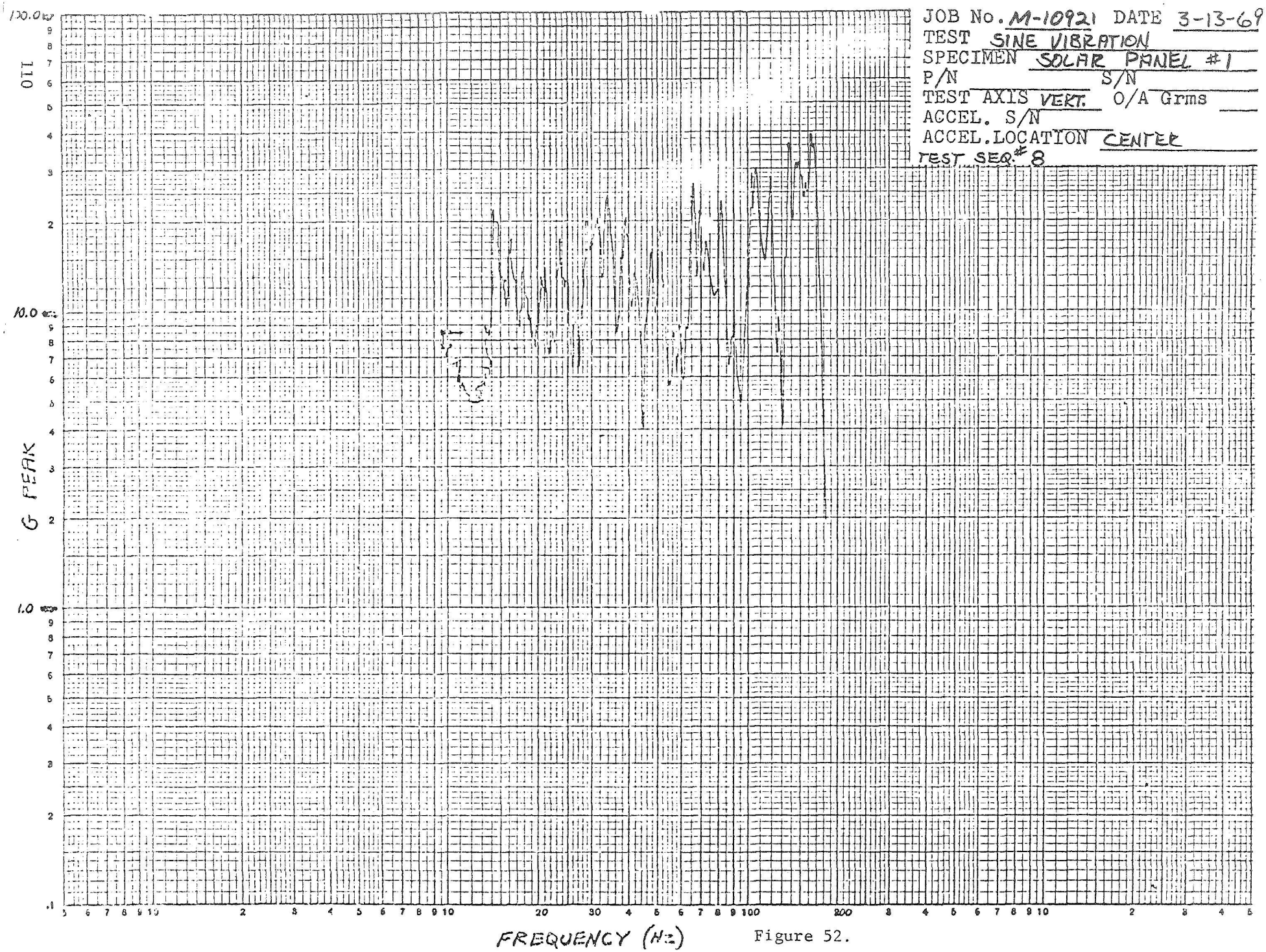
JOB No. M-10921 DATE 3-13-69
TEST SINE VIBRATION
SPECIMEN SOLAR PANEL #1
P/N S/N
TEST AXIS VERT. O/A Grms
ACCEL. S/N
ACCEL. LOCATION CENTER
TEST SEQ.# 8
G PEAK
FREQUENCY (Hz)

Figure 52.

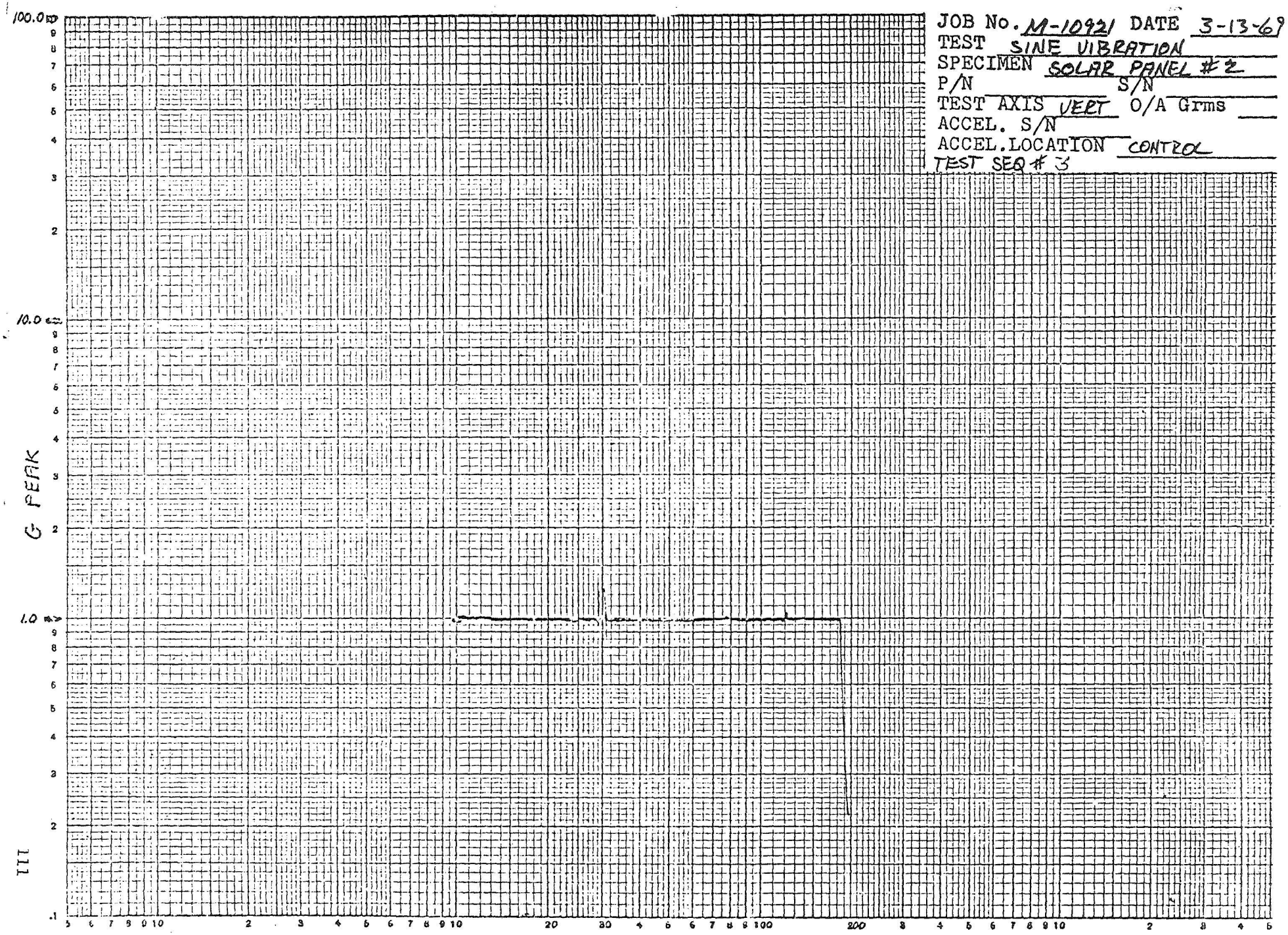
JOB No. M-10921 DATE 3-13-69
TEST SINE VIBRATION
SPECIMEN SOLAR PANEL #2
P/N S/N
TEST AXIS VERT O/A Grms
ACCEL. S/N
ACCEL. LOCATION CONTROL
TEST SEQ # 3
100.0
10.0
1.0
.1
G PEAK
FREQUENCY (Hz)

Figure 53.

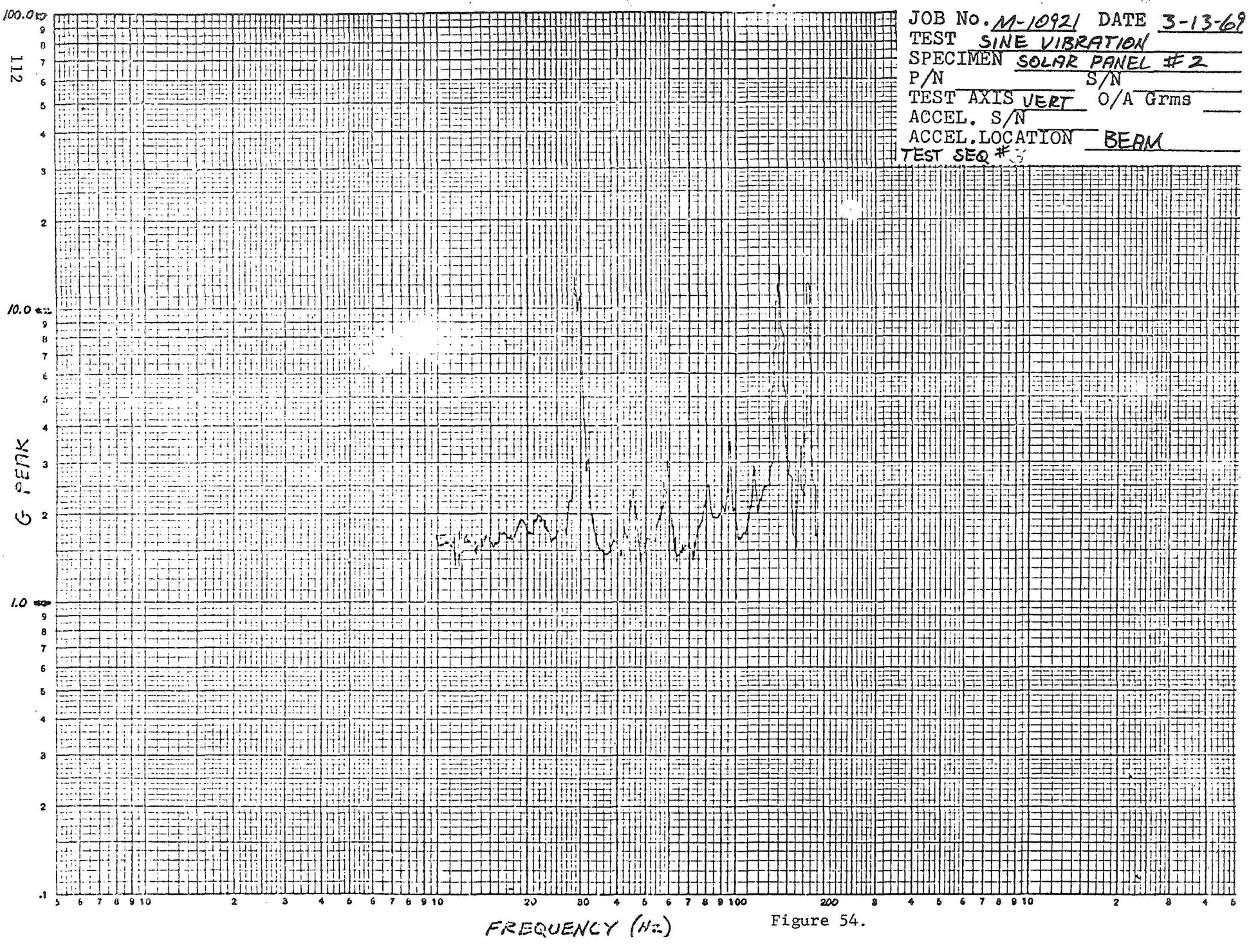
JOB No. M-10921 DATE 3-13-69
TEST SINE VIBRATION
SPECIMEN SOLAR PANEL #2
P/N S/N
TEST AXIS VERT O/A Grms
ACCEL. S/N
ACCEL. LOCATION BEAM
TEST SEQ #3
100.0
10.0
1.0
.1
G PEAK
FREQUENCY (Hz)

Figure 54.

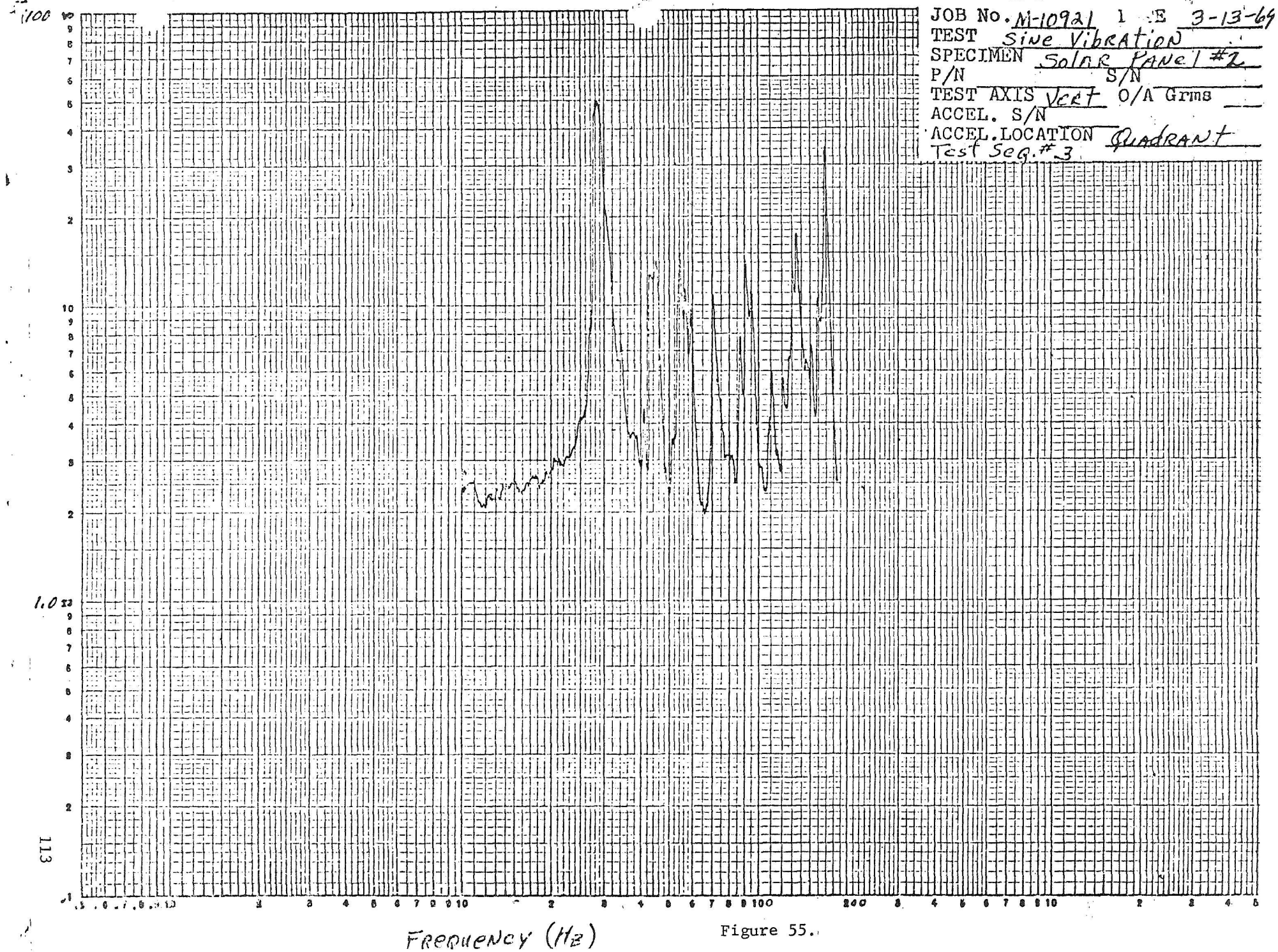
JOB No. M-10921 DATE 3-13-69
TEST Sine Vibration
SPECIMEN Solar Panel #2
P/N S/N
TEST AXIS Vert O/A Grms
ACCEL. S/N
ACCEL. LOCATION Quadrant
Test Seq. #3
100
1.0
Frequency (Hz)

Figure 55.

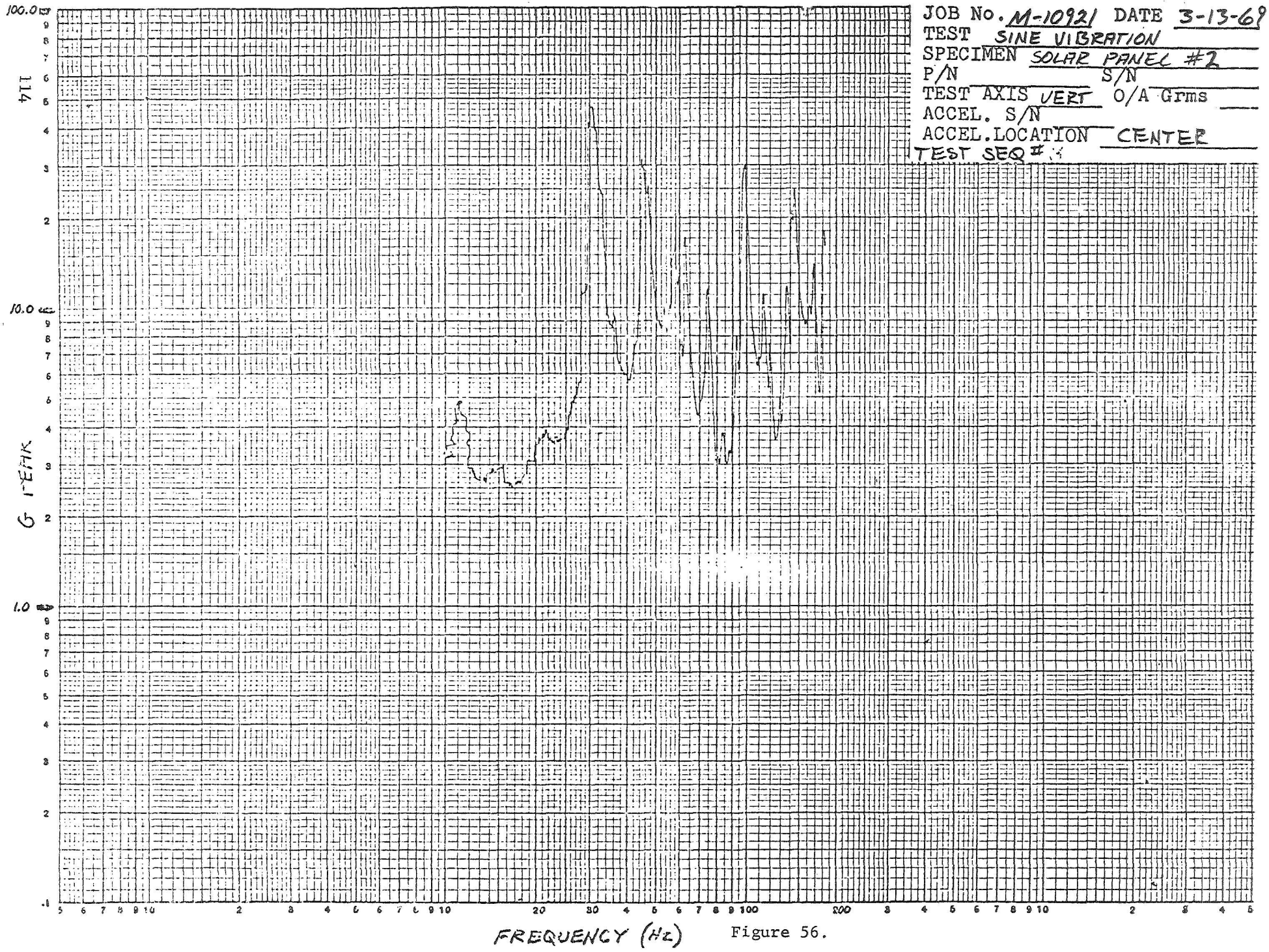
JOB No. M-10921 DATE 3-13-69
TEST SINE VIBRATION
SPECIMEN SOLAR PANEL #2
P/N S/N
TEST AXIS VERT O/A Grms
ACCEL. S/N
ACCEL. LOCATION CENTER
TEST SEQ #
114
G PEAK
100.0
10.0
1.0
.1
FREQUENCY (Hz)

Figure 56.

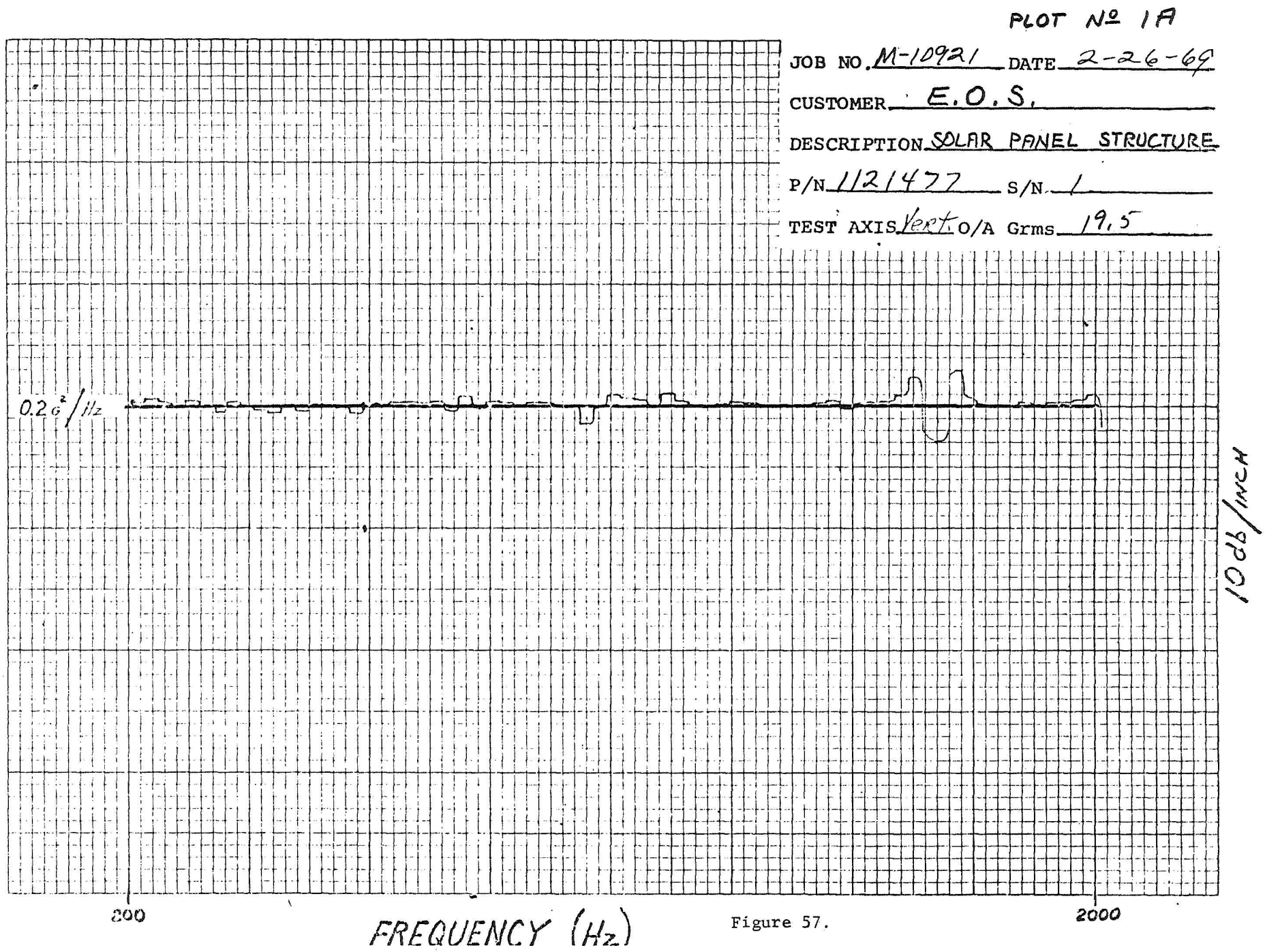
PLOT Nº 1A
JOB NO. M-10921 DATE 2-26-69
CUSTOMER E.O.S.
DESCRIPTION SOLAR PANEL STRUCTURE
P/N 1121477 S/N 1
TEST AXIS Vert. O/A Grms 19.5
0.2 g²/Hz
10 db/INCH
200
2000
FREQUENCY (Hz)

Figure 57.

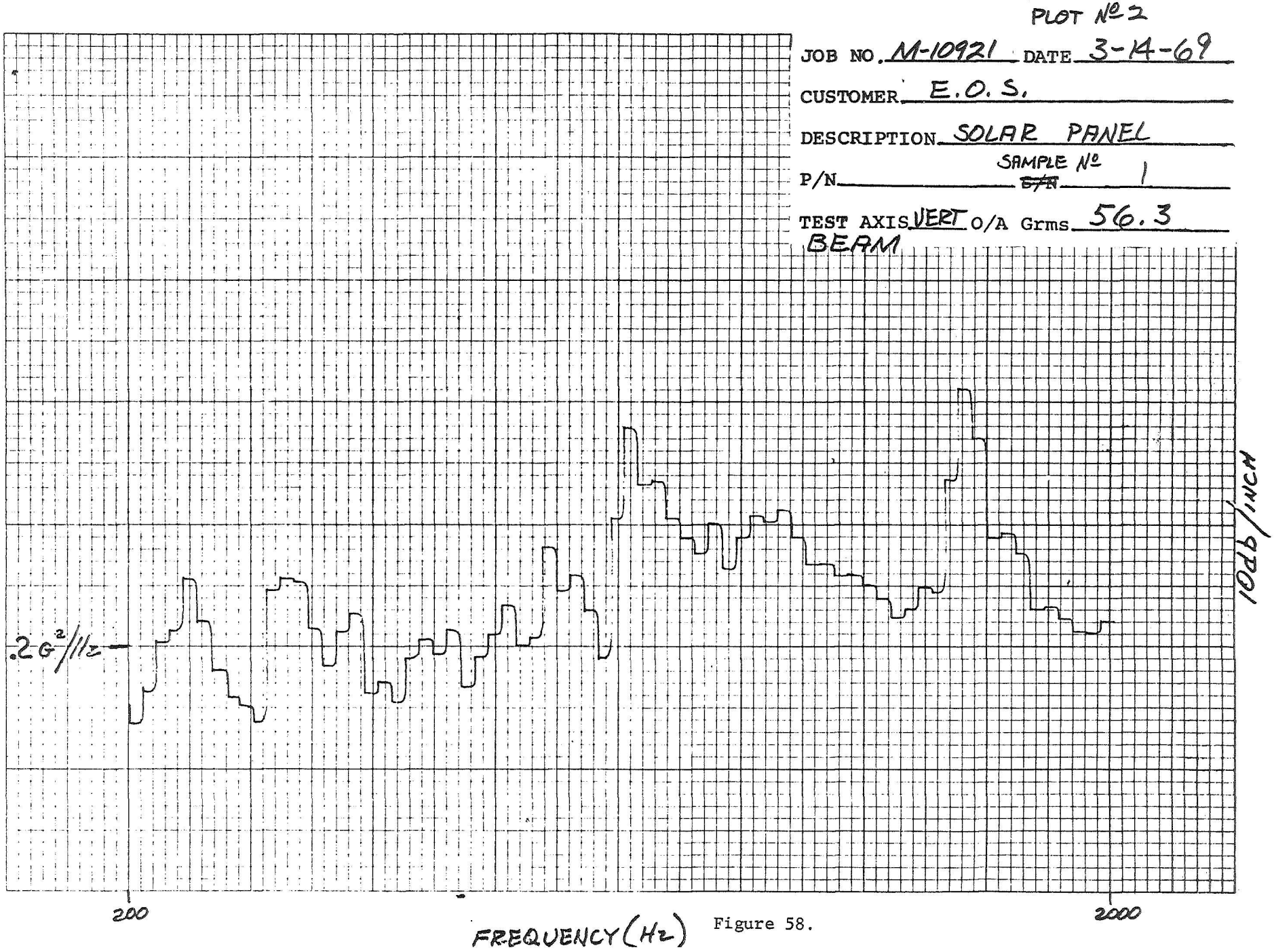
PLOT Nº 2
JOB NO. M-10921 DATE 3-14-69
CUSTOMER E.O.S.
DESCRIPTION SOLAR PANEL
P/N
SAMPLE Nº 1
TEST AXIS VERT O/A Grms 56.3
BEAM
.2 G²/Hz
10db/INCH
200
2000
FREQUENCY (Hz)

Figure 58.

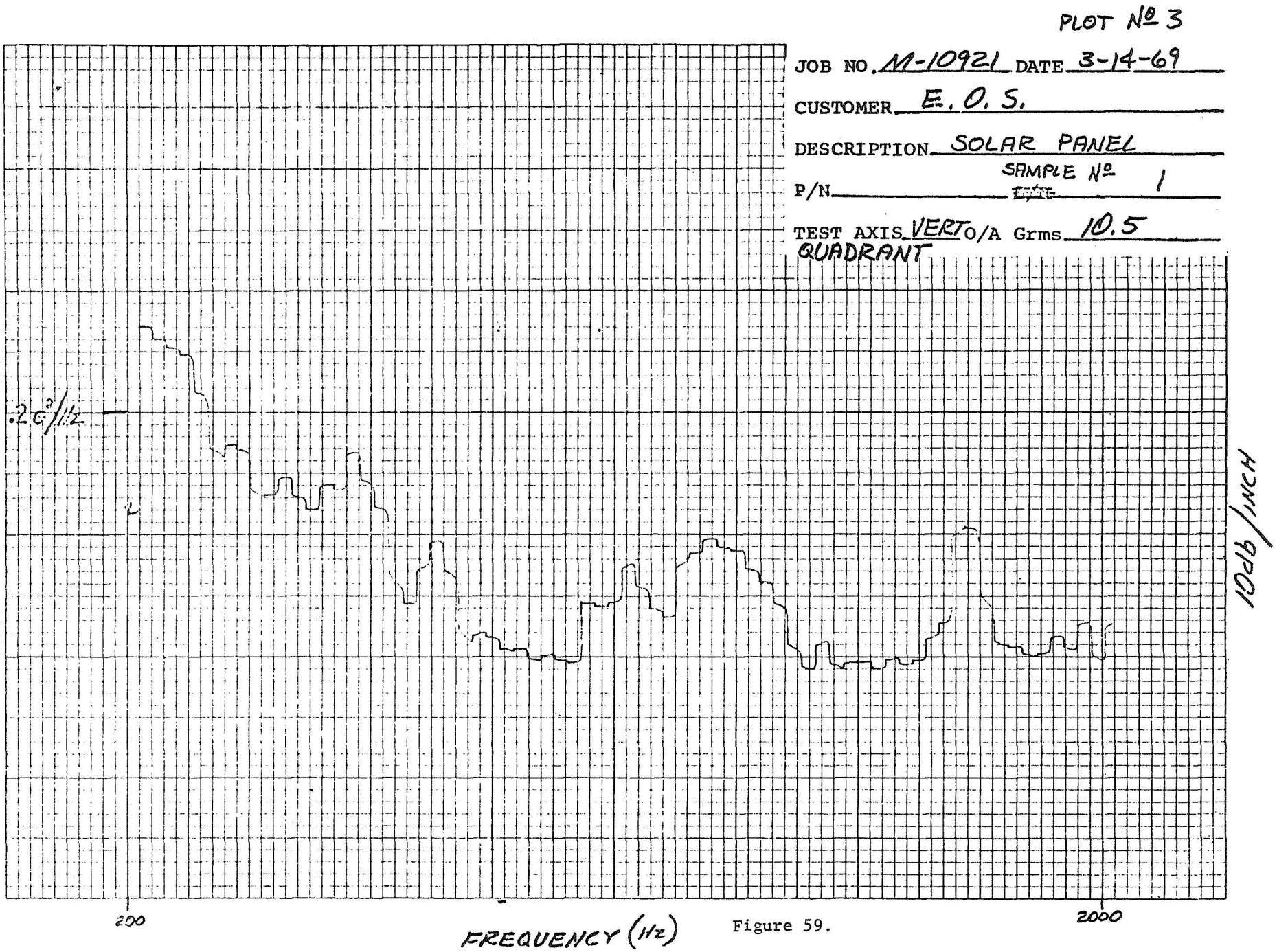
PLOT Nº 3
JOB NO. M-10921 DATE 3-14-69
CUSTOMER E.O.S.
DESCRIPTION SOLAR PANEL
SAMPLE Nº 1
P/N
TEST AXIS VERT O/A Grms 10.5
QUADRANT
.2 G²/Hz
10dB/INCH
200
2000
FREQUENCY (Hz)

Figure 59.

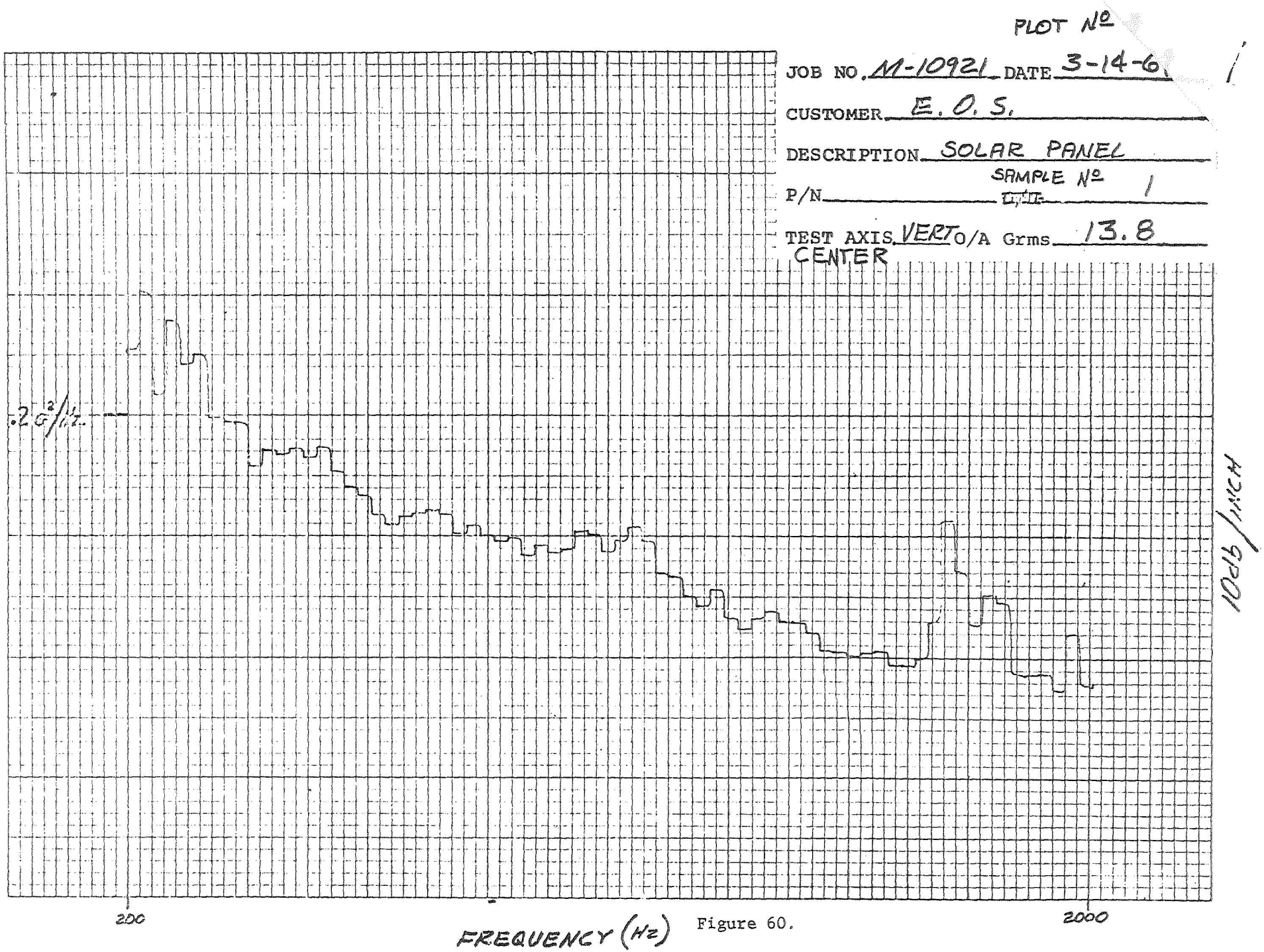
PLOT Nº
JOB NO. M-10921 DATE 3-14-6
CUSTOMER E.O.S.
DESCRIPTION SOLAR PANEL
SAMPLE Nº 1
P/N
TEST AXIS VERT O/A Grms 13.8
CENTER
.2 G²/Hz
10db/INCH
200
2000
FREQUENCY (Hz)

Figure 60.

Electrical Performance Tests

Electrical performance tests for the 6 x 35 cell circuit installed on S/N 2 are shown in Figs. 61 and 62. The I-V curves for the standard cell used for control during the sunlight tests on the roof at EOS are given in Figs. 63 and 64. Figures 61 and 62 were plotted before environmental testing. Figures 63 and 64 are the records of the sunlight tests performed at the completion of all testing. The shapes of the curves taken before and after the environmental tests are identical, indicating no degradation in cell performance. The temperature of the panel was not controlled during sunlight testing. The changes in open circuit voltage and short circuit current are due to the higher ambient temperature and lower solar intensity during the second test.

The power output (AM1) of the single 6 x 35 circuit is approximately 8W.

HEWLETT-PACKARD/MOSELEY DIVISION
9270-1006
FOR USE ON AUTOGRAF RECORDERS
10 UNITS/DIVISION

SOLAR CELL I-V CURVE : BEFORE ENVIRONMENTAL TESTING

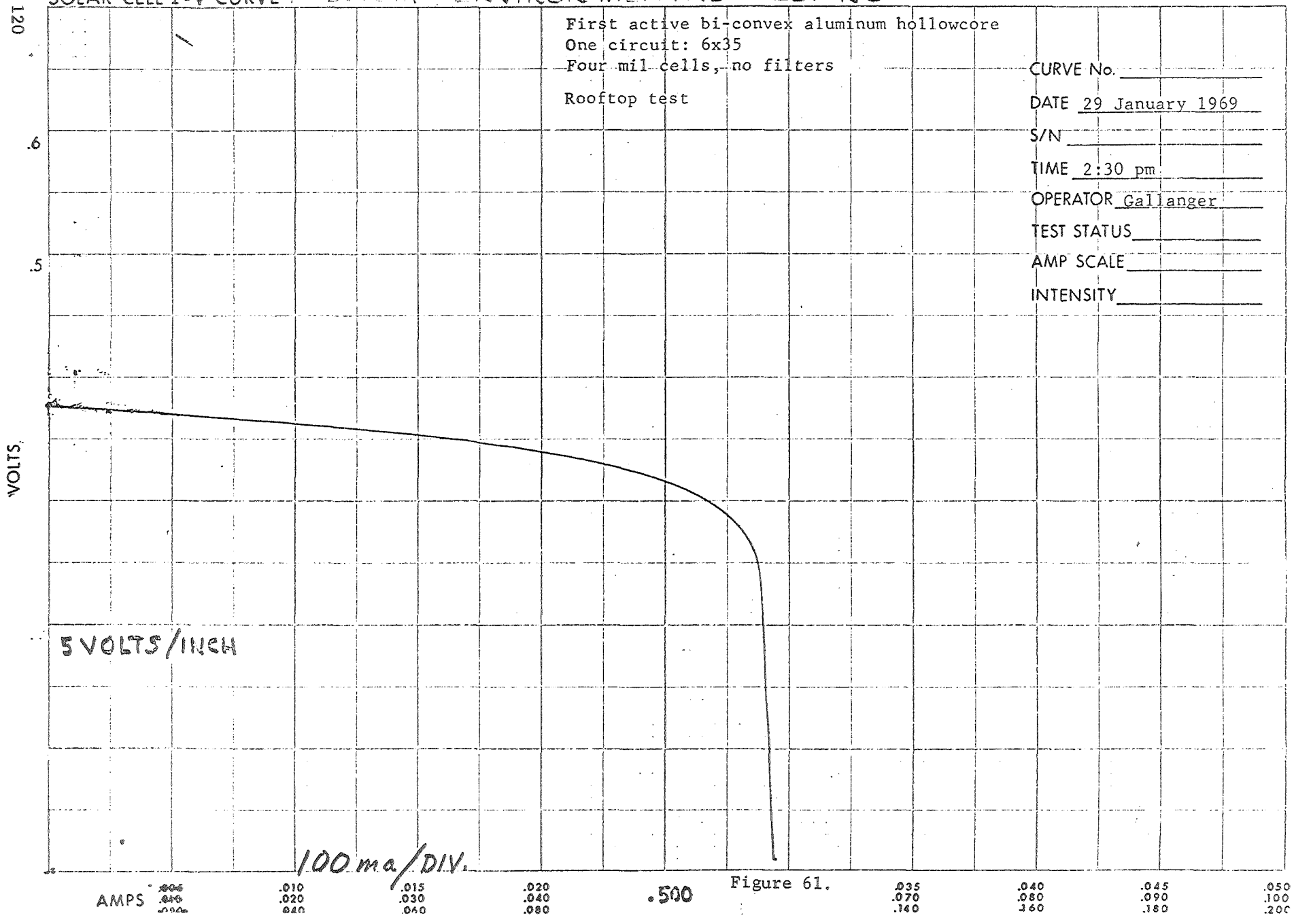

Figure 61.

HEWLETT-PACKARD/MOSELEY DIVISION
9270-1006
FOR USE ON AUTOGRAF RECORDERS
10 UNITS/DIVISION

SOLAR CELL I-V CURVE: AFTER ENVIRONMENTAL TESTING

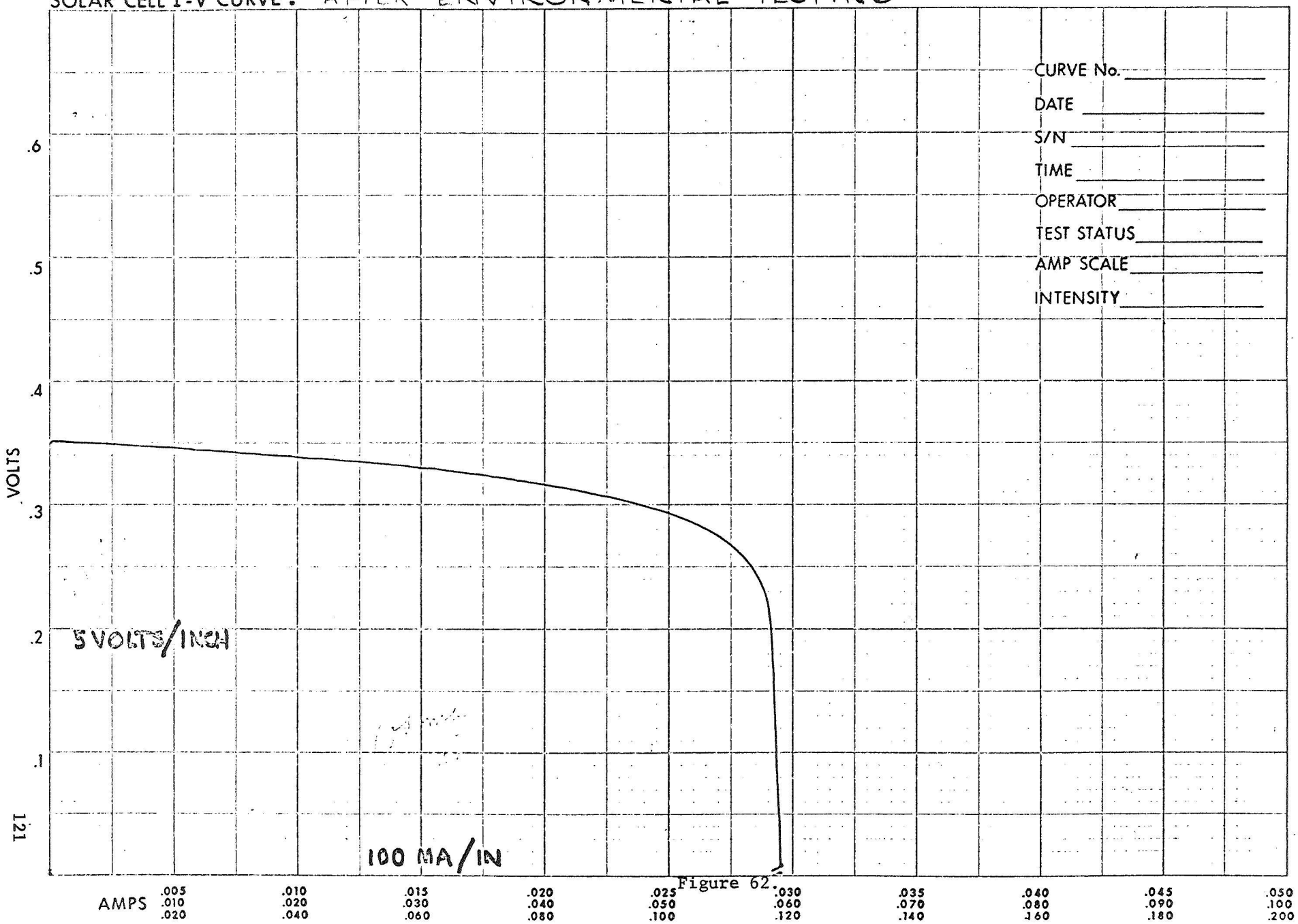

Figure 62.

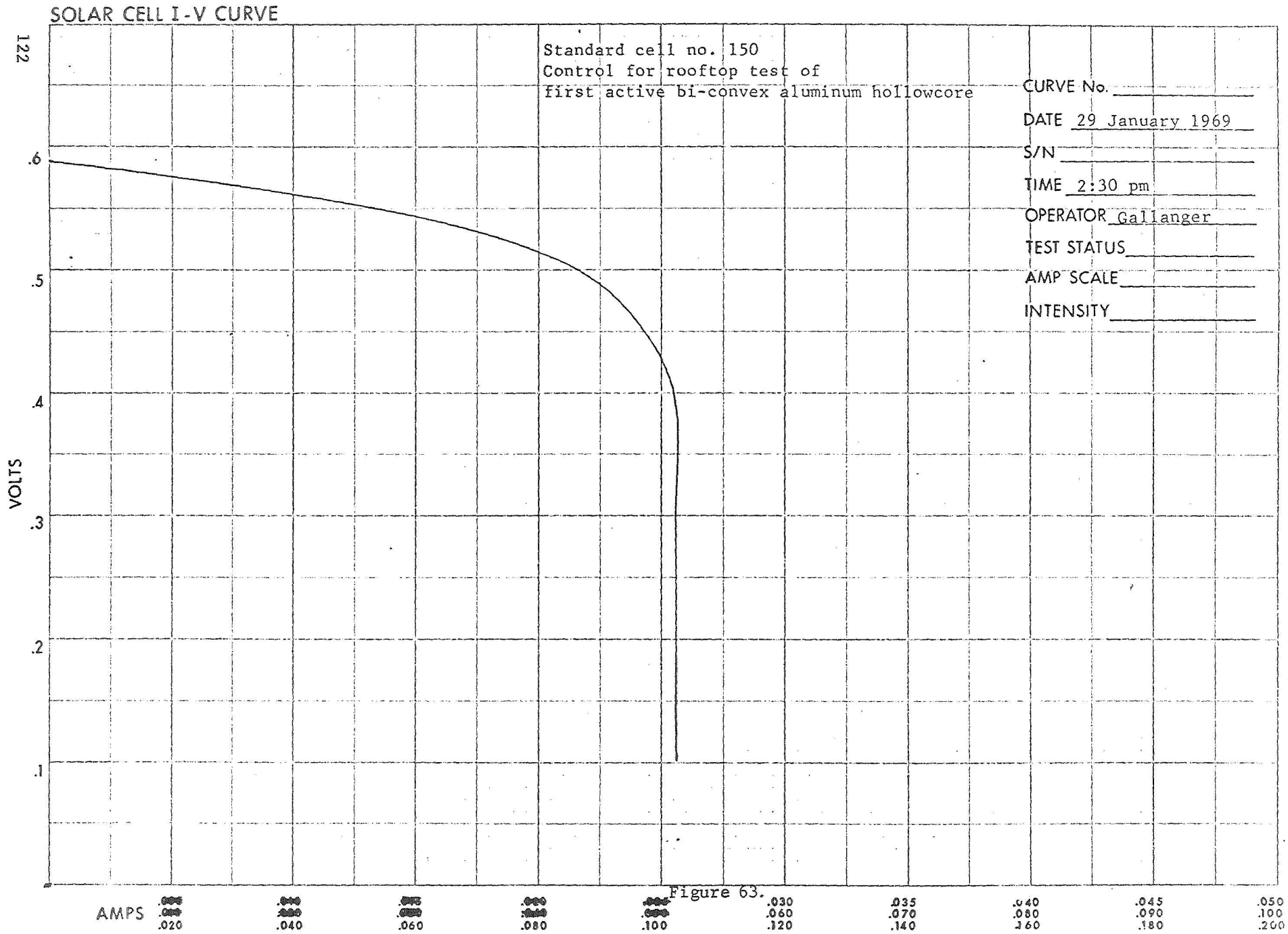
HEWLETT-PACKARD/MOSELEY DIVISION
9270-1006
FOR USE ON AUTOGRAF RECORDERS
10 UNITS/DIVISION
SOLAR CELL I-V CURVE
Standard cell no. 150
Control for rooftop test of
first active bi-convex aluminum hollowcore
CURVE No.
DATE 29 January 1969
S/N
TIME 2:30 pm
OPERATOR Gallanger
TEST STATUS
AMP SCALE
INTENSITY
VOLTS
.6
.5
.4
.3
.2
.1
AMPS
.020
.040
.060
.080
.100
.120
.140
.160
.180
.200
.030
.060
.070
.080
.090
.100
.035
.040
.045
.050

Figure 63.

K+E 10 X 10 TO THE INCH 46 0782
7 X 10 INCHES MADE IN U.S.A.
KEUFFEL & ESSER CO.

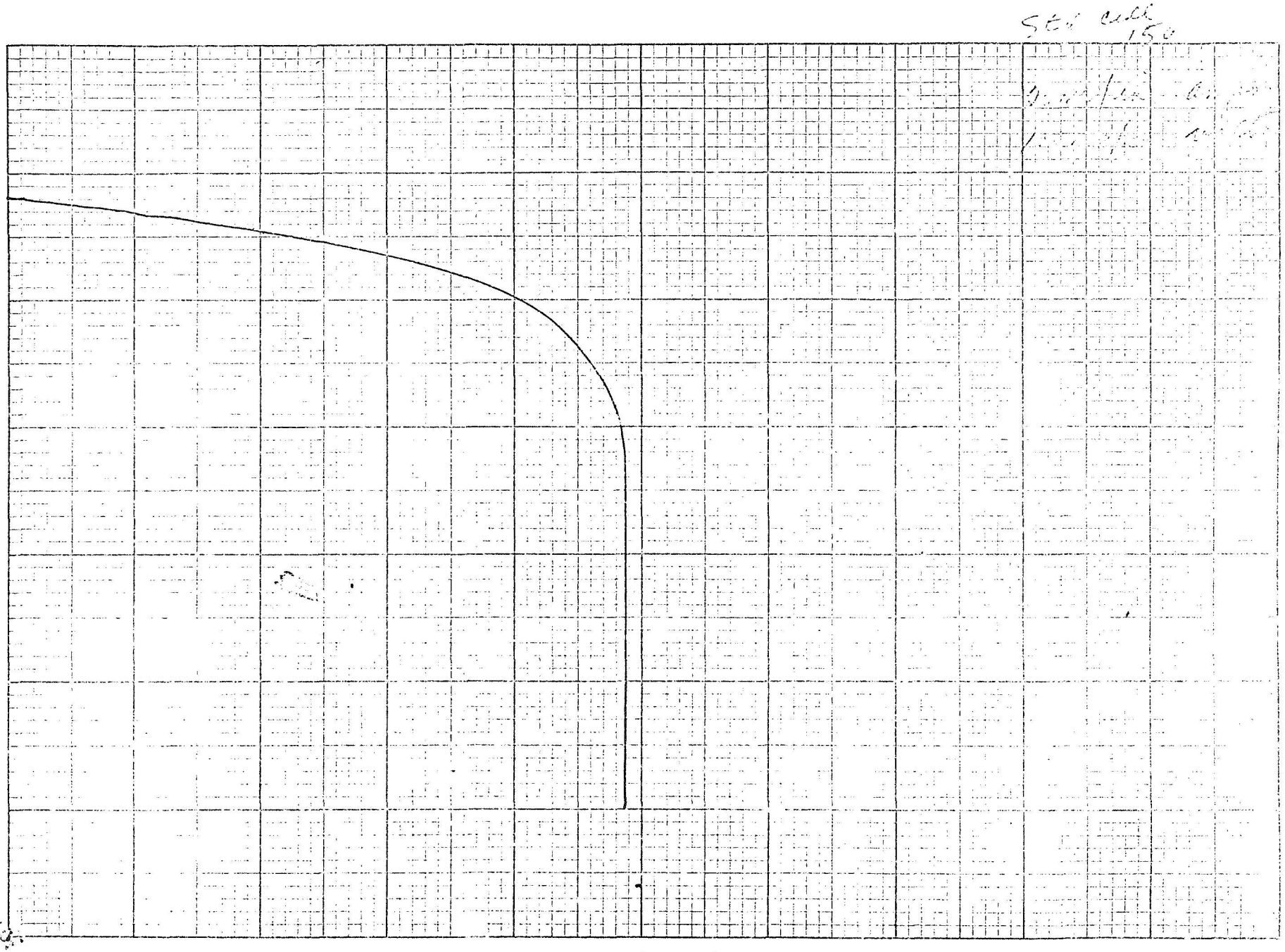

Figure 64.

APPENDIX A

SUBSTRATE ANALYSIS-OPTIMIZATION OF ALUMINUM HOLLOWCORE DESIGN

This analysis follows the procedure outlined in the basic report.

Design Restrictions Due to Hollowcore Fabrication Process

The fabrication process (electroforming) of the hollowcore places the following geometric restrictions on the design:

1. Distance between holes shall not be less than 0.050 inch ($\Delta \geq 0.050$ in.)
2. Hollowcore height shall not be less than 0.100 inch for a planform size of 5 x 5 ft sq ($h \geq 0.100$ in.)
3. Skin thickness of hollowcore shall be equal to or greater than 0.002 inch and equal to or less than 0.006 inch (0.002 in. $\geq t \geq$ 0.006 in.)

The first two restrictions are dictated by the mandrel used in fabricating the hollowcore substrate. At present, a copper sheet is to be used and the holes in it are to be first drilled, then reamed. It has been found that if the distance between holes is less than 0.050 inch the operation of drilling another hole will upset and deform a previously established adjacent hole. If the mandrel thickness is less than 0.100 inch for a 5 x 5 ft sq biconvex shell, it will deform under its own weight when suspended in the electroplating tank.

The last restriction, the allowable range in thickness of the electroplating, is dictated by the state of art of aluminum electroforming.

Frequency Restriction on Solar Panel

There are two factors that dictate the first resonance of the demonstration panel. The first is that it should fall below 50 Hz so as to experience the lowest g level at its first resonant frequency. The second is that it should be as high as possible (close to 50 Hz) so as to lessen the induced displacement and to insure that it will not have a resonance that can couple with the boost vehicle's large amplitude resonances which normally fall below 10 Hz. Therefore, at this time it is arbitrarily stated that the first resonance should be approximately 40 Hz. Once the hollowcore geometry and the cell stack weight are defined, the first frequency can be calculated from the following equation developed in the Phase I portion of the contract. The equation is

$$f_{11} = \frac{1}{2\pi}\sqrt{\frac{1}{\rho h}\left[D(\lambda_1^{\,2} + \mu_1^{\,2})^2 + \frac{Eh'}{R^2}\right]} \qquad \text{(A-1)}$$

where

f_{11} = panel first resonant frequency - Hz
h' = effective height of hollowcore - in.
D = stiffness parameter per unit length - lb in.^{2}/in.
ρh = panel specific mass - lb sec^2/in.^{3}
E = modules of elasticity - lb/in.^{2}
R = radius of curvature - in.

and

$$\lambda_1 = \frac{\pi}{\alpha} \qquad \mu_1 = \frac{\pi}{\beta}$$

It should be noted that this defines the panel frequency for a system with a rigid boundary. Appendix B of this report analyzes the effect of the frame stiffness on the panel first resonant frequency.

Critical Environmental Loading and Structures Dynamic Magnification Factor

Review of the specified design environment defined in the basic report indicates that the sinusoidal vibration of the structure is the most severe loading condition for the solar array. Since the structure is being designed to have a first resonance below 50 Hz, the input acceleration at the attachment points will be 1.5 g rms or 2.12 g zero to peak.

From Phase I testing, it was found that the dynamic magnification factor for this type of structure is about 40.

The acceleration response of the substrate under a sinusoidal vibration input as derived in Phase I (Ref. 1) is

$$\ddot{W} = \frac{16}{\pi^2} Q \sin\left(\frac{n\pi}{\alpha_o}\alpha\right) \sin\left(\frac{m\pi}{\beta_o}\beta\right) \ddot{W}_s \qquad \text{(A-2)}$$

where

$\ddot{W}$ = normal acceleration of substrate surface - g

Q = dynamic manifaction factor - dim.

α = curvilinear coordinate in X direction - in.

β = curvilinear coordinate in Y direction - in.

$\ddot{W}_s$ = input acceleration at boundary - g

The maximum loading is at the center of the substrate where the g loading for the input described above is

$$\ddot{W} = \frac{16}{\pi^2} Q \ddot{W}_s = \frac{16}{\pi^2} (40)\ 2.12\ g$$

or

$$\ddot{W} = 137.5\ g \text{ zero to peak}$$

Panel Dead Load

The panel dead load, that is, the specific weight associated with hardware or structure (i.e. cells, adhesive, etc.) that does not contribute to the overall strength or stiffness is defined as

$$(SpWt)cs = 0.120\ lb/ft^2 = 8.33 \times 10^{-4}\ lb/in.^2$$

The specific weight is developed as follows:

Item	Total Weight	Specific Weight*
Cell	1.332	0.05615
Filter	0.329	0.01387
Interconnectors	0.350	0.01475
Cell adhesive	0.342	0.01441
Circuitry on substrate	0.038	0.00016
Dielectric	0.171	0.00721
Dielectric adhesive	0.044	0.00018
Thermal control paint	0.102	0.00430
		0.11103 lb/ft^2
	+10% contingency	0.01 lb/ft^2
	Design Dead Load =	0.12 lb/ft^2

*Based on substrate area.

Membrane Forces per Unit Length

The membrane force per unit length varies over the surface of the biconvex structure. For the preliminary (first cut) analysis, the maximum membrane forces at the crown of the biconvex panel were approximated by the formula for a spherical shell supported tangentially and loaded by a pressure. The formula is

$$P = \frac{\rho R}{2} \tag{A-3}$$

where

P = membrane force per unit length - lb/in.

R = radius of curvature - in.

ρ = applied pressure - lb/in.^{2}

The applied pressure is defined by

$$\rho = (SpWt)_p \times G \tag{A-4}$$

where the g level is

$$G = \ddot{W} = 137.5 \text{ zero to peak}$$

and the specific weight $(SpWt)_p$ of the total panel is the specific weight of the dead load defined in the preceding subsection and that contributed by the hollowcore. The next section defines the specific weight of the hollowcore and the total panel for various geometric parameters.

Specific weight of hollowcore and panel. - The specific weight of the hollowcore is defined by the following equation:

$$(SpWt)_{HC} = \rho t \left[2 - \frac{\pi}{4\sqrt{3}} \left(\frac{d}{a}\right)^2 + \frac{\pi}{2\sqrt{3}} \left(\frac{h}{a}\right) \left(\frac{d}{a}\right) \right] \qquad \text{(A-5)}$$

where

ρ = density of aluminum = 0.100 lb/in.^{3}

t = thickness of skin - in.

d = cylinder diameter - in.

2a = distance between cylinder centers - in.

h = cross section height of hollowcore - in.

The specific weight for various hollowcore geometric parameters within the restrictions defined in the first subsection of this Appendix is shown in Fig. A-1. This figure shows the total specific weight of the panel with the addition of the dead load specific weight defined in the preceding subsection. The value is defined by

$$(SpWt)_{panel} = (SpWt)_{HC} + 8.33 \times 10^{-4} \text{ lb/in.}^2$$

Membrane force per unit length for various geometric parameters. - Using the first equations of this subsection, A-3 and A-4, the membrane force per unit length is defined in the crown of the structure by

$$P = \frac{R}{2} \times G \times (SpWt)_{panel} = \left(\frac{163.5 \text{ in.}}{2}\right) (137.5) \times (SpWt)_{panel}$$

73628945

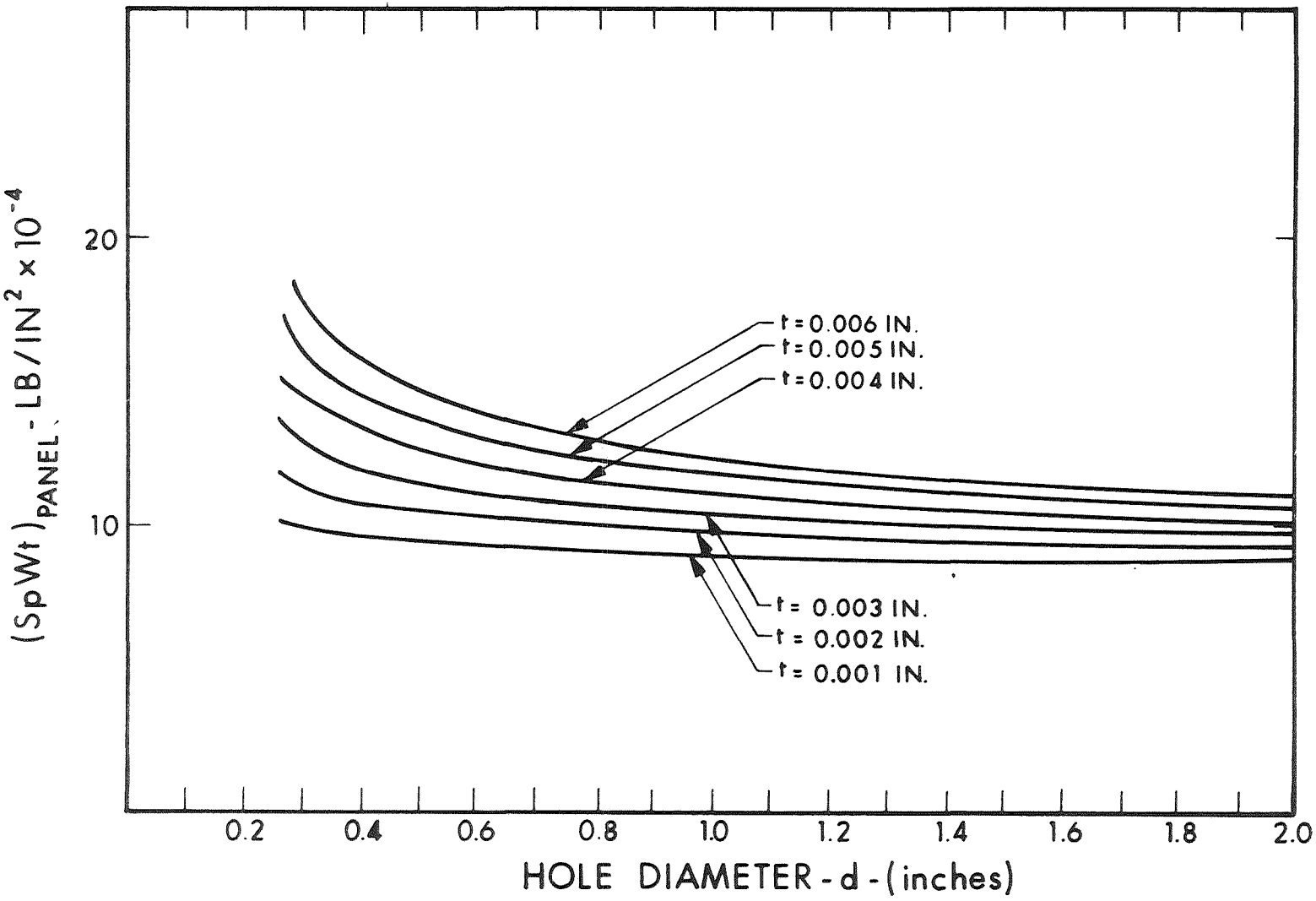

Figure A-1. Hollowcore Optimization, Specific Weight versus Hole Diameter with Skin Thickness as Parameter $(SpW+)_{panel} = (SpW+)_{hollowcore} + (SpW+)_{dead\ load}$

Design Limit Stress in Hollowcore Substrate

Using the membrane load per unit length on a segment of the hollowcore derived in the preceding subsection, the average stress (design limit stress) in the hollowcore can be obtained from the following equation:

$$\sigma = \frac{P}{h'} \tag{A-6}$$

where

σ = average working stress - psi

P = membrane load per unit length - lb/in.

h' = effective height of hollowcore - in.

The effective height of the hollowcore is that cross sectional area per unit length defined by the following equation:

$$h' = \left[2 + \left(\frac{h}{a}\right) - \frac{\sqrt{3}}{2}\left(\frac{d}{a}\right)\right] t \tag{A-7}$$

This equation defines the assumed distribution of membrane stresses between the cylinder walls and the surface between cylinders.

Allowable Stress in Hollowcore

The allowable stress for the hollowcore structure is the minimum value for one of the following: (1) the material ultimate stress (F_{tu}), (2) the critical buckling stress (F_{co}), or (3) the local crippling stress (F_{cc}). The design limit stress (DL) is compared to the allowable stress (AS) using the following formula to determine the margin of safety:

$$MS = \frac{AS}{1.25\ (DL)} - 1 > 0 \tag{A-8}$$

Crippling Stress of the Hollowcore Structure

From the Phase I program, it was determined that the failure mode for the hollowcore structure concept was crippling in the surface between cylinders. It was also determined that this surface could be approximated by an equilateral triangle (see Fig. A-2) loaded in compression along its three sides. The leg dimension(s) of this triangle is defined by

$$s = 4a - \sqrt{3}d \tag{A-9}$$

From NASA Document TN 3781, the critical stress in a triangular sheet, loaded in compression along its boundary, is

$$F_{cc} = K \frac{\pi^2 E}{12(1-\nu^2)} \left(\frac{t}{s}\right)^2 \tag{A-10}$$

The coefficient (K) given in NASA TN 3781 is

K = 5 for simply supported edges

K = 12.5 for coupled edges

In Phase I tests the coefficient was found to be K = 12

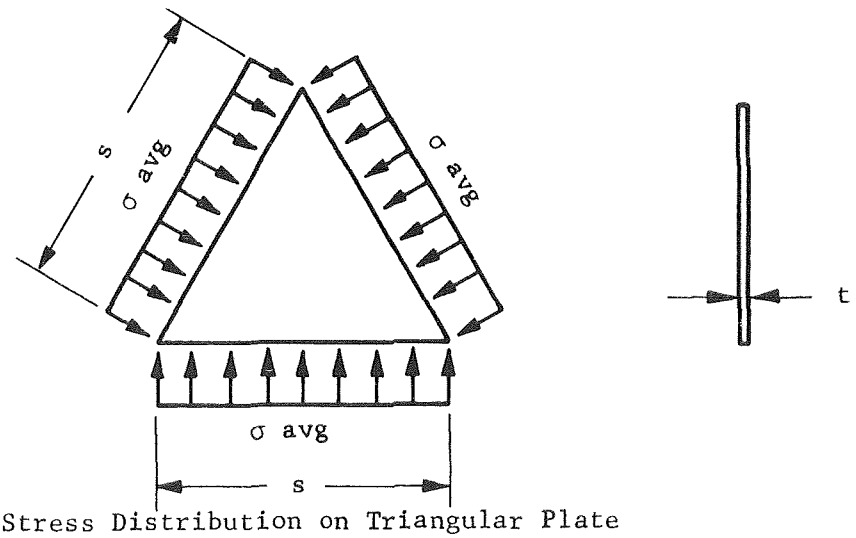

Figure A-2. Stress Distribution on Triangular Plate

Optimum Hollowcore Geometry

Optimum hollowcore geometry is defined as a geometry which meets the restrictions discussed in the first subsection of this appendix and can support the membrane stresses described in the design limit stress portion of this appendix with a margin of safety equal to zero. This set of geometries is determined by superimposing the design limit stress times a factor of 1.25 (see "Allowable Stress in Hollowcore," page for various geometries on a plot of critical crippling stresses for the same geometric parameters. The intersections of two corresponding curves locate the optimum configurations. Figure A-3 is a plot of this analysis.

Minimum Weight Hollowcore Configuration

The specific weight associated with the hollowcore geometry optimized in the preceding subsection can be obtained from Figure A-1. The following tabulation contains this information.

Thickness (in.)	Diameter (in.)	Panel Specific Weight $lb/in^2 \times 10^{-4}$	Panel Specific Weight lb/ft^2	Hollowcore Specific Weight (lb/ft^2)
0.001	0.07	11.47	0.165	0.045
0.002	0.39	10.88	0.157	0.037
0.003	0.77	10.80	0.156	0.036
0.004	1.23	10.73	0.155	0.035
0.005	1.62	10.83	0.156	0.036
0.006	2.24	10.88	0.158	0.038

The data in the tabulation indicates that the minimum weight configuration for the hollowcore structure uses a skin thickness of 0.004 inch and a cylinder diameter of 1.23 inches. The configuration shall also be defined by the restrictions in the first subsection of this appendix.

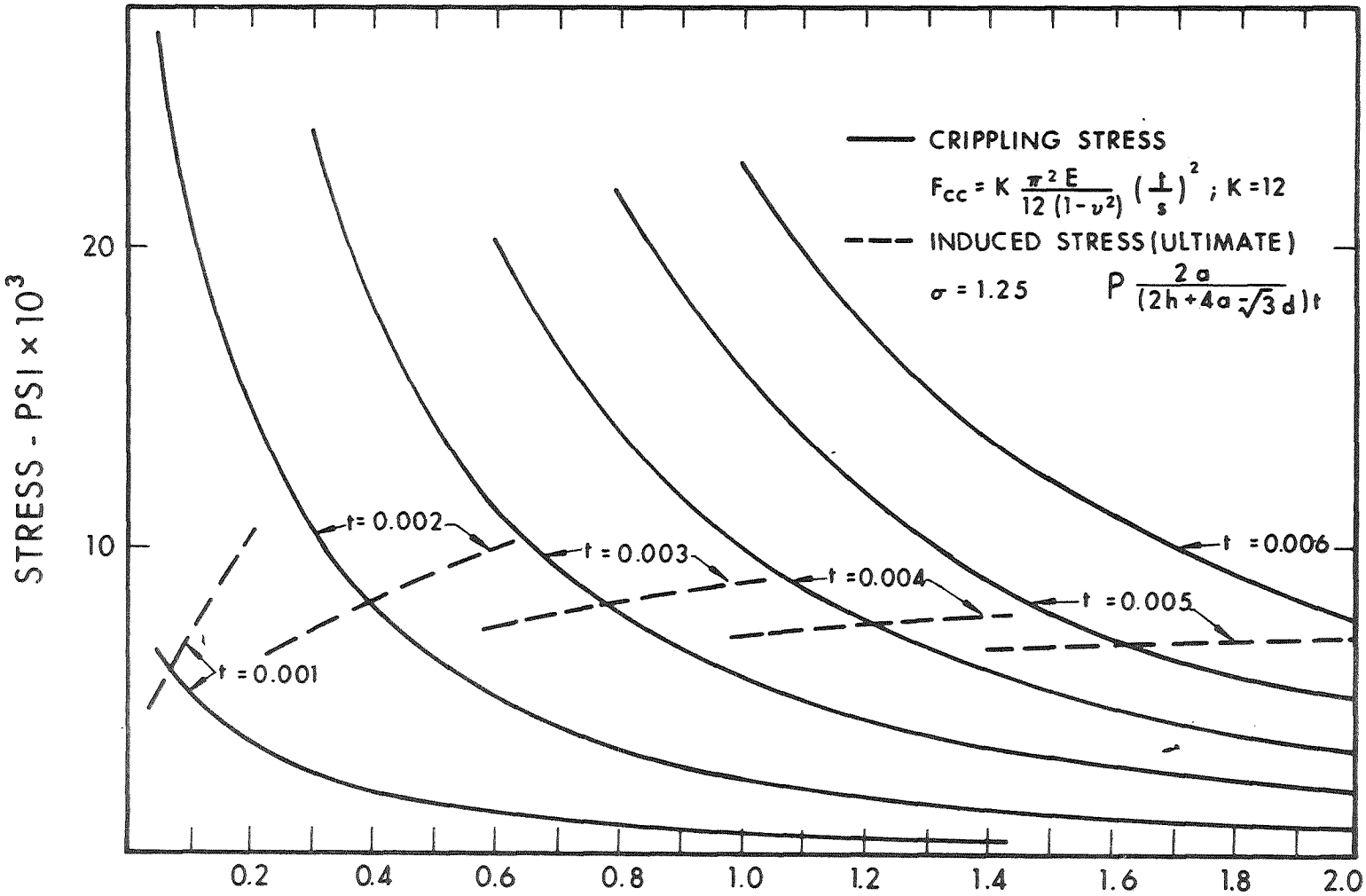

Figure A-3. Hollowcore Optimization, Induced Stress and Crippling Stress versus Geometry

73628946

Verification of Theoretical Buckling Coefficients

Tension tests of electroformed aluminum (mixed ether bath). - A series of tension tests have been performed on 3-mil and 5-mil samples of aluminum electroformed in a mixed ether bath. The purpose of the tests was to verify the values for modulus of elasticity, yield strength, and ultimate strength which were used in the design and analysis of the hollowcore substrate. The tests were performed on an Instron testing machine which records the load versus deflection in a 1-inch gage length on a x-y plotter. The test reports are included in Tables A-1 and A-2.

The modulus of elasticity was calculated from data taken from the plots of the load-deflection history. The calculations are tabulated in Table A-3.

The values for the modulus of elasticity, yield strength, and ultimate strength which were used in the design and analysis of the hollowcore are 7.8×10^6 psi, 20,500 psi, and 24,600 psi, respectively. The tests indicate that these values are acceptable for design.

Hollowcore buckling tests. - The 18 samples shown in Fig. A-4 have been failed in compression to determine the buckling and crippling characteristics of hollowcore panels. The samples had hole diameters of 0.75, 1.00, 1.25, and 1.50 inches and skin thickness ranging from 0.003 to 0.006 inch. The tests were performed on the Instron testing machine shown in Fig. A-5. Load versus deflection data were recorded on an x-y plotter. The ends of the hollowcore samples were potted in epoxy to provide simple support and uniform load distribution.

As the samples are loaded in compression, the load versus deflection records show the three regions depicted in Fig. A-6.

TABLE A-1

TENSION TEST REPORT ON 5-MIL SAMPLE OF ELECTROFORMED ALUMINUM*

Identification Number	Actual Size	Actual Area	Yield Strength: Actual Load Pounds	Yield Strength: Pounds per Sq.In.	Tensile Strength: Actual Load Pounds	Tensile Strength: Pounds Per Sq.In.	Elongation In.—In. 1	Elongation Percent	Reduction of Area Reduced Dimension	Reduction of Area Percent	Reduction of Area Code	Laboratory No.
TENSION TEST AT ROOM TEMPERATURE												18-276P
100-5-H												
1	0.272 **	0.00125	32.3	25800	35.5	28400	0.07	7				
2	0.290 **	0.00174	37.7	21700	42.5	24400	0.08	8				

NOTE: Yield Strength Determined by: 0.2% Offset

(*) FTMS-151a, Method 211.1

(**) Fracture Code

1) 0.0040 in. 0.0052 in. 2) 0.0059 in. 0.0070 in.

TABLE A-2

TENSION TEST REPORT ON 3-MIL SAMPLE OF ELECTROFORMED ALUMINUM

Identification Number	Actual Size	Actual Area	Yield Strength: Actual Load Pounds	Yield Strength: Pounds per Sq.In.	Tensile Strength: Actual Load Pounds	Tensile Strength: Pounds Per Sq.In.	Elongation In.—In. 1	Elongation Percent	Reduction of Area Reduced Dimension	Reduction of Area Percent	Reduction of Area Code	Laboratory No.
TENSION TEST AT ROOM TEMPERATURE												18-277P
100-3-H												
1	0.288 / *	0.000806	17.3	21500	18.9	23400	0.01	1				
2	0.283 / *	0.000736	17.4	23600	19.9	27000	0.01	11				

*Fracture Code

1) 0.0024 in.
0.0032 in.

2) 0.002 in.
0.0032 in.

TABLE A-3

MODULUS OF ELASTICITY

$$E = \frac{PL}{\delta A}$$

Sample	t	A	P	L	δ	E
1.	0.003 0.0024 0.0032	0.000806	13.00	1.00	0.002	8.06×10^6
2.	0.003 0.002 0.0032	0.000736	14.20	1.00	0.002	9.65×10^6
3.	0.005 0.0040 0.0052	0.00125	18.75	1.00	0.002	7.50×10^6
4.	0.006 0.0059 0.0070	0.00174	26.5	1.00	0.002	7.61×10^6

Average $\overline{E} = 8.20 \times 10^6$

$$\text{Probable error} = 0.6745 \sqrt{\frac{\sum_{n=1}^{4} \left(E_n - \overline{E}\right)^2}{3}}$$

Probable error $= 0.67 \times 10^6$

168124

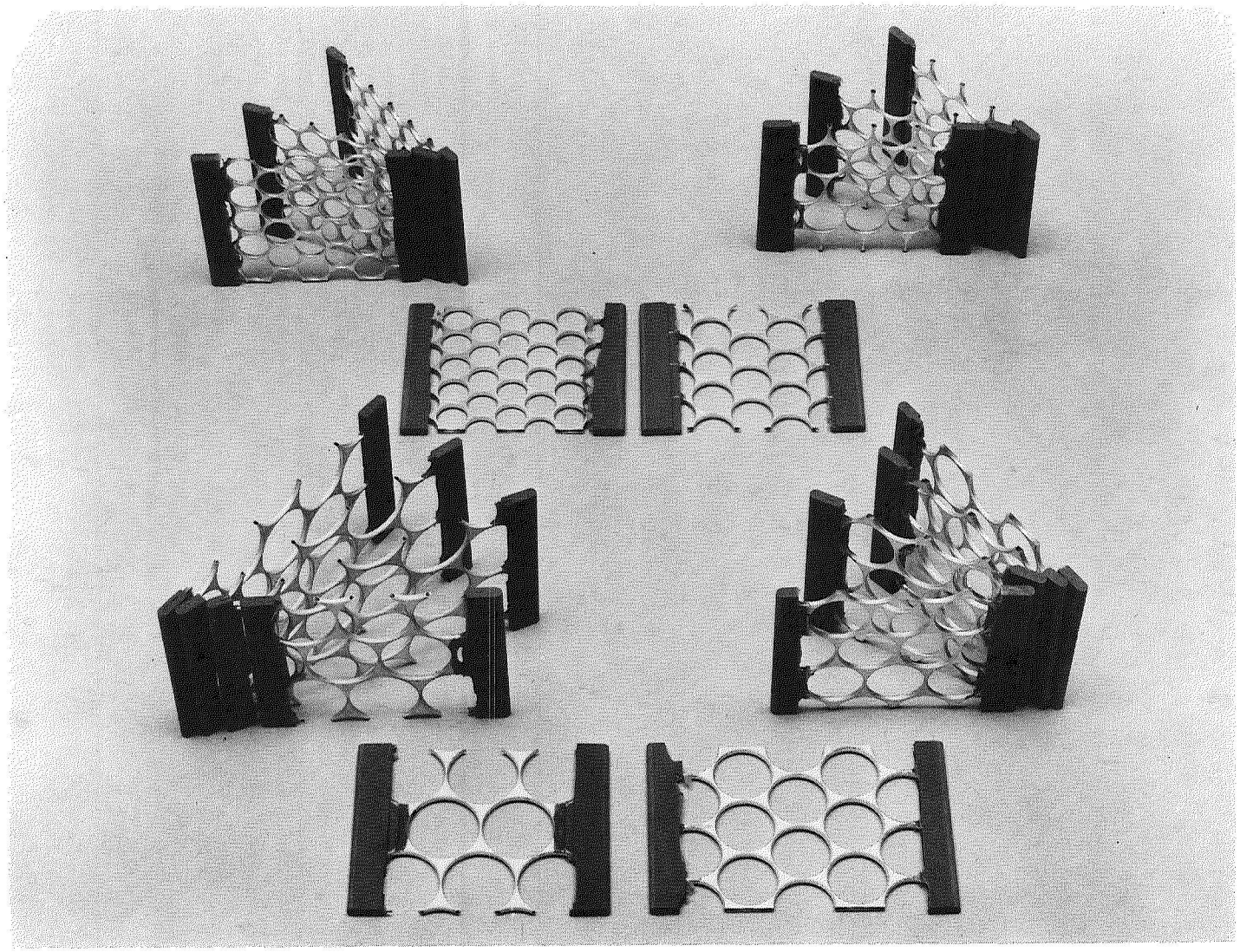

Figure A-4. Buckling Test Samples

168162

Figure A-5. Instron Testing Machine

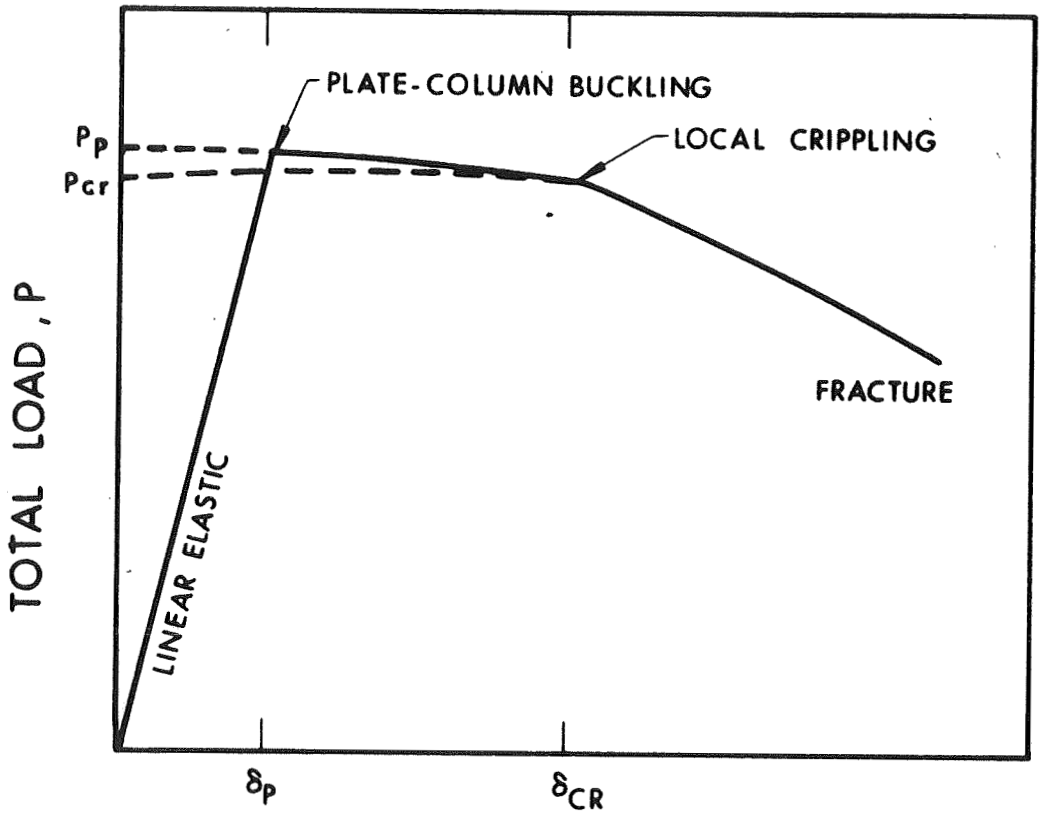

Figure A-6. Typical Load-Deflection Curve for Compression Loading

The data contained in the load versus deflection plots can be used to determine the equivalent bending thickness for the hollowcore.

Equivalent bending thickness: The equivalent bending thickness is determined from the experimental data, using the plate-column buckling load.

$$P_p = \frac{K_b \pi^2 E \ell}{(1-\mu^2)\ 12} \left(\frac{h'^3_{bending}}{L^2}\right)$$

solving the expression for $h'_{bending}$ gives

$$h'_{bending} = \left[\frac{12\ (1-\mu^2) L^2}{\pi^2\ E\ K_b} \left(\frac{P_p}{\ell}\right)\right]^{1/3}$$

where

E = 7.8×10^6 psi

μ = Poisson's ratio = 0.33

L = Length of plate column - inches

ℓ = width of plate column - inches

P_p = total applied load at initiation of plate column buckling, lb

K_b = buckling constant for plate columns $K_b = f\ (\ell/L\sqrt{C})$; $C = 1$ for simply supported boundaries. (See Fig. A-7.)

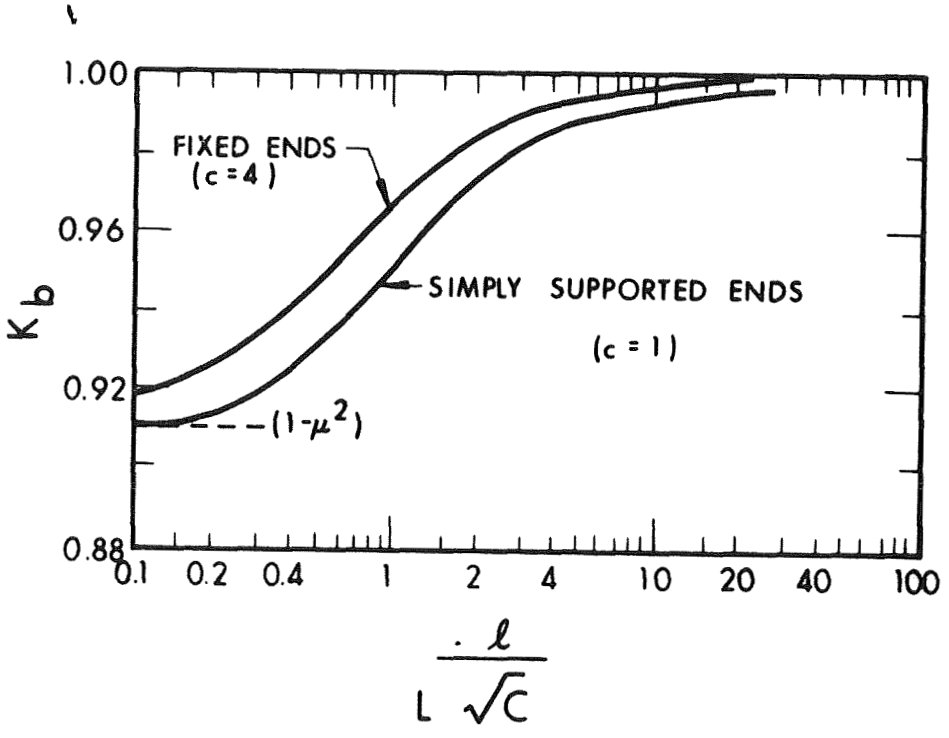

Figure A-7. Plate-Column Buckling Constants

The theoretical equivalent bending stiffness is given by the expression

$$h'_{bending} = \left[\frac{12t}{a}\left\{(2a-d)\left(\frac{h}{2}\right)^2 + \frac{h^3}{12}\right\}\right]^{1/3}$$

The calculated values for $h'_{bending}$, experimental and theoretical, are tabulated in Table A-4. The experimental values are within 10% of the theoretical values in most cases.

The nominal thicknesses, t_N, which were used in the data reduction, were determined from the plating process parameters (current density and time).

Local crippling of the skin: The pattern which forms when the skin of the hollowcore cripples under compression is shown in Fig. A-8. In this series of tests, the stress which produced the crippling was due to the combination axial and bending loads in the postbuckled plate-column. The correlation of the experimental data with the theory requires definition of the complex state of stress which exists in the postbuckled plate-column. To eliminate this difficulty, a series of tests on very short plate-columns, which will assure crippling occurs prior to Euler buckling, are required.

TABLE A-4

EXPERIMENTAL DETERMINATION OF EQUIVALENT BENDING THICKNESS $h'_{bending}$

EXPERIMENTAL $h'_{bending} = 0.00518 \left[\frac{P/\ell}{K_B} L^2\right]^{1/3}$ THEORETICAL $h'_{bending} = \left[\frac{12t}{a}\left\{(2a-d)\left(\frac{h}{2}\right)^2 + \frac{h^3}{12}\right\}\right]^{-1/3}$

Sample	Hole* Orientation	L	ℓ	S	t_N	P_p	P_p/ℓ	ℓ/L	K_B	$h'_{bending}$ experimental	h'_{bend} theoretical
h = 0.1	a = 0.40	d = 0.75									
75-1	L	5.239	4.0	0.28342	0.004	21.25	5.3125	0.763	0.942	0.0278	0.02925
75-2	L	5.207	4.0		0.003	15.00	3.7500	0.768	0.943	0.0246	0.02655
75-3	S	5.189	4.0		0.003	11.25	2.8125	0.770	0.944	0.0223	0.02655
75-4	S	5.271	4.0		0.004	21.75	5.4575	0.758	0.941	0.0281	0.02925
h = 0.1	a = 0.525	d = 1.00									
1001	L	5.339	3.5	0.36795	0.004	19.00	5.4285	0.655	0.937	0.0284	0.02672
1002	L	5.292	3.5		0.005	27.25	7.7857	0.661	0.937	0.0319	0.02875
1003	L	5.200	3.5		0.003	19.25	5.5000	0.673	0.938	0.0280	0.02425
1004	S	5.268	3.6		0.004	23.00	6.3888	0.683	0.938	0.0297	0.02672
h = 0.1	a = 0.650	d = 1.25									
1251	L	5.308	4.0	0.43494	0.004	27.500	6.8750	0.753	0.940	0.0306	0.02487
1252	L	5.317	4.0		0.005	30.75	7.6875	0.752	0.940	0.0318	0.02680
1253	L	5.216	4.0		0.006	34.75	8.6875	0.766	0.943	0.0326	0.02850
1254	S	6.210	4.0		0.004	15.00	3.7500	0.644	0.936	0.0278	0.02487
1255	S	6.290	4.0		0.006	24.00	6.0000	0.636	0.935	0.0327	0.02850
h = 0.1	a = 0.775	d = 1.50									
1501	L	5.348	2.7	0.50193	0.006	13.25	4.9075	0.504	0.930	0.0275	0.02682
1502	L	5.318	2.7		0.004	10.75	3.9815	0.507	0.930	0.0255	0.02346
1503	S	7.290	4.0		0.006	11.00	2.7500	0.548	0.932	0.0279	0.02682
1504	S	7.290	4.0		0.004	7.00	1.7500	0.548	0.932	0.0240	0.02346
1505	S	7.290	4.0		0.005	8.25	2.0625	0.548	0.932	0.0255	0.02528

*L = in line with load; S = staggered

468162

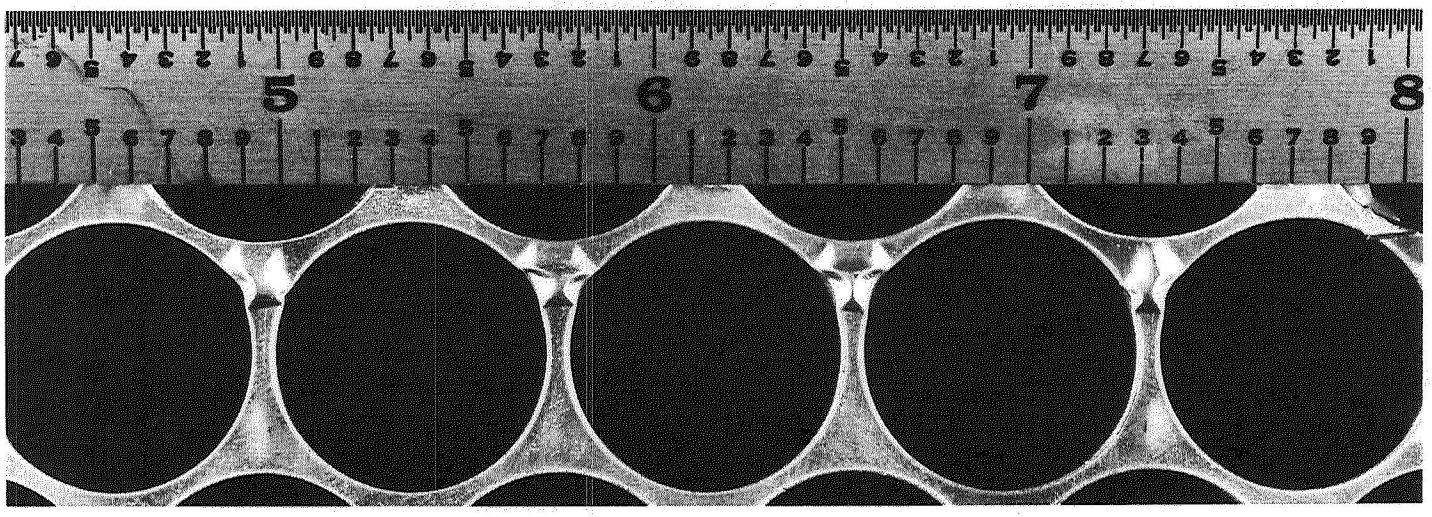

Figure A-8. Hollowcore Crippling Pattern Under Compression

APPENDIX B

BEAM ANALYSIS

Estimate of Effect of Frame Stiffness on Panel Resonant Frequency

The decrease in natural frequency of the curved panel due to flexibility of the frame is shown below.

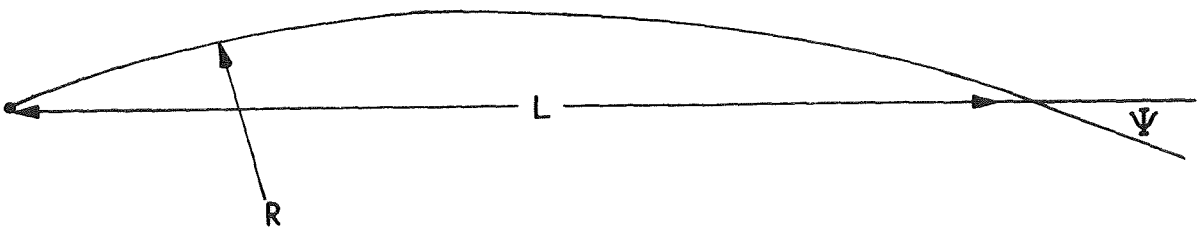

The frequency of the shell is given by

$$\omega_{mn}^{2} = \frac{1}{\rho h}\left[D\,(\lambda_n^{2} + \mu_m^{2})^{2} + \frac{Eh}{R^2}\right] \qquad \text{(B-1)}$$

where the first term is flat plate frequency and the second term is the addition due to curvature. The second term is the predominant term for low frequencies. Therefore,

$$\omega_{11}^{2} \cong \frac{E}{\rho R^2} \qquad \text{(B-2)}$$

E = Young's modulus

R = Radius of curvature

ρ = Mass density of shell

To get an idea of the effect of the elastic support frame on the fundamental frequency, form the differential of ω_{11}

$$2\omega_{11}\, d\omega_{11} = -\frac{2E\, dR}{\rho\, R^3} \tag{B-3}$$

Assuming the arc length, S, of the shell does not change

$$S = 2R\Psi = \text{constant} \tag{B-4}$$

Then

$$\begin{aligned} 2R\, d\Psi + 2\Psi\, dR &= 0 \\ d\Psi &= -\Psi \frac{dR}{R} \end{aligned} \tag{B-5}$$

Also

$$\begin{aligned} L &= 2R \sin\Psi \\ dL &= 2R \cos\Psi\, d\Psi + 2 \sin\Psi\, dR \end{aligned} \tag{B-6}$$

Substituting Eq. 5 in Eq. 6

$$dL = (-2\Psi \cos\Psi + 2 \sin\Psi)\, dR$$

so that

$$dR = \frac{dL}{2\,(\sin\Psi - \Psi \cos\Psi)} \tag{B-7}$$

Substituting Eq. 7 in Eq. 3 gives

$$\omega_{11}\, d\omega_{11} = \frac{E\, dL}{2\rho R^3\,(\Psi \cos\Psi - \sin\Psi)} \tag{B-8}$$

Solving Eq. 8 for dL gives

$$\frac{dL}{2} = \frac{\rho R^3}{E} (\Psi \cos\Psi - \sin\Psi)\ \omega_{11}\ d\omega_{11} \tag{B-9}$$

dL/2 can be interpreted as the deflection of the frame; that is, if the frame deflects dL/2, the frequency is reduced by $d\omega_{11}$.

$$v_2 = \frac{dL}{2} = \frac{\rho R^3}{E} (\Psi \cos\Psi - \sin\Psi)\ \omega_{11}\ d\omega_{11} \tag{B-10}$$

Let

$$d\omega_{11} = K\ \omega_{11} \tag{B-11}$$

Then

$$v_2 = \frac{\rho R^3}{E} (\Psi \cos\Psi - \sin\Psi)\ K\ \omega_{11}{}^2 \tag{B-12}$$

Substituting Eq. 2 in Eq. 12 gives

$$v_2 = K\ R\ \ (\Psi \cos\Psi - \sin\Psi) \tag{B-13}$$

Evaluating Eq. 13 for the specific geometry

$$R = 163.25 \text{ in}$$

$$\Psi = 10^{\circ} = \pi/18 = 0.17453 \text{ rad}$$

$$\sin\Psi = 0.17365$$

$$\cos\Psi = 0.98481$$

$$v_2 = K\ 163.25\ \ (0.17453 \times 0.98481 - 0.17365)$$

$$v_2 = -0.29058K$$

To limit the decrease in the frequency to 20% of the rigid boundary frequency, v_2 must be $v_2 \leq 0.058$ inch.

Load Distribution on the Beryllium Beam

The maximum response at the center of the shell was predicted to be 137.5 g.

Using a panel specific weight of 10.83×10^{-4} lb/in.^{2}, the maximum pressure at the center of the panel is

$$P_o = 137.5 \times 10.83 \times 10^{-4} = 0.149 \text{ psi} \tag{B-14}$$

Assuming a double sinusoidal distribution of the loading, the average pressure over the surface is

$$P_{avg} = \frac{4}{\pi^2} P_o = 0.0604 \text{ psi} \tag{B-15}$$

The membrane force at the crown of the spherical shell is

$$P_s = P_{avg} \frac{R}{2} = 0.0604 \frac{\text{lb}}{\text{in.}^2} \frac{163.25 \text{ in.}}{2}$$

$$P_s = 4.93 \text{ lb/in.} \tag{B-16}$$

This load is assumed to vary sinusoidally as shown in Fig. B-1. The forces acting on the beam, P_B, are determined as follows:

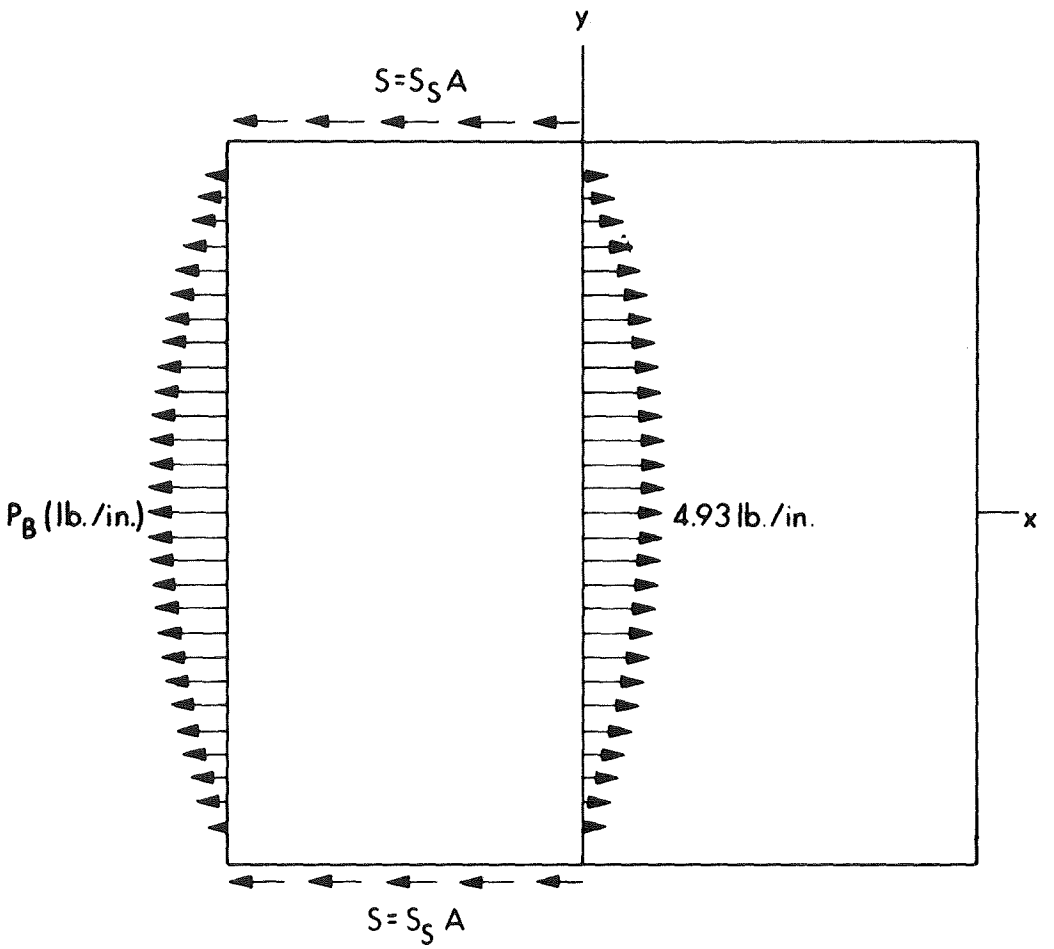

Figure B-1. Forces on Biconvex Shell

35386

Equilibrium of forces in the x direction gives the following equation:

$$\int_o^L P_s \sin \frac{\pi y}{L} dy = \int_o^L P_B \sin \frac{\pi y}{L} dy + 2S \qquad \text{(B-17)}$$

or

$$P_s \frac{(2\ L)}{\pi} = \frac{2\ L}{\pi} (P) + 2\ S$$

Solving for P_B gives

$$P_B = P_s - \frac{\pi}{L} S \qquad \text{(B-18)}$$

$$S = S_s A$$

where, S_s is the limit stress in shear for the hollowcore
A is the minimum shear area of the hollowcore

S_s will be taken as 3000 psi. Since the limit stress in tension is about 6000 psi, a shear limit stress of 3000 psi will give equal margin of safety for tension and shear.

$$A = \frac{[2(2a - d) + 2h]\ t\ L}{4a}$$

$$A = \frac{0.3\ (0.004)(L)}{0.3 \qquad 2}$$

$$A = 0.00092 \frac{L}{2}$$

$$S = 3000\ (0.00092) \frac{L}{2}$$

Therefore,

$$P_B = 4.93 - \frac{\pi}{2}(3000)(0.00092)$$

$$P_B = 0.60 \text{ lb/in.}$$

The average loading on the beam is

$$P_{B_{AVG}} = \frac{2}{\pi} 0.6 = 0.38 \text{ lb/in.}$$

Analysis of Curved Beams in the Supporting Frame

Definition of Symbols

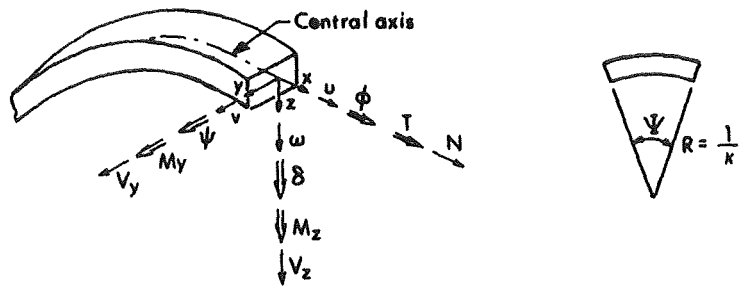

Figure B-2. Coordinates and Definition of Forces on a Segment of the Curved Beam

List of Symbols

E	Young's modulus
G	shear modulus
$K = 1/R$	curvature of central axis
Ψ	central arc
GJ_T	torsional stiffness
EJ_Z	bending stiffness about Z axis
P	tension (compression) load in membrane lb/in
d	width of beam

Mathematical Model

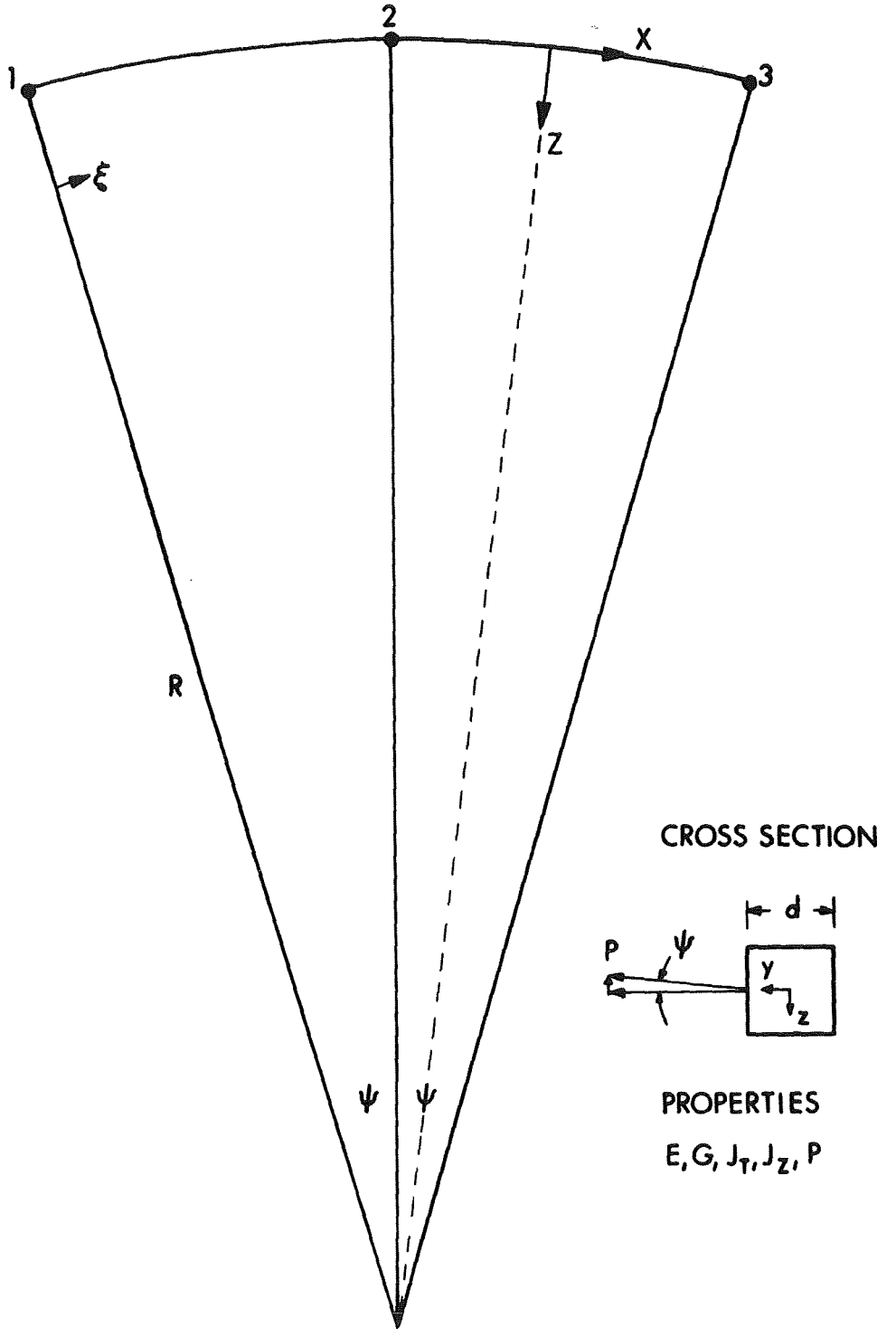

Analysis

The state vectors at sections 1, 2, and 3 are

$$Z_1 = \{\phi_1 \; v_1 \; \theta_1 \; M_{Z_1} \; - V_{y_1} \; T_1\}$$

$$Z_2 = \{\phi_2 \; v_2 \; \theta_2 \; M_{Z_2} \; - V_{y_2} \; T_2\}$$

$$Z_3 = \{\phi_3 \; v_3 \; \theta_3 \; M_{Z_3} \; - V_{y_3} \; T_3\}$$

The transfer matrix which relates these state vectors is shown in Table B-I.

TABLE B-I

TRANSFER MATRIX

$$U = \begin{bmatrix} \cos\Psi & 0 & \sin\Psi & \left(\frac{1}{GJ_T} + \frac{1}{EJ_Z}\right)\frac{R\Psi}{2}\sin\Psi & \left(\frac{1}{GJ_T} + \frac{1}{EJ_Z}\right)R^2F_3 & \frac{RF_1}{GJ_T} - \frac{RF_3}{EJ_Z} \\ -R(1-\cos\Psi) & 1 & R\sin\Psi & u_{24} & u_{25} & -\left(\frac{1}{GJ_T} + \frac{1}{EJ_Z}\right)R^2F_3 \\ -\sin\Psi & 0 & \cos\Psi & u_{34} & u_{35} & -\left(\frac{1}{GJ_T} + \frac{1}{EJ_Z}\right)\frac{R\Psi}{2}\sin\Psi \\ 0 & 0 & 0 & \cos\Psi & R\sin\Psi & -\sin\Psi \\ 0 & 0 & 0 & 0 & 1 & 0 \\ 0 & 0 & 0 & \sin\Psi & R(1-\cos\Psi) & \cos\Psi \end{bmatrix}$$

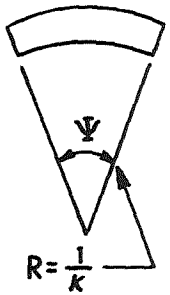

where $u_{24} = u_{35} = R^2/2EJ_Z\ \Psi\sin\Psi - R^2/GJ_T\ F_5$

$u_{25} = R^3/EJ_Z\ F_3 - R^3/GJ_T\ F_6$

$u_{34} = R/EJ_Z\ F_1 - R/GJ_T\ F_3$

TABLE B-I (concluded)

TRANSFER MATRIX

Where we use the following abbreviations:

$$F_1(\Psi) = 1/2\ (\Psi \cos\Psi + \sin\Psi) = \Psi - \frac{2}{3!}\Psi^3 + \frac{3}{5!}\Psi^5 - \frac{4}{7!}\Psi^7 + \frac{5}{9!}\Psi^9 - \ldots$$

$$F_2(\Psi) = \Psi \sin\Psi + \cos\Psi - 1 = \frac{1}{2!}\Psi^2 - \frac{3}{4!}\Psi^4 + \frac{5}{6!}\Psi^6 - \frac{7}{8!}\Psi^8 + \ldots$$

$$F_3(\Psi) = 1/2\ (\sin\Psi - \Psi \cos\Psi) = \frac{1}{3!}\Psi^3 - \frac{2}{5!}\Psi^5 + \frac{3}{7!}\Psi^7 - \frac{4}{9!}\Psi^9 + \ldots$$

$$F_4(\Psi) = 2 \sin\Psi - \Psi \cos\Psi - \Psi = \frac{1}{3!}\Psi^3 - \frac{3}{5!}\Psi^5 + \frac{5}{7!}\Psi^7 - \frac{7}{9!}\Psi^9 + \ldots$$

$$F_5(\Psi) = 1/2\ (2 - 2 \cos\Psi - \Psi \sin\Psi) = \frac{1}{4!}\Psi^4 - \frac{2}{6!}\Psi^6 + \frac{3}{8!}\Psi^8 - \frac{4}{10!}\Psi^{10} + \ldots$$

$$F_6(\Psi) = 1/2\ (2\Psi + \Psi \cos\Psi - 3 \sin\Psi) = \frac{1}{5!}\Psi^5 - \frac{2}{7!}\Psi^7 + \frac{3}{9!}\Psi^9 - \frac{4}{11!}\Psi^{11} + \ldots$$

The matrix relations are

$$Z_2 = U \; Z_1$$

$$Z_3 = U \; Z_2$$

The loading conditions resulting in the beam from the membrane forces can be calculated by forming the extended transfer matrix $\tilde{U}$ using the relations in Table B-II.

$$\tilde{U} = \left[\begin{array}{c|c} & r_1 \\ & r_2 \\ & r_3 \\ U & r_4 \\ & r_5 \\ & r_6 \\ \hline 0\;0\;0\;0\;0\;0 & 1 \end{array}\right]$$

$$\tilde{Z}_2 = \tilde{U} \; \tilde{Z}_1$$

$$\tilde{Z}_3 = \tilde{U} \; \tilde{Z}_2$$

$$\tilde{Z} = \{ Z \;\vdots\; 1 \}$$

The matrix equations which relate the extended state vectors are:

$$\tilde{Z}_2 = \tilde{U} \; \tilde{Z}_1$$

$$\tilde{Z}_3 = \tilde{U} \; \tilde{Z}_2$$

TABLE B-II

TRANSFER MATRIX RELATIONS

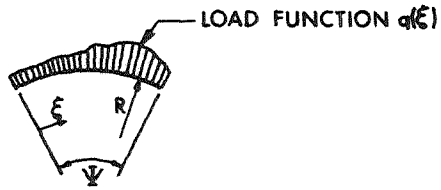

Load acting perpendicular to plane of arch

$q_y(\epsilon)$ = distributed load in y direction = $P \cos\Psi$

$t_x(\epsilon)$ = distributed torque about x axis = $1/2\ pd \sin\Psi$

$m_z(\epsilon)$ = distributed moment about z axis = 0

Load column vector r (seventh column in extended transfer matrix $\tilde{U}$):

$$r = U(\Psi)\{r_1\ r_2\ r_3\ r_4\ r_5\ r_6\}$$

$$r_1 = \phi = R^2 \int_0^{\Psi} \left[t_x\left(\frac{1}{GJ_T} F_1 - \frac{1}{EJ_z} F_3\right) - m_z \frac{1}{2}\left(\frac{1}{EJ_z} + \frac{1}{GJ_T}\right) \epsilon \sin\epsilon - q_y R\left(\frac{1}{EJ_z} + \frac{1}{GJ_T}\right) F_3 \right] d\epsilon$$

$$r_2 = \tilde{v} = R^3 \int_0^{\Psi} \left[- t_x\left(\frac{1}{EJ_z} + \frac{1}{GJ_T}\right) F_3 - m_z\left(\frac{1}{2}\frac{1}{EJ_z} \epsilon \sin\epsilon - \frac{1}{GJ_T} F_5\right) - q_y R\left(\frac{1}{EJ_z} F_3 - \frac{1}{GJ_T} F_6\right) \right] d\epsilon$$

Solution for particular case:

$$\Psi = 10^{o}$$
$$R = 163.25 \text{ in.}$$

Boundary conditions

$$v_1 = 0$$
$$v_3 = 0$$
$$\phi_1 = 0$$
$$\phi_3 = 0$$
$$T_1 = T_3$$
$$M_{z_1} = M_{z_3}$$
$$\theta_1 = 0$$
$$\theta_2 = 0$$
$$\theta_3 = 0$$
$$V_{y_1} = -V_{y_3}$$

The deflection normal to the plane of curvature of the beam at the center of the span for uniformly distributed load is given by

$$v_2 = \alpha P + \beta M_1$$

where v_2 = Deflection at center span
P = Uniform load - lb/in.
M_1 = Bending moment at end of beam

$$\alpha = R^4 (r_1 a + r_2 b) + \frac{R^3 d}{2} (r_3 a + r_4 b)$$

$$\beta = -R^2 \left[\frac{\Psi \sin\Psi}{2 \cos\Psi} a + \left(\frac{\Psi \sin\Psi}{2 \cos^2\Psi} - \frac{1-\cos\Psi}{\cos\Psi} \right) b \right]$$

$$a = \frac{1}{EJ_z} ; \qquad b = \frac{1}{GJ_T}$$

$$M_1 = \frac{RP[(Ra \cos\Psi - d/2 \{a + b\}\sin\Psi)(\Psi - \sin\Psi \cos\Psi) + Rb\Psi \cos\Psi(\cos\Psi-1)^2]}{a (\Psi + \sin\Psi \cos\Psi) + b (\Psi - \sin\Psi \cos\Psi)}$$

Solving these expressions for the case where d = 2.00, E = 42.0 x 10^6, and G = 19.3 x 10^6.

t	v_2/P
0.004	0.32085
0.006	0.21385
0.008	0.16040
0.010	0.12832
0.012	0.10694
0.014	0.09164
0.016	0.08024

APPENDIX C

THERMAL ANALYSIS

This appendix presents the analysis performed to predict the steady-state operating temperature for a sun-oriented hollowcore panel in earth space, and to estimate the overall heat transfer coefficient for these conditions.

Mathematical Model

Figure C-1 shows a cross section of the hollowcore panel which defines the geometry and thermal properties. Figure C-2 is the thermal network used in the analysis. Radiation between the dielectric and the aluminum hollowcore is neglected.

The quantities in Fig. C-2 are defined as follows:

A_1 = Unit area on sun side

A_2 = Percent of unit area which exposes H-film on back side

A_3 = Percent of unit area which is hollowcore surface

α_{11} = Absorptivity of solar cell with 1 mil filter, assume $\alpha_{11} = 0.82$

ϵ_{11} = Emissivity of silicon, assume $\epsilon_{11} = 0.80$

σ = Stefan-Boltzmann constant, 0.173×10^{-8} Btu/ft^2 hr $(^oR)^4$

μ = Fraction of solar radiation converted to electricity, assume $\mu = 0.0938$

G_s = Intensity of solar radiation in earth space, 130 watts/ft^2

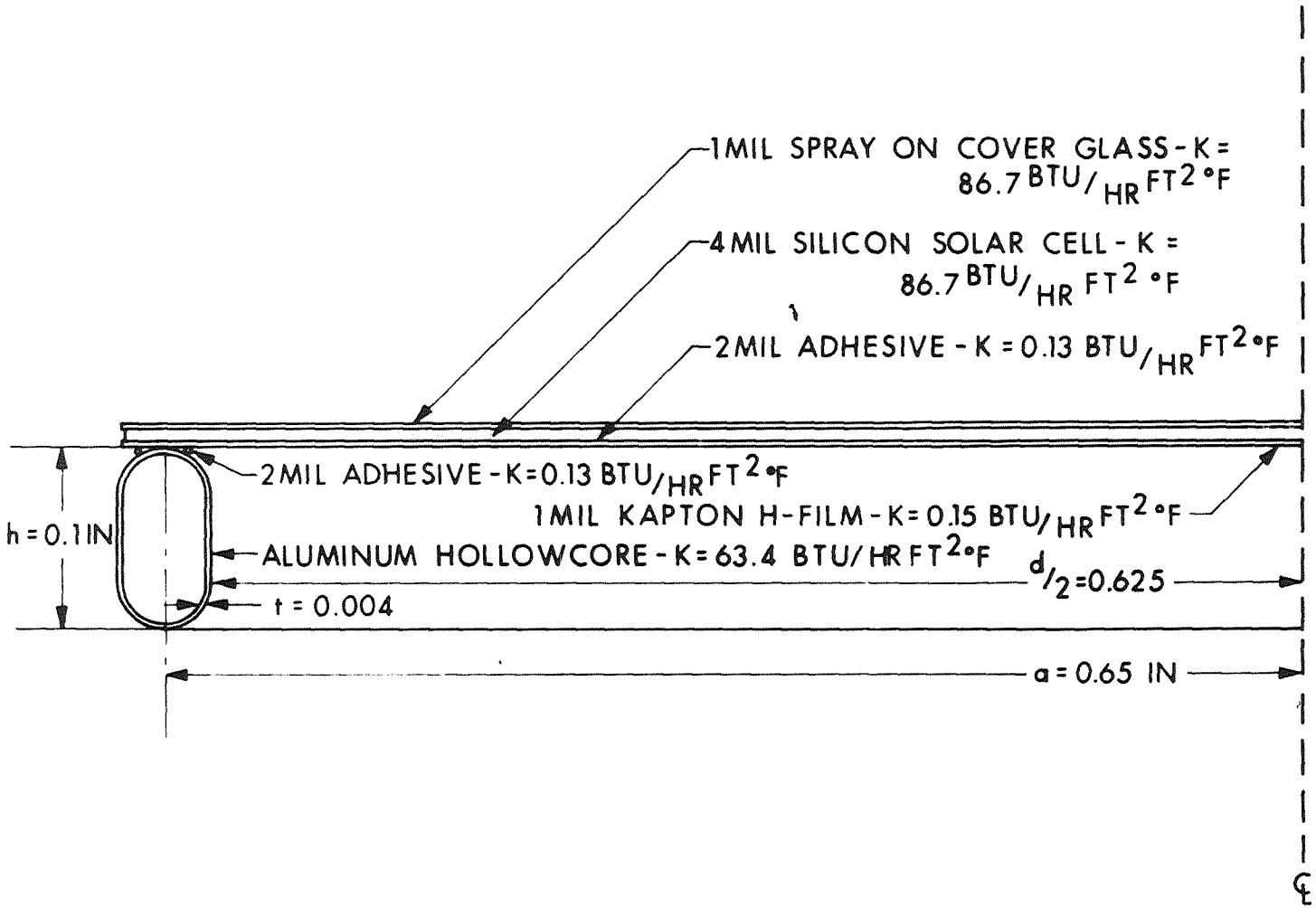

Figure C-1. Cross Section of Hollowcore Panel

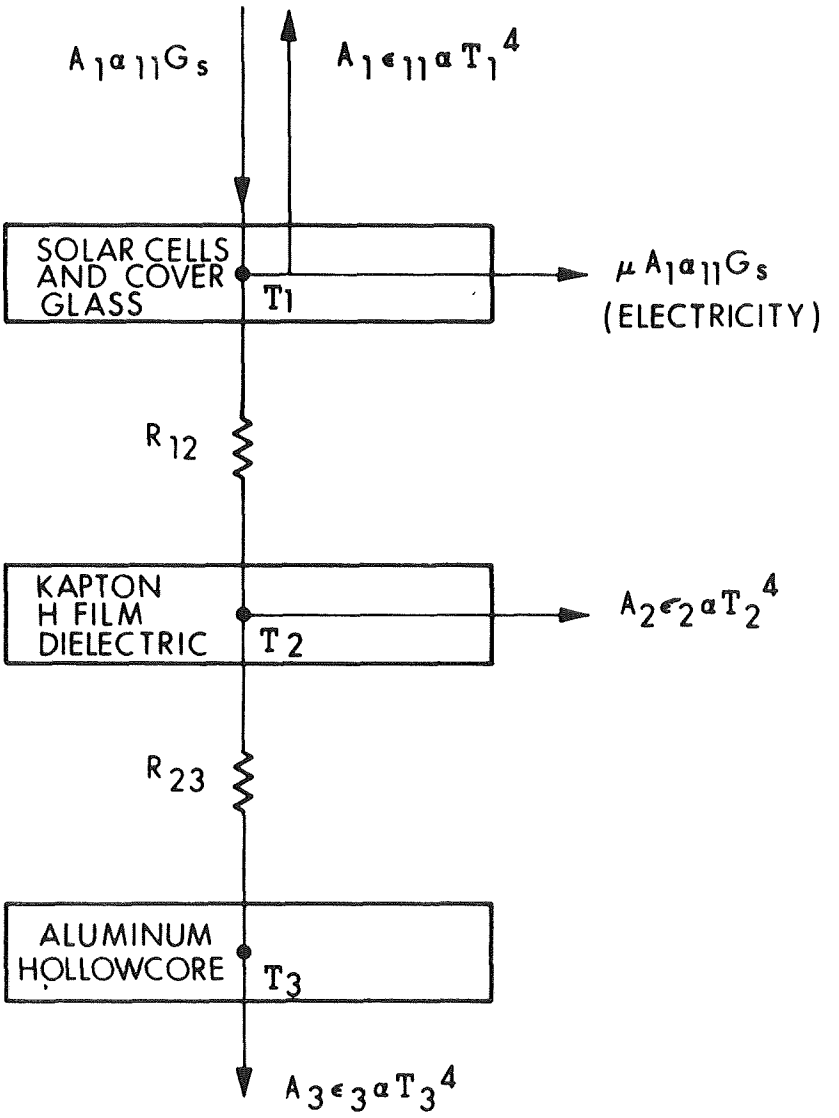

Figure C-2. Thermal Network

30684

ϵ_2 = Emissivity of Kapton H-film, assume ϵ_2 = 0.80

ϵ_3 = Emissivity of aluminum hollowcore surface with thin thermal control coating, ϵ_2 = 0.70

R_{12} = Thermal resistance of cover glass, cell, cell adhesive, and H-film dielectric

R_{23} = Thermal resistance of dielectric adhesive and aluminum hollowcore

T_1 = Average cell temperature, ^oR

T_2 = Average temperature of back surface of the H-film, ^oR

T_3 = Average temperature of the back surface of the hollowcore

Calculation of Percent Open Area in Hollowcore Substrate and Areas A_1, A_2, A_3, and $A_{cylinder}$

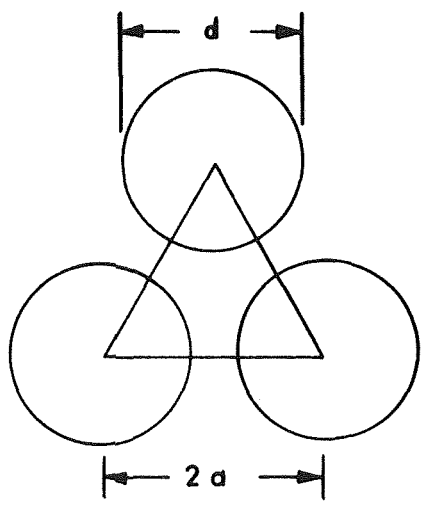

$$\text{Open area} = \frac{1}{2}\pi\left(\frac{d}{2}\right)^2$$

$$\text{Total area} = \sqrt{3}\ a^2$$

$$\frac{\text{Open area}}{\text{Total area}} = \frac{\pi}{8\sqrt{3}} \left(\frac{d}{a}\right)^2$$

$$\% \text{ open area} = 22.673 \left(\frac{d}{a}\right)^2$$

for $d = 1.25$ in.

$a = 0.65$ in.

$$\% \text{ open area} = 83.85$$

A_1 will be taken as 1.0 ft^2

then,

A_2 is 0.8385 ft^2

and,

A_3 is 0.1615 ft^2

The percentage of the unit area which is conducting from the front surface to the back surface is called $A_{cylinders}$ and is calculated as follows:

$$A_{cylinders} = \frac{\pi d t}{2\sqrt{3}\ a^2}$$

$d = 1.25$

$t = 0.004$

$a = 0.65$

$$A_{cylinders} = 0.0107$$

Calculation of Thermal Resistances

$$R_{12} = \frac{\Delta X_{cell}}{K_{s1} A_1} + \frac{\Delta X_{adhesive}}{K_{adhesive} A_1} + \frac{\Delta X_{H\text{-}film}}{K_{H\text{-}film} A_1}$$

Since T_1 is the average cell temperature, ΔX_{cell} is one-half the total cell and spray-on coverglass thickness:

$$\Delta X_{cell} = (0.004 + 0.001)/2 = 0.0025 \text{ in.}$$

$$R_{12} = \frac{0.0025}{86.7 \times 12} + \frac{0.002}{0.13 \times 12} + \frac{0.001}{0.15 \times 12}$$

$$R_{12} = (0.0024 + 1.282 + 0.555) \times 10^{-3} = 1.84 \times 10^{-3} \frac{\text{hr } ^{\circ}\text{F}}{\text{Btu}}$$

$$R_{23} = \frac{\Delta X_{adhesive}}{K_{adhesive} A_3} + \frac{\Delta X_{hollowcore}}{K_{hollowcore} A_{cylinders}}$$

$$R_{23} = \frac{0.002}{0.13 \times 0.1615 \times 12} + \frac{0.10}{69.4 \times 0.0107 \times 12}$$

$$R_{23} = (7.938 + 11.222) \times 10^{-3} = 19.16 \times 10^{-3} \frac{\text{hr } ^{\circ}\text{F}}{\text{Btu}}$$

Equations of Steady-State Thermal Equilibrium

Node 1 $$(1 - \mu) A_1 \alpha_{11} G_s = A_1 \epsilon_{11} \sigma T_1^4 + \frac{(T_1 - T_2)}{R_{12}}$$

Node 2 $$\frac{(T_1 - T_2)}{R_{12}} = A_2 \epsilon_2 \sigma T_2^4 + \frac{(T_2 - T_3)}{R_{23}}$$

Node 3 $$\frac{(T_2 - T_3)}{R_{23}} = A_3 \epsilon_3 \sigma T_3^4$$

Substituting the known or assumed quantities in these equations gives

$$\text{Node 1} \quad 329.693 = 393.174\ \sigma T_1^4 + 978.261\ (T_1 - T_2)$$

$$\text{Node 2} \quad 978.261\ (T_1 - T_2) = 329.676\ \sigma T_2^4 + 93.946\ (T_2 - T_3)$$

$$\text{Node 3} \quad 93.946\ (T_2 - T_3) = 55.56\ \sigma T_3^4$$

If the blackbody emissive power (σT_i^4) is in watts/in.^{2} and temperatures in $^{\circ}$K, rearranging and simplifying gives

$$\text{Node 1} \quad \sigma T_1^4 - 0.8385 + 2.488\ (T_1 - T_2) = 0$$

$$\text{Node 2} \quad \sigma T_2^4 - 2.967\ (T_1 - T_2) + 0.285\ (T_2 - T_3) = 0$$

$$\text{Node 3} \quad \sigma T_3^4 - 1.691\ (T_2 - T_3) = 0$$

These nonlinear equations were solved by iteration to give the following results:

$$\text{Node 1} \quad T_1 = 328.10^{\circ}\text{K} = 590.58^{\circ}\text{R} = 130.6^{\circ}\text{F}$$

$$\text{Node 2} \quad T_2 = 327.93^{\circ}\text{K} = 590.27^{\circ}\text{R} = 130.3^{\circ}\text{F}$$

$$\text{Node 3} \quad T_3 = 327.68^{\circ}\text{K} = 589.82^{\circ}\text{R} = 129.8^{\circ}\text{F}$$

This is the greatest differential that would be encountered. The panel is assumed to be in near earth space, but without a large view factor of the earth. In a very low orbit it will stabilize at a higher temperature. However, the gradient across the panel is always less since the back side is heated by sunlight reflected from the earth.

APPENDIX D

DYNAMIC ANALYSIS

Prediction of Fundamental Resonant Frequency of the Biconvex Shell - Simply Supported Boundary

The natural frequency of the biconvex shell, assuming simply supported boundarys, is calculated as follows:

$$f_{11} = \frac{1}{2\pi}\sqrt{\frac{1}{\rho h}\left[D\,(\lambda_1^2 + \mu_1^2)^2 + \frac{Eh'}{R^2}\right]}$$

(see EOS Report 7027-IDR, 18 May 1966, Appendix E)

$$\rho h = \frac{0.155 \text{ lb sec}^2 \text{ ft}^2}{386 \text{ in. ft}^2 \ (144)\text{in.}^2} = 2.7885 \times 10^{-6} \frac{\text{lb sec}^2}{\text{in}^3}$$

$$D = \frac{Et}{a}\left[\left\{(2a - d)\left(\frac{h}{2}\right)^2 + \frac{h^3}{12}\right\}\right]$$

$a = 0.65$

$d = 1.25$

$h = 0.10$

$E = 7.8 \times 10^6$

$t = 0.004$

$D = 10$

$$\lambda_1 = \mu_1 = \frac{\pi}{58.13} = 0.05404$$

$$D(\lambda_1^2 + \mu_1^2)^2 = 3.41 \times 10^{-4}$$

$$h' = \left[2 + \frac{h}{a} - \frac{\sqrt{3}}{2}\left(\frac{d}{a}\right)\right] t = 0.00195$$

$$R = 163.25$$

$$\frac{Eh'}{R^2} = 0.57071$$

$$f_{11} = \frac{10^3}{2\pi}\sqrt{\frac{1}{2.7885}\left[0.000341 + 0.57071\right]} = \frac{10^3}{2\pi}\sqrt{0.20478} = 72.02 \text{ Hz}$$

Prediction of the Resonant Frequencies of the Solar Panel Structure Including the Eleastic Effect of the Frame

The first six resonant frequencies and the associated mode shapes of the shell-frame combination have been computed using the STAR DYNE structural analysis routine on the Control Data Corporation 6600 digital computer.

Mathematical Model. - The geometry of the mathematical model used in the computer analysis is shown in Fig. D-1. One quadrant of the panel structure was modeled, and the conditions of symmetry were used to establish appropriate boundary conditions for symmetric and antisymmetric modes.

The stiffness matrix for this model was constructed using the elemental stiffness matricies for homogeneous, flat, triangular plates and uniform cross-sectional straight beams. The stiffnesses of the plates were derived based on the equivalent thickness and mechanical properties of electroformed aluminum hollowcore. The stiffnesses of the beam elements were derived based on the mechanical properties of cross-rolled beryllium sheet. The section properties of the aluminum and magnesium beam elements were scaled to equivalent beryllium sections.

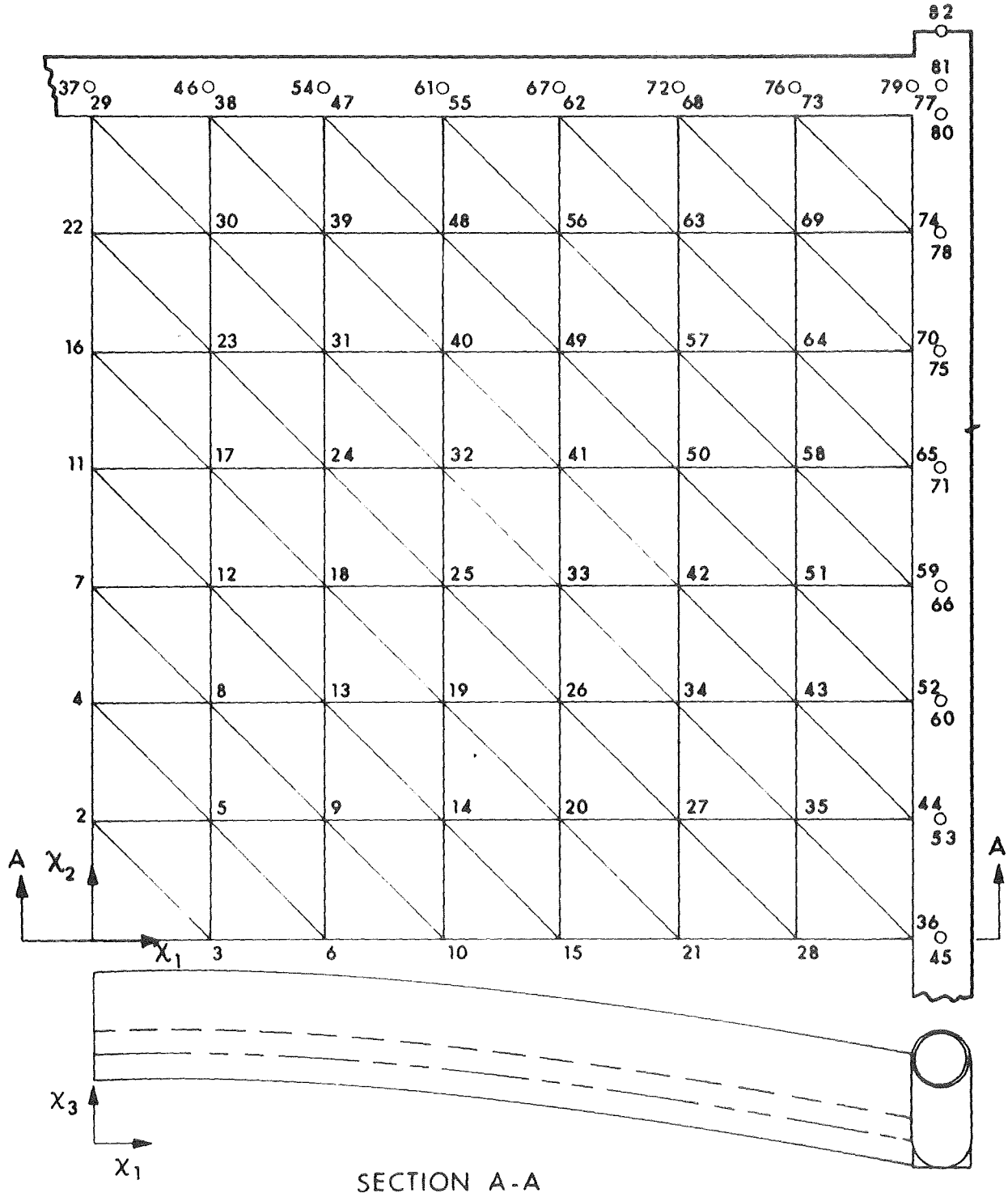

Figure D-1. Geometry of Mathematical Model for Computer Analysis

30683

The mass of the panel was lumped at the nodes of the model. The calculation of the distribution is included in Subsection 2.2.2.2.5.

Each of the sets of three coordinates which define the position of a triangular plate element is connected with two plate elements in the mathematical model. One plate has the equivalent thickness of the hollowcore based on area, and carries in-plane loads only. The other plate has the equivalent thickness based on cross sectional moment of inertia, and carries bending and transverse shear loads.

Calculation of input for computer analysis. - The equivalent stiffness fo for the bars which simulate the clip and attachment to the beryllium b beam was calculated as follows:

The mathematical model in Fig. D-2 simulates the element shosn in Fig. D-3.

The deflection of a cylinder, of length under a line load P = pl, is

$$\xi_1 = 0.0305 \left[12 (1 - \nu^2)\right]^{5/8} \frac{R^{3/4} \ell^{1/2} P}{t^{9/4} E} \quad \text{(from Roark)}$$

The deflection of the model element is

$$\xi_1 = \frac{P\ell_E}{EA}$$

The area of the model element is obtained by equating these two expressions and solving for A,

$$A = \frac{\ell_E t^{9/4}}{0.0305 \left[12(1 - \nu^2)\right]^{5/8} R^{3/4} \ell^{1/2}}$$

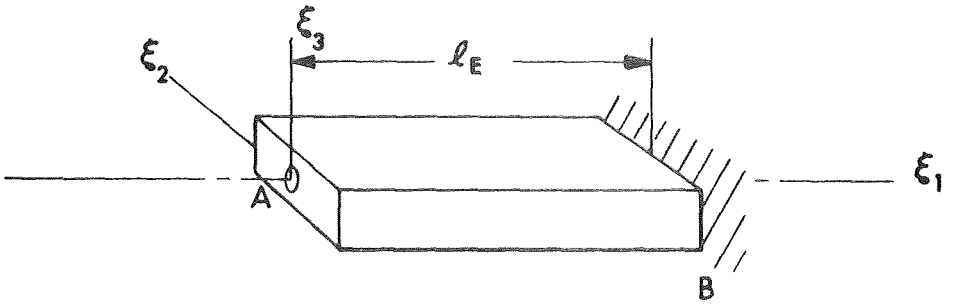

Figure D-2. Mathematical Model

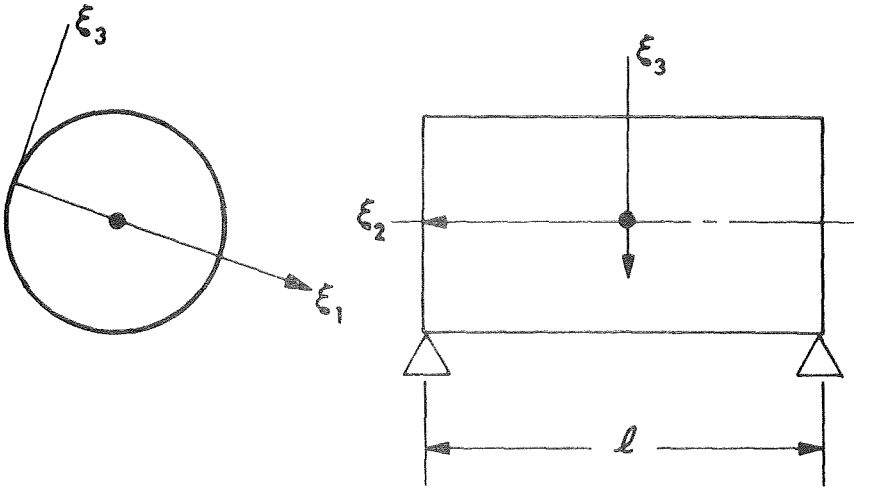

Figure D-3. Section of the Beryllium Beam

30682

$$\ell_E = 1.0 \text{ in.}$$

$$t = 0.012 \text{ in.}$$

$$R = 1.0 \text{ in.}$$

$$\ell = 4.15 \text{ in.}$$

$$= 0.1$$

$$A = \frac{(0.012)^{9/4}}{0.0305\ [12(0.99)]^{5/8}\ (4.15)^{1/2}}$$

$$A = \frac{4.76 - 6 \times 10^{-5}}{0.0305\ (5.33)\ (2.03715)}$$

$$A = 1.44 \times 10^{-4} \text{ in.}^2$$

The torsional deflection of the mathematical model is

$$\theta = \frac{T_{\xi_1}\ \ell_E}{JG}$$

The corresponding deflection of the actual member is

$$\theta = \frac{T_{\xi_1}\ \ell}{E\ I}$$

The torsional stiffness constant for the model is obtained by equating these expressions,

$$J = \frac{\ell_E\ EI}{1\ G}$$

$$\ell_E = 1.0 \text{ in.}$$

$$\ell = 4.15 \text{ in.}$$

$$E = 42 \times 10^6 \text{ psi}$$

$$G = 20 \times 10^6 \text{ psi}$$

$$I = \pi R^3 T = 0.03769$$

$$J = \frac{\ell\ (42)\ (0.03769)}{4.15\ (20)} = 0.01907$$

The bending stiffnesses about the ξ_2 and ξ_3 axes are large, i.e., the bars connecting joints such as 36 and 45, 44 and 53, etc., are essentially rigid members in bending. The elements will be assigned a section moment of inertia of 0.2 in.^{4} about both ξ_2 and ξ_3.

The section properties of the beryllium beam are

$$\text{Area} = A\ \pi r^3 t = 2\pi\ (1.0)\ (0.012) = 0.07538 \text{ in.}^2$$

$$\text{Torsional } J = 2\pi r^3 t = 0.07538$$

$$\text{Bending } I = \pi r^3 t = 0.03769$$

$$\text{Shear coefficient } K = \frac{2(1 + \nu)}{4 + 3\nu} + 0.51$$

$$E = 42 \times 10^6 \text{ psi Young's modulus}$$

$$\nu = 0.1$$

The section properties of the aluminum hollowcore are calculated below.

The equivalent membrane thickness of the aluminum hollowcore is

$$h' = \left[2 + \frac{h}{a} - \frac{3}{2}\left(\frac{d}{a}\right)\right] t = 0.00195$$

For

$$h = 0.10$$

$$a = 0.65$$

$$d = 1.25$$

$$t = 0.004$$

The equivalent thickness of the hollowcore, based on bending stiffness, is

$$h'_{bend} = \left[\frac{12t}{a}(2a - d)\left(\frac{h}{2}\right)^2 + \frac{h^3}{12}\right]^{1/3}$$

$$h'_{bend} = 0.02475$$

The modulus of electroformed aluminum is 7.8×10^6 psi; Poisson's ratio is 0.33.

The section properties of the end fitting are

$$A = \frac{1}{2}(2bt + rbt)$$

$$\text{Average} = 3bt = 0.360$$

$$\text{A model 81-82} = \frac{E_{MG}}{E_{BE}}(0.360) = 0.05571$$

The torsional section is

$$J_{AVG} = \left(b^3t + \frac{2}{3}bt^3\right)$$

$$= \left[8\,(0.060) + 1.333\,(0.06)^3\right]$$

$$J_{AVG} = 0.48$$

$$J_{81-82} = \frac{E_{MG}}{E_{BE}}(0.48) = 0.07$$

The bending section moment-of-inertia is

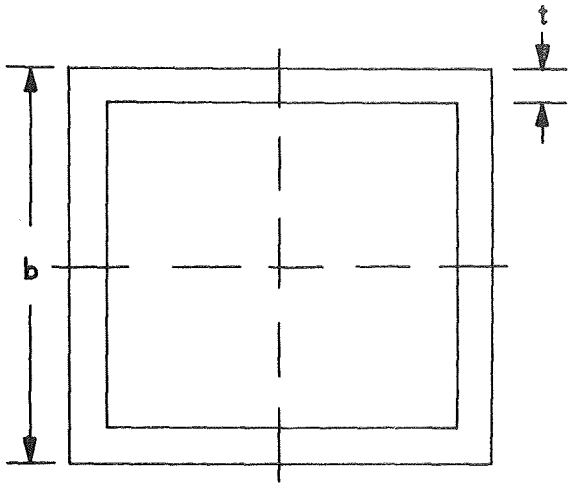

$$I = 2bt\left(\frac{b}{2}\right)^2 + 2\,\frac{1}{12}\,tb^3$$

$$I = t\left(4 + \frac{4}{3}\right)$$

$$I = 0.060\ (5.333) = 0.31999$$

$$I_{model} = \frac{E_{MG}}{E_{BE}}\,(0.32) = 0.04952$$

The weight distribution was developed as described below.

The effects of rotary inertia will be neglected.

Each node of the shell not on the outside boundary will be assigned the weight corresponding to 4.15^2 in.^{2}.

$$W_s = 0.155\ \frac{lb}{ft^2} \times \frac{ft^2}{144\ in.^2} \times 4.15^2\ in.^2 = 0.01853\ lb$$

The nodes on the boundary of the shell will be assigned a weight which includes the weight of the clip.

$$W_{BS} = 1/2\ W_S + \left(\frac{4.15}{12} \times 0.018\ \frac{lb}{ft}\right)$$

$$W_{BS} = 0.009265 + 0.00622 = 0.01549\ lb$$

The nodes on the center line of the beryllium beam will be assigned a weight calculated as follows:

$$W_{BE} = \rho AL = 0.065 \frac{lb}{in.^3} \times 0.07539 \text{ in.}^2 \times 4.15 \text{ in.}$$

$$W_{BE} = 0.02033 \text{ lb}$$

Joints 79 and 80 will have 1/2 W_{BE}

Joint 81 will have the weight of the hinge fitting

$$W_F = 0.10 \text{ lb}$$

No weight will be assigned to joint 82.

Results of Computer Analysis. - The first six symmetric modes and associated natural frequencies of the solar panel structure have been determined by extracting the lowest six eigenvalues and eigenvectors from the set of equations.

$$([K] - \omega_r^2 [M]) \{q^{(r)}\} = 0$$

where:

$[K]$ = stiffness matrix (492 x 492)

$[M]$ = diagonal mass matrix

$\omega_r^2 = (2\pi f_r)^2$ = r^{th} eigenvalue

$q^{(r)}$ = r^{th} eigenvector

The boundary conditions were set to give zero rotation about the X_2 axis at nodes on the line 1 to 37 and zero rotation about the X_1 axis at nodes on the line 1 to 45. These conditions establish the symmetric modes. The first six natural frequencies of symmetric modes are:

Symmetric Mode No.	Frequency (Hz)
1	55.94
2	65.65
3	71.11
4	82.65
5	87.73
6	109.66

This analysis shows that the elastic boundary conditions produced by the beryllium frame structure reduce the frequency of the shell from 72 Hz, calculated previously, to 55.74 Hz.

Overall Buckling of Substrate

The critical pressure for overall buckling of the biconvex shell is given by

$$|P_{CR}| = \frac{D(\lambda_n^2 + \mu_m^2)^2 + \frac{Eh'}{R^2}}{\frac{R}{2}(\lambda_n^2 + \mu_m^2)}$$

Using the values for the parameters listed with the natural frequency calculation,

$$|P_{CR}| = \frac{(3.141 + 10^{-4} + 0.57071)}{\frac{163.25}{2}(0.00584)}$$

$$|P_{CR}| = \frac{2 \times 0.57105}{163.25\ (0.00584)} = 1.2 \text{ psi}$$

The margin of safety of overall buckling is

$$MS = \frac{\text{critical pressure}}{\text{applied pressure} \times FS} - 1$$

A conservative estimate of the maximum applied pressure is obtained by multiplying the panel specific weight by the maximum predicted acceleration response. The maximum response is predicted to be 137.6 g at the center of the panel. The actual effective pressure will follow a sinusoidal distribution (zero on the boundaries, maximum at the center), but, for this calculation, the maximum pressure will be assumed to act over the entire surface. Then,

$$\begin{aligned} \text{Applied pressure} &= 137.5\ (\text{SpWt})\ \text{Panel} \\ &= 137.5\ (0.00176) \\ &= 0.148 \text{ psi} \end{aligned}$$

The margin of safety is

$$MS = \frac{1.20}{0.148 \times 1.25} - 1 = 5.49$$

APPENDIX E

SAFETY AND OPERATING PROCEDURES

Safety

Electroforming cell housing. - The electroforming cell was engineered for maximum control of the environmental variable which is known to react with any or all of the ethereal plating solution constituents. Should there be an accidental explosion or fire, the housing has been designed for a controlled release of any excess pressure (directed away from personnel and equipment) and extinguishing of fire. The above provisions were implemented by the following:

1. The plating room will support a maximum explosive condition involving less than 1 gal of diethyl ether solvent, based on the stoichiometric principle of oxygen to flammable material ratio.

2. The facility has a release wall constructed to relieve excess pressure of approximately 25 to 30 psi.

3. All equipment is explosive-proof, Class I, Division II, as spelled out in Article 22, Title 8, State of California Division of Industrial Safety Electronic Orders. All equipment is grounded internally as well as externally.

4. This room is ventilated by a once-through air change per minute system with pickups at floor level.

5. An Ansul No. 150 dry chemical dump system, the sensing heads of which are actuated by a rapid rate of rise to 160°F, provides fire control. The air ventilation system is interlocked to shut down prior to discharge of the dry chemical. Additionally, the dump system acuates an air-horn alarm.

Personnel control. - Only personnel assigned to the aluminum electroforming program, and safety and security personnel, have access to these facilities. EOS or Government visitors must clear through the manager of this program. Visitor access to this facility for observation must be cleared through the Safety Systems manager. All personnel are indoctrinated and trained to handle emergency situations. The Pomona Fire Department units who will respond to a fire condition have been indoctrinated and furnished safety information.

Emergency procedures. - If it is necessary for the operator to shut down during plating because of a malfunction in the system which may present a hazardous condition, one of the operators will call 222 and have the guard stand by. The guard will notify Pomona Plant Safety, extension 451.

If a fire or explosion occurs in the plating facility, the plating operator will notify Plant Security, extension 222. The guard will call the Pomona Fire Department and the Pomona Security Officer (who will notify the nurse and doctor, and make any necessary announcements over the public address system.

Personnel will retreat, when it is safe, to the main entrance of the plating area and don special fire fighting gear. Dry chemical wheel units will be readied for action. Personnel are not to attempt to fight the ether fire but to contain it. Personnel should remain up-wind from fire and fumes.

Personnel in charge of the facility will meet the incoming fire trucks and brief the fire captain. Only ether plating personnel and safety and security personnel are permitted access to the area. Security and safety personnel will keep the area clear of other employees. Employees are to ramain in the main buildings.

Safety equipment. - Each operator shall have the following minimal safety equipment:

1. fire-retardant smock
2. face shield
3. face mask - mild caustic
4. gloves
5. safety shoes and grounding wire.

The following fire fighting equipment shall be available:

1. thermal barrier suit
2. 150 lb roll-tank, dry chemical fire extinguisher
3. 20 lb Ansul foray extinguisher
4. Scott breathing equipment

All incidents and accidents will be reviewed by an ad hoc committee composed of the managers of plating operations, safety systems, and facility engineering.

Operating Procedure

The electrolyte used in the plating operation is flammable and, in some circumstances, explosive. Also, solvents such as aluminum chloride and lithium aluminum hydride are potentially hazardous under certain conditions.

In order to avoid unsafe conditions, all equipment must be maintained in safe operating condition and safety procedures must be adhered to during operation.

The following operational procedures for loading, mixing, plating, and equipment servicing shall be used. A control panel schematic diagram is shown in Fig. E-1 and an operational flow plan is illustrated in Fig. E-2.

Flushing of the electroforming cell. - The air in the entirely enclosed electroforming cell must be replaced with nitrogen.

1. Mixing tank
   a. Close valves Nos. 15 and 17 and the butterfly valve leading to the mixing tank. Close the 1/2 in. and 3/8 in. valves in the glove box.
   b. Open the nitrogen valve and pressurize the mixing tank to 5 psig.
   c. Open the vacuum valve and evacuate the mixing tank to 10 in. Hg.
   d. Repeat steps b and c for a total of 10 cycles.
   e. Fill the mixing tank with nitrogen gas to 1 psig.
2. Storage tank
   a. Close valves Nos. 10, 13, 18, and 19.
   b. Open the nitrogen valve and pressurize the storage tank to 5 psig.
   c. Open the vacuum valve and evacuate the storage tank to 10 in. Hg of vacuum.
   d. Repeat steps b and c for a total of 5 cycles.
   e. Fill the storage tank with nitrogen gas to 1 psig.
3. Plating tank
   a. Close valves Nos. 14 and 16.
   b. Open the nitrogen valve and pressurize the plating tank to 5 psig.
   c. Open the vacuum valve and evacuate the plating tank to 10 in. Hg of vacuum.

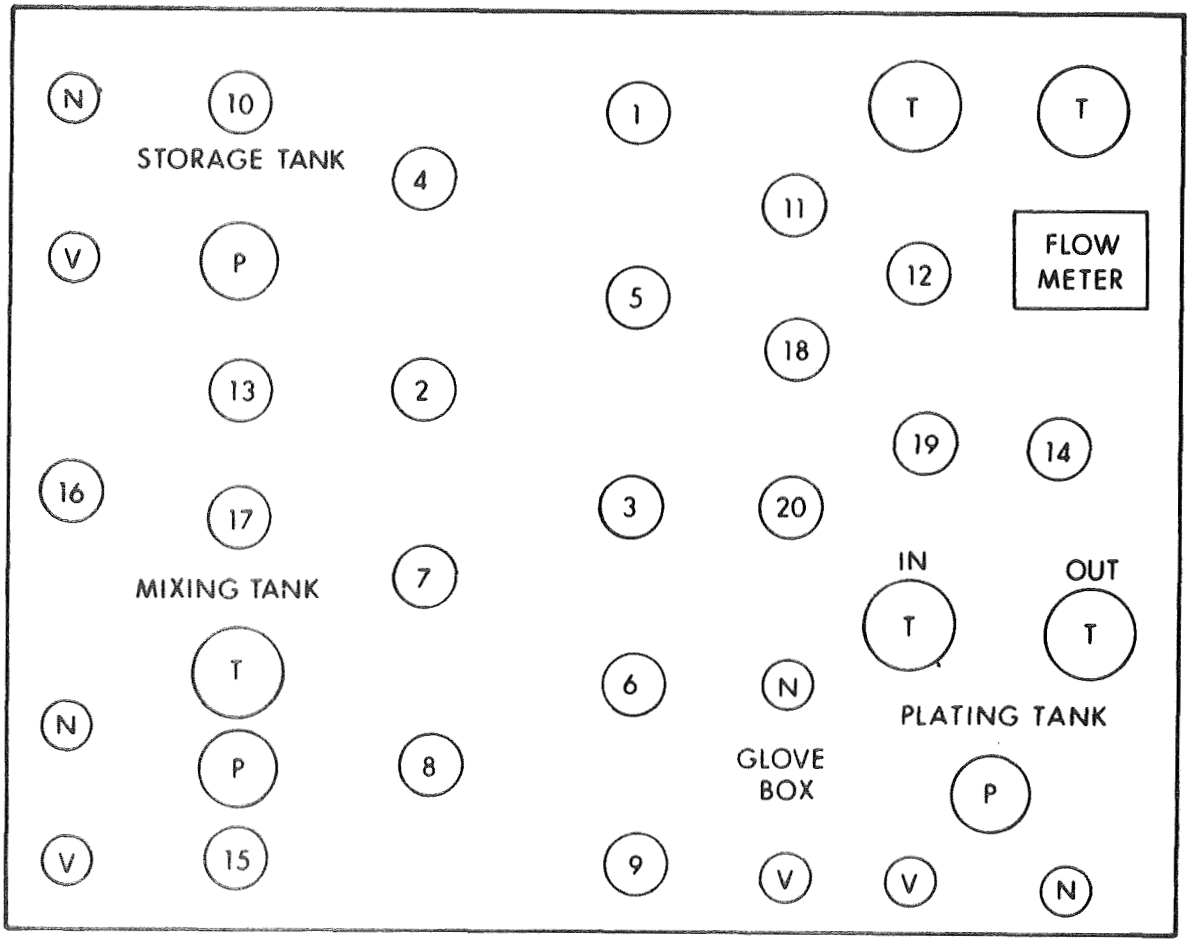

N NITROGEN VALVE

V VACUUM VALVE

4 NO. 4 PNEUMATIC VALVE

P PRESSURE GAGE

T TEMPERATURE GAGE

Figure E-1. Control Panel Schematic Diagram

35398

35397

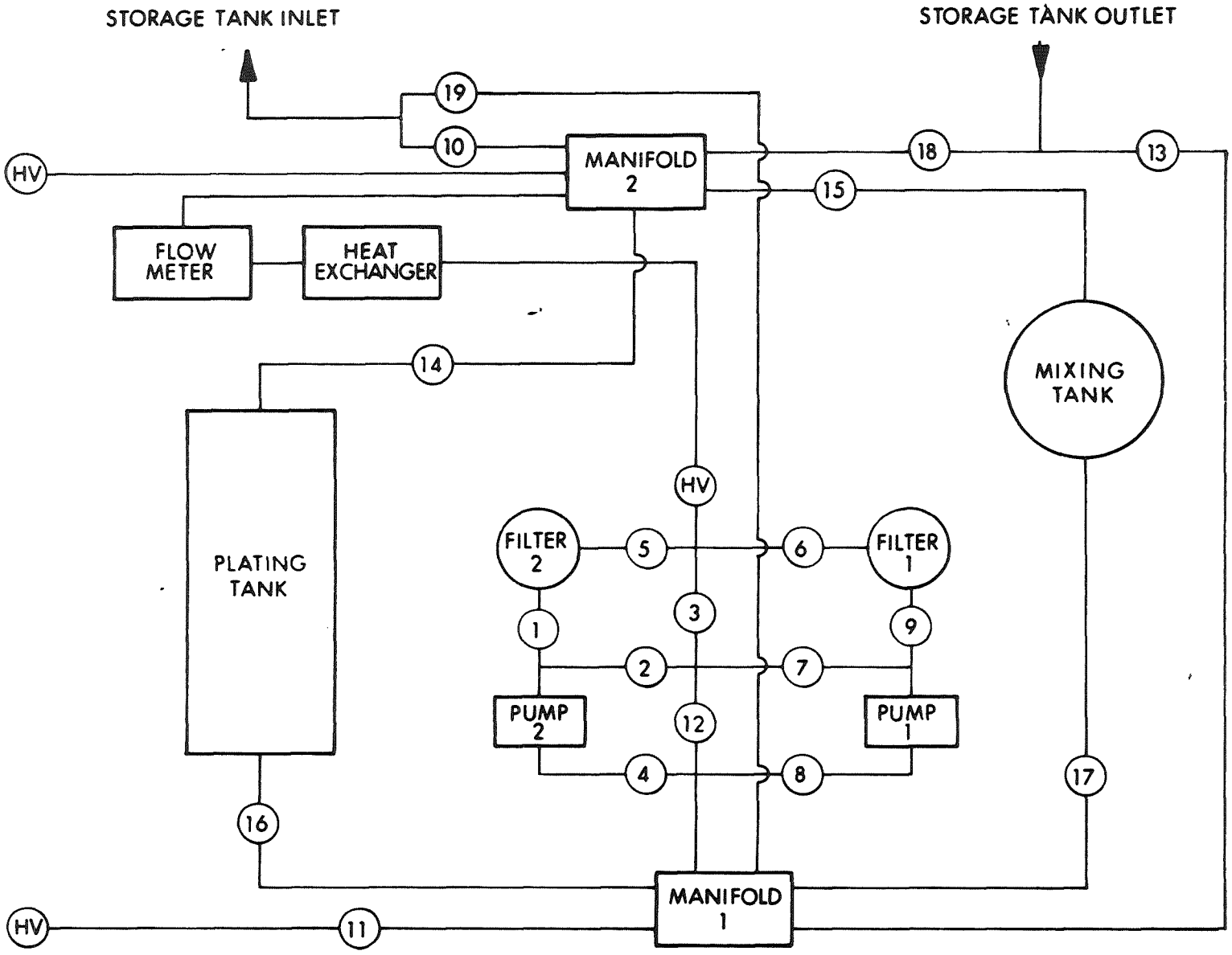

Figure E-2. Operational Flow Plan

d. Repeat steps b and c for a total of 5 cycles.

e. Fill the plating tank with nitrogen gas to 1 psig.

4. Electrolyte lines, filters, pumps and heat exchanger

Electrolyte lines, filters, pumps and heat exchangers can not be flushed alone. They must be flushed together with other pieces of equipment such as a plating tank. The following procedure demonstrates such an operation:

a. Open all valves, except Nos. 10, 11, 13, 15, 17, 18, 19, and hand valves Nos. 2 and 3.

b. Follow steps 3-b, c, d, and e.

Transportation of fluid. - The following procedure covers the transfer of fluid from 55-gal drums to the storage tank or the mixing tank. All 55-gal drums of diethyl ether or anisole loading into the storage tank or mixing tank are handled under the conditions listed below.

1. All 55-gal drums are grounded to the facility grounding system and grounding is not removed until all lines have been disconnected.

2. Prior to transferring the ether to the storage tank or the mixing tank, the drum is purged with dry nitrogen gas to drive off all air that may have been introduced to the drum while hooking up the transfer lines.

3. Personnel shall observe the following safety procedures:

a. The transfer of solvents is a 2-man operation.

b. All personnel shall wear fire-retardant smocks, face shields and protective gloves.

c. Fire fighting equipment shall be ready for use at all times.

d. The 55-gal drums of ether or plating solution shall not be stored on the premises over 48 hours.

After the electroforming system has been properly flushed, the fluid can be introduced into the storage tank according to the following procedure:

1. Connect the nitrogen line and the flexible intake line to the barrel with the hand valve, H_2, closed.

2. Open valves Nos. 11, 4, 1, 5, 8, 9, 6, 10 (No. 15 for mixing tank), as well as hand valve H_1, which is to be kept open at all times.

3. Open the vacuum valve, evacuate and maintain the storage tank at 5 in. Hg of vacuum.

4. Open the nitrogen valve, pressurize and maintain the barrel at 10 psig.

5. Open the hand valve H_2.

6. Wait 30 seconds and turn on pumps P_1 and P_2.

7. When all ether has been transferred, (as indicated by the flow meter), turn off pumps P_1 and P_2 immediately.

8. Close valves Nos. 11, 4, 1, 5, 8, 9, 6, 10 (No. 15 for mixing tank), and H_2.

9. Open the nitrogen valve and pressurize the storage tank, (mixing tank), to 1 psig.

10. Disconnect the nitrogen line to the barrel.

11. Disconnect the flexible intake line to the barrel.

12. Repeat the above process if more than one barrel of ether is to be transferred into the storage tank.

The following steps cover the transfer from the mixing tank into the storage tank or to the plating tank.

1. Open valves Nos. 17, 4, 1, 5, 8, 9, 6 and 10 (No. 14 for plating tank).

2. Open the nitrogen valve, pressurize and maintain the mixing tank at 6 psig.

3. Open the vacuum valve, evacuate and maintain the storage tank at 2 in. Hg.

4. Turn on pumps P_1 and P_2 until all fluid has been transferred.

5. Turn off pumps P_1 and P_2 immediately.

6. Close valves Nos. 17, 4, 1, 5, 8, 9, 6 and 10 (No. 14 for plating tank).

7. Open the vacuum valve and reduce the pressure in the mixing tank to 1 psig.

8. Open the nitrogen valve and pressurize the storage tank to the plating tank to 1 psig.

The following steps cover the transfer from the storage tank into the plating tank or mixing tank.

1. Open valves Nos. 1, 3, 4, 1, 5, 8, 9, 6, and 14 (No. 15 for mixing tank).

2. Open the nitrogen valve and pressurize the storage tank to 9 psig.

3. Open the vacuum valve, evacuate and maintain the plating tank, or the mixing tank, at 2 in. Hg.

4. Turn on pumps P_1 and P_2.

5. When the desired amount of fluid has been transferred, turn off pumps P_1 and P_2 immediately.

6. Close valves Nos. 13, 4, 1, 5, 8, 9, 6 and 14 (No. 15 for mixing tank).

7. Open the vacuum valve and reduce the pressure in the storage tank to 1 psig.

8. Open the vacuum valve and pressurize the plating tank, or the mixing tank, to 1 psig.

To transfer fluid from the plating tank into the storage tank, or the mixing tank, follow the steps listed below.

1. Open valves Nos. 16, 4, 1, 5, 8, 9, 6 and 10 (No. 15 for mixing tank).

2. Open the nitrogen valve, pressurize and maintain the plating tank at 6 psig.

3. Open the valve, evacuate and maintain the storage tank, mixing tank, at 2 in. Hg.

4. Turn on pumps P_1 and P_2.

5. When the desired amount of fluid has been transferred, turn off pumps P_1 and P_2 immediately.

6. Close valves 16, 4, 1, 5, 8, 9, 6 and 10 (No. 15 for mixing tank).

7. Open the vacuum valve and reduce the pressure in the plating tank to 1 psig.

8. Open the nitrogen valve and pressurize the storage tank, or the mixing tank, to 1 psig.

The following steps cover the circulation of electrolyte for cooling during electroforming.

1. Close the water inlet and outlet valves for the mixing tank cooling jacket.

2. Open the hand valve for the water line into the heat exchange.

3. Turn on the compressor.

4. Open valves Nos. 16, 4, 1, 5, 8, 9, 6 and 14.

5. Open the nitrogen valve, pressurize and maintain the plating tank at 6 psig.

6. Turn on pumps P_1 and P_2.

7. When cooling is no longer needed, turn off pumps P_1 and P_2.

8. Close valves Nos. 16, 4, 1, 5, 8, 9, 6 and 14.

9. Open the vacuum valve and reduce the pressure in the plating tank to 1 psig.

Preparation of electrolyte. - The proper quantities of aluminum chloride and lithium aluminum hydride must be added to the mixed ether at a controlled rate to prevent overheating due to exothermic heat. The aluminum chloride and lithium aluminum hydride are added to the mixed ether solvent as indicated in the steps listed below.

CAUTION

The operator must wear gas mask during the operation.

Aluminum chloride shall be added as follows:

1. Flush the mixing tank according to the flushing procedure described previously.

2. Add solvent to mixing tank according to the procedure described under "Transportation of Fluid."

3. Open the water inlet and outlet valves for the mixing tank cooling jacket and close the hand valve for the water line into the heat exchange. Turn on the compressor and the agitator.

4. Flush the glove box for approximately 2 hours by repeat pressurizing with nitrogen gas and evacuation.

5. Open the outside door of the transferring box.

6 Place one 50 pound $AlCl_3$ container in the transferring box and tightly close the outside door.

7. Open the vacuum valve and evacuate the transferring box to 10 in. Hg of vacuum.

8. Open the nitrogen valve and reduce the vacuum in the transferring box to 1 in. Hg.

9. Repeat f and g for a total of 5 cycles and bring the pressure in the transferring box to ambient pressure.

10. Open the inner door of the transferring box and open the cover of the $AlCl_3$ container.

11. Empty the $AlCl_3$ into the hopper of the feeder.

12. Set the feeder speed at 6.

13. Open the vacuum valve, evacuate and maintain the mixing tank pressure at 1 in. Hg of vacuum.

14. Open the butterfly valve.

NOTE

Personnel must now leave the plating room and enter the control room. No one shall be permitted into the plating room during the mixing cycle of the aluminum chloride.

15. Turn on feeder.

16. Remove empty container by placing it into transferring box and tightly close inner door before opening outside door.

17. Repeat steps f, g, h, i, j, k, and p, if more $AlCl^3$ is to be added.

18. When desired amount of $AlCl_3$ has been added, close butterfly valve.

19. Turn off feeder. The solution in the mixing tank is ready for adding lithium aluminum hydride.

Lithium aluminum hydride shall be added as follows:

1. Place five 1-gal jars of 5M lithium aluminum hydride solution in the transferring box. Tightly close its outside door.

2. Flush out the transferring box according to steps 7, 8, and 9 from the preceding operation.

3. Open the inner door of the transferring box and put all lithium aluminum hdyride solution inside the glove box.

4. Open the cover of the jar and insert the flexible lithium aluminum hydride feeding tube.

NOTE

Personnel must now leave the plating room and enter the control room. No one shall be permitted to enter the plating room during the mixing cycle of the lithium aluminum hydride.

5. Make sure the mixing tank is maintained at 1 in. Hg of vacuum.

6. Open the 3/8 in. lithium aluminum hydride delivery valve carefully. Due to gas generation, the initial addition of hydride must be slowly controlled so that the gas generated in the mixing tank can be removed immediately. However, later additions can be proceeded at a high rate.

7. Close the 3/8-in. hydride delivery valve immediately when the jar is empty. Repeat steps 4, 5, 6, and 7 until all 5 jars have been added.

8. Remove the empty jar into the transferring box and tightly close the inner door.

9. Repeat steps 1 through 8 until all the hydride needed has been added.

10. Turn off the compressor.

11. Transfer all electrolyte into the storage tank according to this procedure.

12. Turn off the agitator.

Electroforming. - This operation consists of five different steps. The procedures for each of these five steps are as follows:

11. Mounting the electrode package
    a. Close valves Nos. 11 and 16.
    b. Disconnect the nitrogen, vacuum, pressure gage lines and carefully open the plating tank cover.
    c. Place the electrode package into the plating tank by fitting the package on the holders.
    d. Connect the anode and cathode leads.
    e. Check continuously between the electrode from the outside leads. The circuit between the anode and the cathode should be open.

NOTE

Before securing the cover to the plating tank, personnel shall make a visible inspection of the inside to ensure that all tools and any other foreign materials have been removed.

f. Secure the cover by tightening all nuts and bolts.

g. Connect the nitrogen, vacuum and pressure gage lines.

NOTE

Personnel must now leave the plating room and enter the control room.

h. Flush the tank according to the flushing procedure described previously.

2. Filling electrolyte

Electrolyte is introduced into the plating tank in the manner described in the steps for transferring fluid from the storage tank to the plating tank.

NOTE

After the plating tank has been secured and filled, the plating operation will be placed in the cycling mode without power to the electrodes. The ventilation system is turned off for three minutes, during which time the operator will observe the general monitor's system (GMS) for any indications of significant rise in explosive atmosphere within the plating room. Any abnormal readings require returning of the plating solution to the storage tank and investigation. Under no circumstances does any operator enter the plating room until all plating solutions have been placed in storage.

3. Startup

   a. Start cooling electrolyte according to the procedure described previously.

   b. Set the current limit on the power supply.

   c. Turn on the d-c power supply.

NOTE

The operator maintains a close surveillance of the flow rates and temperature levels of the plating load; any significant rise in temperature, decrease in flow rates and/or pressure change will indicate an abnormal operation. The plating solution is returned to the storage tank until an analysis of the condition can be made.

4. Termination of electroforming

   a. Turn off the d-c power.

   b. Stop cooling by turning off the compressor and pumps 1 and 2.

   c. Transfer all electrolyte into the storage tank according to the procedure described previously.

   d. Remove the remaining few gallons of electrolyte through the 3/8-in. valves (located near the outlet of plating tank) into some small container.

   e. Flush the plating tank according to the flushing procedure described.

NOTE

When the solution has been stored and the system purged, the operator once again shuts down the ventilation system for three minutes and observes the GMS.

5. Remove electroformed object

NOTE

The operator must wear a protecting mask and clothes during these operations.

a. Disconnect nitrogen, vacuum, pressure gage lines, outside electrical leads, electrolyte inlet and outlet lines.

b. Move the plating tank outside of the plating room.

NOTE

The plating tank shall be moved to at least 20 ft away from the plating facility. Personnel moving the tank and removing the plated object are fully suited with face shields, respirators, gloves and fire smocks. There is always one person whose specific duty is to man the fire extinguishers during this operation. Should a fire erupt, the fire safety person shall completely flood the unit, as well as anyone close to it with the dry chemical fire extinguisher. The 150 lb portable unit shall be on standby and shall be located at least 25 ft away from the operation.

NOTE

All flow-line fitting connections shall be thoroughly washed before any wrench is applied to disconnect bolts from the plating tank cover.

c. Open and remove the plating tank cover.

d. Wash the electroformed object with ether.

e. Remove the electrode package from the plating tank.

f. Wash the electrode package with water.

g. Separate the anode and cathode.

h. Clean the plating tank and the cover.

Services. - An incident in which a fire occurred resulted from servicing the filter. It is included here to illustrate the importance of proper safety procedures in the maintenance of equipment which has been exposed to the ethereal electrolyte.

The fire incident of 7 April 1968 involved the filter component of the aluminum electroforming system. The incident occurred during the replacement of filter elements used in preparation of the aluminum plating solution. Apparently, some filter cake contained lithium aluminum hydride which reacted with air, causing a flash fire. The Ansul dump system accuated and extinguished the fire.

The following corrective measures have been made to prevent similar accidents:

1. A back wash system for filters has been set up to remove accumulated hydride, particularly before replacement of the filter elements.

2. The filters have been relocated for easier access.

The aluminum plating solution contains 3.4 molar of aluminum hydride and approximately 0.3 molar of lithium aluminum hydride in anhydrous diethyl ether. In preparing the plating solution the aluminum and lithium aluminum hydride (in the form of 5-M diethyl ether solution) are slowly added to diethyl ether solvent in a reactor. Prepared solution is then transferred from the reactor into a storage tank, through two filters of 10 gallon capacity, and each containing 6 all-woven polypropylene filter elements. These elements must be replaced when cumulated particles, mainly from aluminum hydride and lithium aluminum hydride, appear to hinder the electrolyte flow. The detailed operating procedure of changing such elements are given in the attached sheets. They are being back washed with wash ether to remove as much as possible

hydride particles before being replaced. Used elements are then stored in a steel container and subsequently carefully washed with water before being disposed of. The back wash ether is fed into the filter from an external source. The drainage is a dilute solution of lithium aluminum hydride and can be safely disposed of after allowing to react slowly with moisture in the air.

The filter cartridges must be replaced using the following procedure:

NOTE

Operators must wear protective mask and clothin during the following operations.

1. Close valves Nos. 1, 5, 9, and 6.

2. Flush the filter with wash ether from an external source.

3. Carefully open the filter and discard all filter elements immediately into a steel container.

4. Remove the filter base from its mounting by disconnecting the electrolyte lines and mounting screws.

5. Carefully wash and clean the filter component with water.

6. Dry out the filter components.

7. Install the filter back into the electrolyte line and put in new filter elements.

8. Pressure-check all connections.

9. Flush the filter with nitrogen by pressurizing the plating tank to 5 psig. Open valves Nos. 16, 12, 2, 1, 7, 9 and the 1-in. draining valve on each filter.

10. After sufficient flushing, close the 1-in. hand draining valves as well as valves Nos. 16, 12, 2, 1, 7 and 9 in the electrolyte line.

11. Open the vacuum valve and reduce the pressure in the plating tank to 1 psig.

12. The filters are now ready for further use.

REFERENCES

1. Staff, Power Systems Division, Electro-Optical Systems: Development of Lightweight Rigid Solar Panels. NASA CR-75370, 1966.

2. Lui, K; Guidotti, R: Electroforming of Magnesium/Aluminum for Solar Concentrators. NASA CR-66427, 1967.

APPENDIX A

SUBSTRATE ANALYSIS-OPTIMIZATION OF ALUMINUM HOLLOWCORE DESIGN

This analysis follows the procedure outlined in the basic report.

Design Restrictions Due to Hollowcore Fabrication Process

The fabrication process (electroforming) of the hollowcore places the following geometric restrictions on the design:

1. Distance between holes shall not be less than 0.050 inch ($\Delta \geq 0.050$ in.)
2. Hollowcore height shall not be less than 0.100 inch for a planform size of 5 x 5 ft sq ($h \geq 0.100$ in.)
3. Skin thickness of hollowcore shall be equal to or greater than 0.002 inch and equal to or less than 0.006 inch (0.002 in. $\geq t \geq$ 0.006 in.)

The first two restrictions are dictated by the mandrel used in fabricating the hollowcore substrate. At present, a copper sheet is to be used and the holes in it are to be first drilled, then reamed. It has been found that if the distance between holes is less than 0.050 inch the operation of drilling another hole will upset and deform a previously established adjacent hole. If the mandrel thickness is less than 0.100 inch for a 5 x 5 ft sq biconvex shell, it will deform under its own weight when suspended in the electroplating tank.

The last restriction, the allowable range in thickness of the electroplating, is dictated by the state of art of aluminum electroforming.

It should be noted that this defines the panel frequency for a system with a rigid boundary. Appendix B of this report analyzes the effect of the frame stiffness on the panel first resonant frequency.

Critical Environmental Loading and Structures Dynamic Magnification Factor

Review of the specified design environment defined in the basic report indicates that the sinusoidal vibration of the structure is the most severe loading condition for the solar array. Since the structure is being designed to have a first resonance below 50 Hz, the input acceleration at the attachment points will be 1.5 g rms or 2.12 g zero to peak.

From Phase I testing, it was found that the dynamic magnification factor for this type of structure is about 40.

The acceleration response of the substrate under a sinusoidal vibration input as derived in Phase I (Ref. 1) is

$$\ddot{W} = \frac{16}{\pi^2} Q \sin\left(\frac{n\pi}{\alpha_o}\alpha\right) \sin\left(\frac{m\pi}{\beta_o}\beta\right) \ddot{W}_s \qquad \text{(A-2)}$$

where

$\ddot{W}$ = normal acceleration of substrate surface - g

Q = dynamic manifaction factor - dim.

α = curvilinear coordinate in X direction - in.

β = curvilinear coordinate in Y direction - in.

$\ddot{W}_s$ = input acceleration at boundary - g

Membrane Forces per Unit Length

The membrane force per unit length varies over the surface of the biconvex structure. For the preliminary (first cut) analysis, the maximum membrane forces at the crown of the biconvex panel were approximated by the formula for a spherical shell supported tangentially and loaded by a pressure. The formula is

$$P = \frac{\rho R}{2} \tag{A-3}$$

where

P = membrane force per unit length - lb/in.

R = radius of curvature - in.

ρ = applied pressure - lb/in.^{2}

The applied pressure is defined by

$$\rho = (SpWt)_p \times G \tag{A-4}$$

where the g level is

$$G = \ddot{W} = 137.5 \text{ zero to peak}$$

and the specific weight $(SpWt)_p$ of the total panel is the specific weight of the dead load defined in the preceding subsection and that contributed by the hollowcore. The next section defines the specific weight of the hollowcore and the total panel for various geometric parameters.

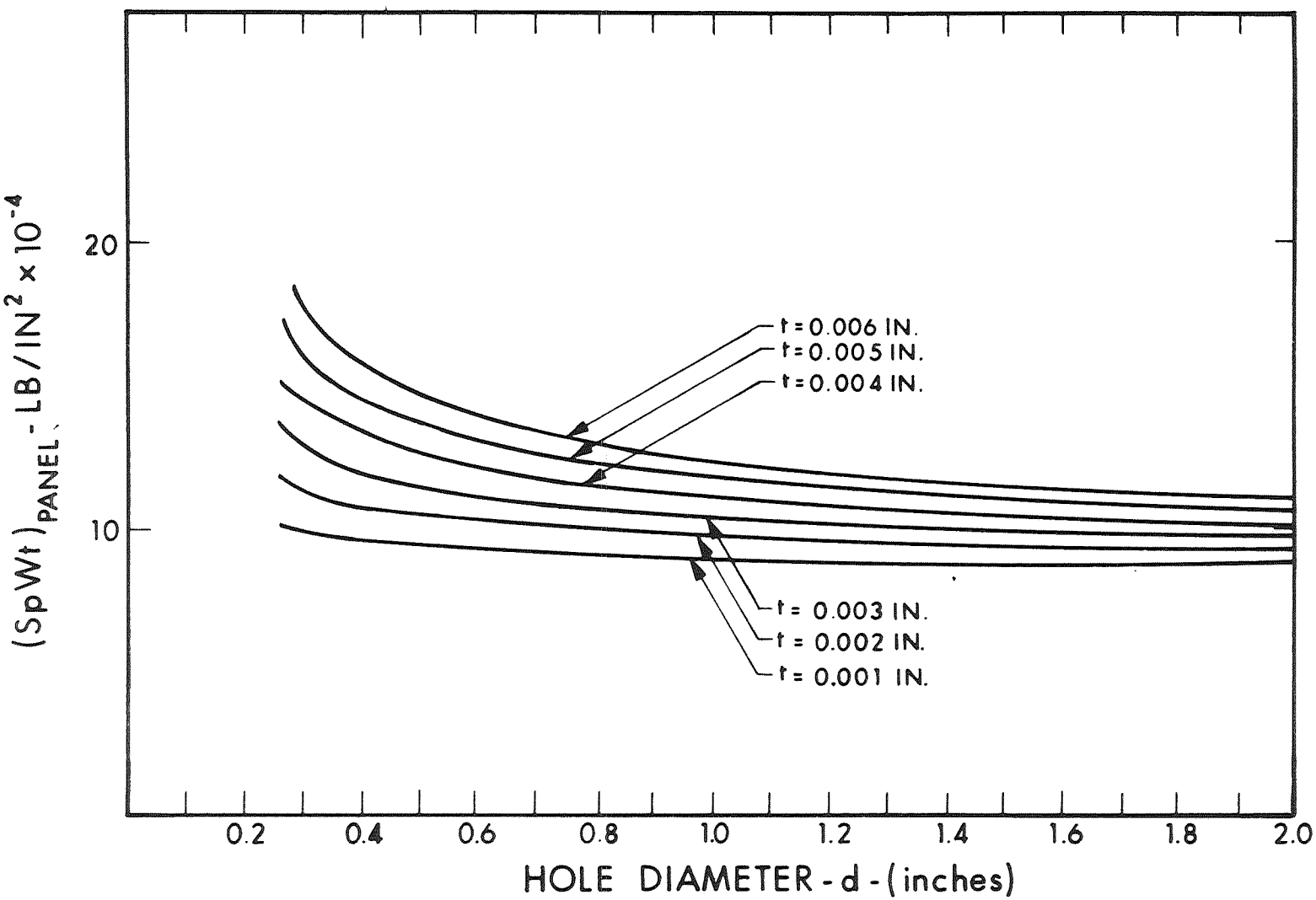

Figure A-1. Hollowcore Optimization, Specific Weight versus Hole Diameter with Skin Thickness as Parameter $(SpW+)_{panel} = (SpW+)_{hollowcore} + (SpW+)_{dead\ load}$

Crippling Stress of the Hollowcore Structure

From the Phase I program, it was determined that the failure mode for the hollowcore structure concept was crippling in the surface between cylinders. It was also determined that this surface could be approximated by an equilateral triangle (see Fig. A-2) loaded in compression along its three sides. The leg dimension(s) of this triangle is defined by

$$s = 4a - \sqrt{3}d \tag{A-9}$$

From NASA Document TN 3781, the critical stress in a triangular sheet, loaded in compression along its boundary, is

$$F_{cc} = K \frac{\pi^2 E}{12(1-\nu^2)} \left(\frac{t}{s}\right)^2 \tag{A-10}$$

The coefficient (K) given in NASA TN 3781 is

K = 5 for simply supported edges

K = 12.5 for coupled edges

In Phase I tests the coefficient was found to be K = 12

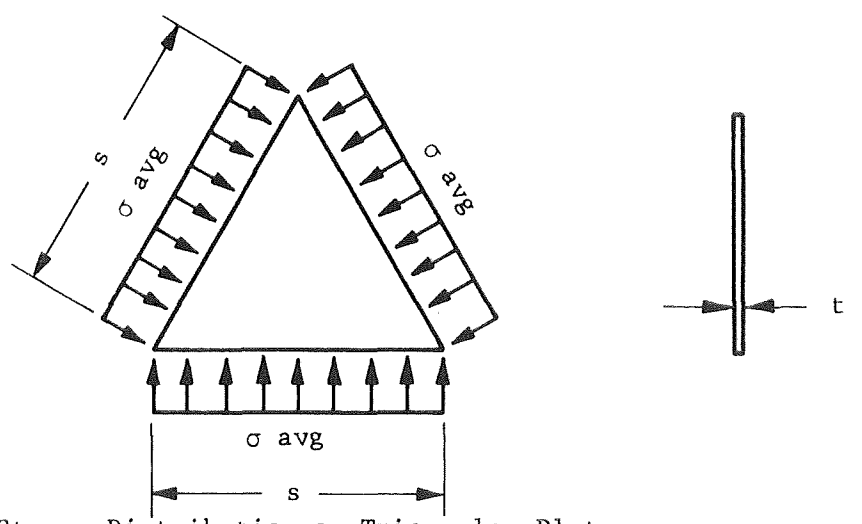

Figure A-2. Stress Distribution on Triangular Plate